Drivers, development, and impact of tillering plasticity mechanisms for corn yield stability in Kansas environments

by

Rachel Lynn Veenstra

B.S., Missouri State University, 2018

AN ABSTRACT OF A DISSERTATION

submitted in partial fulfillment of the requirements for the degree

DOCTOR OF PHILOSOPHY

Department of Agronomy
College of Agriculture

KANSAS STATE UNIVERSITY
Manhattan, Kansas

2022

Abstract

Historic breeding efforts in corn (*Zea mays* L.) have resulted in uniform, single-stalked phenotypes with limited environmental plasticity potential. Therefore, plant density is a critical yield component for corn, as it is unable to successfully compensate for a deficit of grain-bearing shoots. Enhancing corn yield stability across plant densities has potential benefits, particularly considering diverse yield environments and seasonal weather uncertainties due to climate change. Research and actionable information regarding branching ("tillering") utility in corn production are largely unavailable. This is particularly relevant in environments where plant density is typically resource-limited or environments in which the target density is not properly achieved. Therefore, the objectives of this dissertation were to determine the following based on tillered corn phenotypes in a range of environment (E) × management (M) scenarios: 1) the impact of tiller development on corn yields; 2) the plastic extent and relative importance of yield components; 3) the drivers and predictability of corn tiller development; and 4) the effect of tiller expression on biomass accumulation, carbon economy, and subsequent reproductive efficiency. This extensive field study evaluated tiller presence (removed or intact) with two commercial hybrids (P0657AM and P0805AM, Corteva Agriscience, Johnston, IA) in a range of plant densities (25000, 42000, and 60000 pl ha^{-1}) across the state of Kansas. In total, 17 site-years were evaluated – comprised of 9 unique field locations across 3 seasons (2019-2021).

Yields were increased or unaffected by greater plant densities and tiller presence. Environments varied in yield responsiveness to tiller density, but plant density was key to maximizing yield. Favorable soil properties and higher photothermal quotient (PTQ) values were important correlates of tiller productivity (Chapter 2*).* Ear number and kernel number per area were less dependent on plant density with tillered phenotypes. Kernel number remained key to

yield stability. Although ear number was less related to yield stability, ear source and type were significant yield predictors, with tiller axillary ears as stronger contributors than main stalk secondary ears in high-yielding environments (Chapter 3). Plant density interactions with cumulative growing degree days (GDD), PTQ, mean minimum and maximum daily temperatures, cumulative vapor pressure deficit (VPD), soil nitrate (NO_3), and soil phosphorus (P) were important predictive factors of tiller density – many of these with stark non-limiting thresholds. Out-of-season prediction errors were seasonally variable, highlighting the importance of representative training datasets (Chapter 4). Tiller expression stabilized aboveground biomass across plant densities at the hectare scale. Greater tiller biomass was not correlated with any changes in reproductive efficiency. Additional stem tissue allowed tillered corn phenotypes to accumulate a greater reserve of water-soluble carbohydrates in low plant densities and support main stem remobilization demand (Chapter 5).

Overall, tillering in corn presents itself as a potentially useful plasticity mechanism in non-uniform field situations with unexpectedly reduced or inadequate plant densities. While limits to tiller productivity are apparent, the branching ability of modern corn hybrids may lend itself to improving resilience of defensive strategies in water-limited environments. It should be noted that although this study explored a range of environments, severe drought scenarios were not explored. The utility of tillering as a plasticity mechanism in corn remains an area of active study.

Drivers, development, and impact of tillering plasticity mechanisms for corn yield stability in Kansas environments

by

Rachel Lynn Veenstra

B.S., Missouri State University, 2018

A DISSERTATION

submitted in partial fulfillment of the requirements for the degree

DOCTOR OF PHILOSOPHY

Department of Agronomy
College of Agriculture

KANSAS STATE UNIVERSITY
Manhattan, Kansas

2022

Approved by:

Major Professor
Dr. Ignacio A. Ciampitti

Copyright

Abstract

Historic breeding efforts in corn (*Zea mays* L.) have resulted in uniform, single-stalked phenotypes with limited environmental plasticity potential. Therefore, plant density is a critical yield component for corn, as it is unable to successfully compensate for a deficit of grain-bearing shoots. Enhancing corn yield stability across plant densities has potential benefits, particularly considering diverse yield environments and seasonal weather uncertainties due to climate change. Research and actionable information regarding branching ("tillering") utility in corn production are largely unavailable. This is particularly relevant in environments where plant density is typically resource-limited or environments in which the target density is not properly achieved. Therefore, the objectives of this dissertation were to determine the following based on tillered corn phenotypes in a range of environment (E) × management (M) scenarios: 1) the impact of tiller development on corn yields; 2) the plastic extent and relative importance of yield components; 3) the drivers and predictability of corn tiller development; and 4) the effect of tiller expression on biomass accumulation, carbon economy, and subsequent reproductive efficiency. This extensive field study evaluated tiller presence (removed or intact) with two commercial hybrids (P0657AM and P0805AM, Corteva Agriscience, Johnston, IA) in a range of plant densities (25000, 42000, and 60000 pl ha^{-1}) across the state of Kansas. In total, 17 site-years were evaluated – comprised of 9 unique field locations across 3 seasons (2019-2021).

Yields were increased or unaffected by greater plant densities and tiller presence. Environments varied in yield responsiveness to tiller density, but plant density was key to maximizing yield. Favorable soil properties and higher photothermal quotient (PTQ) values were important correlates of tiller productivity (Chapter 2*).* Ear number and kernel number per area were less dependent on plant density with tillered phenotypes. Kernel number remained key to

yield stability. Although ear number was less related to yield stability, ear source and type were significant yield predictors, with tiller axillary ears as stronger contributors than main stalk secondary ears in high-yielding environments (Chapter 3). Plant density interactions with cumulative growing degree days (GDD), PTQ, mean minimum and maximum daily temperatures, cumulative vapor pressure deficit (VPD), soil nitrate (NO_3), and soil phosphorus (P) were important predictive factors of tiller density – many of these with stark non-limiting thresholds. Out-of-season prediction errors were seasonally variable, highlighting the importance of representative training datasets (Chapter 4). Tiller expression stabilized aboveground biomass across plant densities at the hectare scale. Greater tiller biomass was not correlated with any changes in reproductive efficiency. Additional stem tissue allowed tillered corn phenotypes to accumulate a greater reserve of water-soluble carbohydrates in low plant densities and support main stem remobilization demand (Chapter 5).

Overall, tillering in corn presents itself as a potentially useful plasticity mechanism in non-uniform field situations with unexpectedly reduced or inadequate plant densities. While limits to tiller productivity are apparent, the branching ability of modern corn hybrids may lend itself to improving resilience of defensive strategies in water-limited environments. It should be noted that although this study explored a range of environments, severe drought scenarios were not explored. The utility of tillering as a plasticity mechanism in corn remains an area of active study.

Table of Contents

List of Figures

List of Tables

Acknowledgements

My acknowledgements must begin with the solemn truth that I would not have the opportunity to write these words without the grace of my Lord and Savior, Jesus Christ. Every step to reach this moment was so obviously, carefully planned and orchestrated, and I found myself awed every day as I watched it unfold. Thank you to everyone who opened doors and participated in the events that led me here to K-State – my dear family and friends, my advisers at Missouri State University (Dr. Melissa Bledsoe, particularly), Steve and Barb Frank of Westmoreland, and Dr. Laura Mayor of Corteva Agriscience.

I extend special gratitude to my mentor and adviser, Dr. Ignacio Ciampitti, who offered his time and experience as I worked to accomplish my goals, as well as the freedom to explore my ideas and find my own path during my program. My gratitude is also extended to Dr. Kevin Donnelly, who entrusted me with priceless teaching responsibilities and opportunities and inspired me to chase my dreams of teaching. Both of these mentors reinforced the value of not only sharing my passion with others, but doing so in a way that fosters meaningful connection.

I thank my committee members, Dr. Trevor Hefley, Dr. P.V. Vara Prasad, Dr. Charlie Messina, and Dr. Lucas Haag for their support and encouragement during my Ph.D. program. I am also grateful for the support of Dan Berning and Dr. Paul Carter, who have offered meaningful perspectives and direction throughout this project. Field implementation of this project was successful because of Sean Wallace, Lisa Currie, and Mike Legleiter from Corteva Agriscience, who offered their time and assistance from the Garden City and Wamego, KS stations.

The data used to compile this dissertation would not exist without the visiting scholars and interns of the 2019-2022 KSUCrops and Ciampitti Lab teams who worked so hard, day in

and day out, to collect and process it. I was blessed by the support of my lab mates who made the hard days easier and the good days even better. My heartfelt thanks are extended to all.

I extend sincere gratitude for the financial support of Kansas State University, the Kansas Corn Commission, and Corteva Agriscience. These organizations funded and facilitated my Ph.D. work, and individuals associated with each played a pivotal role in my professional development and graduate student experience.

Dedication

To my family – Leon, Lynette, Jessica, and Aaron – for their endless support and love.

To my friends who became family.

To the families who welcomed me as their own along the way.

I love you all with my entire heart.

This dissertation is possible because of you.

Chapter 1 - Introduction to Cereal Crop Plasticity

1.1 What is crop plasticity?

Phenotypic plasticity, an inherent characteristic of plants, is often intertwined with modern conversations of climate-smart agriculture. This plasticity is essentially variation caused by a change in management practices and/or environment and mediated by a change in the physiology and/or morphology of plants. Adaptation is the expression of alternative phenotypes or maintenance of a desirable phenotype providing an evolutionary advantage to the plant. Resilience is the ability to recover or maintain a phenotype of interest without external intervention following a disruption due to a change in the environment. Therefore, plastic plants may be well-adapted or not, resilient plants may be plastic or not, and well-adapted plants may be resilient or not. Ultimately, crop domestication resulted in plants more dependent on humans for successful seed production than their wild relatives. Consequently, adaptations may be regional, plasticity may be suppressed, and resilience may be impacted as well.

Crop plasticity broadly refers to the responsiveness of a cultivated plant genotype to environmental stimuli via an expression of alternate phenotypes (Laitinen & Nikoloski, 2019). Because plasticity is expressed in different ways, to different extents, and with different productivity results across species, quantification of crop plasticity is not uniform throughout available literature. For example, plasticity may be measured as the modification of a specific trait (structural plasticity) or as functional differences in contrasting stress regimes (physiological plasticity) at various scales (Pierik et al., 2021). Prediction of specific plasticity mechanisms can prove difficult, and recent literature indicates mounting research interest in crop plasticity expression. Historic crop improvement efforts have defined frameworks to quantify plasticity and make selections based on traits of interest – yield response to evapotranspiration as a drought

sensitivity indicator, for example. Many traditional breeder frameworks target high-yielding (favorable environments) and stable (restrictive environments) genotypes (Eberhart & Russell, 1966; Finlay & Wilkinson, 1963). Because crop plasticity is expressed and quantified uniquely across species, plasticity has historically been perceived and pursued differently for various crop species.

1.2 Modern advancement in cereal crop plasticity

Cereals (including rice [*Oryza sativa* L.], wheat [*Triticum aestivum* L.], corn [*Zea mays* L.], grain sorghum [*Sorghum bicolor* L.], and the millets [including *Pennisetum glaucum* L.R. Br., *Panicum miliaceum* L., *Eleusine coracana*]) are known to be very stable cropping species, with an enhanced ability to withstand stress early in the growing season, accumulate substantial amounts of carbon in vegetative organs for redistribution, produce high quantities of seed, and even persist as perennials. Ultimately, crop domestication processes identified traits that improved efficiency and intensity of human management in mediated environments and exploited them. Plasticity can be accomplished both from source (resource accrual or provision) and sink (resource allocation) perspectives, but identifying advantages of its expression (yield production and variation, biomass production and variation, etc.) to in-field crop production is crucial (Abdelrahman et al., 2020; Dingkuhn et al., 2020; Gambín & Borrás, 2007). Modern advancements in cereal crop plasticity mechanisms generally fall into one of three areas highlighted by Passioura's framework – resource use, use efficiency, and harvest index, where key resources are light, water, and nutrients (Passioura, 1977, 2006). The implementation of such mechanisms in production through the marriage of breeding and agronomic decision-making is also a key area of advancement. Contextual examples are presented below.

1.2.1 Light capture

Light capture can be altered and maximized through the modification of multiple plant traits – including leaves, branches, and molecular function. Leaf number, size, and shape impact canopy coverage and crop leaf area index (LAI). For example, flag leaf size of wheat is plastic under contrasting water regimes (Fatiukha et al., 2021), but leaf size and shape are less plastic than leaf number when adjusting LAI in rice (U. Kumar et al., 2017). Leaf angle has been extensively selected in high-density targeted crops rice and corn (Cao et al., 2022; Duvick, 2005; Duvick et al., 2004). However, opportunities may exist in the less-manipulated sorghum genome for greater environmental plasticity exploitation (Pfeiffer et al., 2019; Zhi et al., 2022). Shoot architecture plasticity can have pseudo-biodiversity impacts in agroecosystems and thus facilitate successful implementation of management practices like intercropping (Ajal et al., 2022; Zhu et al., 2015).

Tillers, vegetative branches of Poacea species, impact leaf traits and shoot morphology and have been a focal point for crop domestication and improvement. In rice, wheat, and sorghum, tiller number plasticity has been linked to environmental factors impacting available plant C at time of initiation (Choi et al., 2013; Lafarge et al., 2010) and growth rate (Kamiji et al., 2011). As plant density increases, shading and stress are more likely, resulting in reduced tillering potential of all cereal crops (Adriani et al., 2016). While key to plant density adaptation, rice tiller expression has been shown less plastic than sink modifications in response to climate variations (U. Kumar et al., 2017). In the case of corn, genotypes with greater intensification potential have been historically preferred, resulting in the masking of tillering traits from modern hybrids (Duvick et al., 2004). In spite of this, tiller expression is a focus of efforts to sustain corn

production in vulnerable growing environments, where it has potential as a useful plasticity mechanism (Rotili et al., 2021b; Veenstra et al., 2021).

Molecular adaptations are an excellent example of a plasticity mechanism. Wheat drought resilience has been identified in genotypes able to situationally express proteins altering stomatal regulation, mitigating reactive oxygen species, and redirecting C allocation (R. R. Kumar et al., 2017; X. Wang et al., 2014). However, photosynthetic response to light intensity does not implicate biomass changes in the case of rice, and genotype plays a key role in determining efficacy of all plasticity mechanisms, including photochemistry (Chen et al., 2021).

1.2.2 Energy allocation

Sink plasticity has been highlighted as a critical opportunity for adaptation to alternative climate conditions (Dingkuhn et al., 2020). Cereal crops differ in the remobilization process of pre-anthesis C reserves, most of which are stored in stems. In stressed conditions, remobilization becomes more important as photosynthetic capacity is reduced. In wheat, genotypes with greater plasticity in stem C allocation are more tolerant of drought stress (Liu et al., 2020).

Although critical to water and nutrient uptake, root plasticity is less explored largely due to soil nutrient and moisture management in intensified systems (Schneider & Lynch, 2020). The persisting challenge of realistically measuring in-field root architecture and plasticity contributes to a lack of studies (Aguilar et al., 2021; Karlova et al., 2021). However, root plasticity allowing for exploration of soil profiles is particularly important in variable or marginal cropping conditions (Schneider & Lynch, 2020). In wild accessions of *Aegilops tauschii* and *Triticum dicoccoides* (wheat relatives), root C partitioning plasticity under contrasting moisture conditions improves drought adaption while maintaining shoot productivity – a trait with donor potential for modern wheat varieties (Suneja et al., 2019). Similarly, sorghum and millet root development

plasticity, particularly the inhibition of lateral roots and expression of deep, steep rooting structures is critical to remaining productive in water-limited conditions (Liang et al., 2017; Rostamza et al., 2013). In corn, root architecture of modern hybrids has adapted to increased plant populations – improving yields through an increased reliance on plant density and not improved root efficacy (Messina et al., 2021).

Inflorescence development has been identified as key to successful environmental adaptation, particularly with climate-based stressors (Dingkuhn et al., 2020; Faye et al., 2019; Jacott & Boden, 2020). Increased harvestable inflorescence size was a key part of crop domestication processes (Y. Wang & Li, 2011), but genetic selection for stable phenotypes has negatively impacted plasticity in most crops. Less-intensified species like pearl millet can more easily manipulate grain size via the grain filling duration, thus providing a moisture stress advantage (Ghatak et al., 2021). Grain size in cereals is typically dependent on both source availability and the sink capacity established in reproductive development phases. However, sorghum is capable of adjusting sink capacity throughout the grain-filling period to capitalize on available energy reserves if C exceeds the sink limits (Gambín & Borrás, 2007). Corn, however, has a more determinate sink size per grain (Gambín et al., 2008).

1.2.3 Crop production utility

While mentioned examples may be of situational interest, relevance to modern agroecosystems is contingent on practical applications. Conclusions of many presented examples are based on observations from a greenhouse or otherwise unrealistic production environment. In addition, although some studies included a wide variety of genotypes, relatively few environmental conditions were considered (e.g., one “water-limited” versus one “well-watered”). Each study discussed plasticity mechanisms from a relatively circumstantial, unique perspective,

highlighting the lack of standardization in this realm of crop ecology. In fact, the conclusions of many highlighted studies were the simple existence of plasticity mechanisms rather specific examples of their usefulness. Crop simulation models are an avenue to integrate such data into a usable platform. Examining plasticity mechanisms as individual components in not sufficient to inform breeding or agronomic management decisions – the whole system must be considered.

While plasticity mechanism exploration is intriguing and progressive, discussion of its practical implementation in modern production systems is apparently lacking. Perhaps this is largely due to the fact that "crop plasticity" quantification remains vague and abstract. I find this stagnant nature puzzling, considering the call to explore plasticity in production agriculture has echoed for decades (Loomis & Connor, 1992; Nicotra & Davidson, 2010). How can we implement something not collectively understood, even if it has been defined for some time? To what extent must environmental variation exist for a genotype to be deemed plastic? How can usefulness be highlighted and targeted in field studies? What can be done to facilitate more meaningful, impactful conclusions?

1.3 Forward-facing perspectives

Intentional utilization of plasticity in cropping systems and breeding programs is more difficult to achieve than to conceptualize. Several obstacles must be overcome to truly implement the strategies that have been discussed in crop breeding for decades (Brooker et al., 2022). Comprehensive, standardized crop ecology studies must be conducted to identify the practical implications and limitations of plasticity from the perspective of large-scale production systems. Perhaps the development of a targeted crop trait framework similar to the proposal of Nicotra et al. (2010) could be used to standardize these efforts. Crop simulation models provide an avenue

to address these challenges, and use of such tools should increase in the future. Combinations of these advancements must culminate in tangible targets for breeding programs.

Plasticity expression, by definition, requires multiple genetic candidates and a variety of growing conditions, which is very resource-intensive. For this reason, singular efforts cannot adequately explore the complex interactions of practical application. Understanding plasticity mechanisms and potential in our crop species will require well-documented protocols and quality data from different studies covering a wide variety of genotype × environment interactions. Although resource-intensive, standardized reporting of singular studies can facilitate the broad-scale efforts necessary to properly explore trait plasticity and utility in diverse global environments. However, as mentioned previously, plasticity utility in large-scale production agriculture remains untested and uncertain, and additional work must be done prior to breeding program incorporation.

While breeding programs have considered resilience and plasticity in their selections over time, refining our knowledge of the mechanisms of such plasticity expression in our crop species and agricultural production systems is crucial. This process centers on recognizing crop tolerance as a useful but indefinite solution to climate change. From this standpoint, plasticity has potential in breeding programs as a tool rather than an obstacle. It is important to emphasize that long-term impacts of climate change are ultimately unknown and plasticity is not proposed as a catch-all solution. Increasing temperatures and altered weather patterns could bring additional pressures such as more severe or regionally displaced pest outbreaks, which will compound effects of altered temperature and moisture. Considering all of these factors, affirming potential displacement of invariable, predictable crop genotypes from current agroecosystems is pertinent. Crop plasticity requires further exploration. This understanding is necessary to equip ourselves

as possible for an uncertain future. Societal complacency presents a unique challenge to the incorporation of alternative climate adaptation strategies, as impacts appear gradual and tolerable. Perception shifts are needed, however, for proactive response to forecasted environmental thresholds, which we may not be able to accurately predict or even perceive (Hughes et al., 2013). Perhaps instead of perpetuating a sense of normality in established agroecosystems experiencing fundamental changes, we must consider ways to conform our cropping systems, including species selection and phenotypic preferences, to alternative climate states.

1.4 Dissertation objectives

Considering this background, authors sought to quantify, characterize, and appropriately describe utility of a generally unstudied plasticity mechanism in dent corn – tillering. Research and actionable information regarding tillering in corn production are largely unavailable. This area of study is particularly relevant in environments where plant density is typically resource-limited or is not reliably optimized due to variable climate. Therefore, the objectives of this dissertation were to determine the following based on tillered corn phenotypes in a range of E × M scenarios: 1) the impact of tiller development on corn yields; 2) the plastic extent and relative importance of yield components; 3) the drivers and predictability of corn tiller development; and 4) the effect of tiller expression on biomass accumulation, carbon economy, and subsequent reproductive efficiency. Following chapters address each of these general objectives.

Chapter 2 - Effect of tillers on corn yield: Exploring trait plasticity potential in unpredictable environments

**Published in Crop Science.*

Veenstra, RL, Messina, CD, Berning, D, Haag, LA, Carter, P, Hefley, TJ, Prasad, PVV, Ciampitti, IA. Effect of tillers on corn yield: Exploring trait plasticity potential in unpredictable environments. *Crop Science*. 2021; 61: 3660– 3674. https://doi.org/10.1002/csc2.20576

Abstract

Long-term selection in corn (*Zea mays* L.) favored single-stalked phenotypes limiting vegetative growth. However, reduced plant densities create conducive environments to the expression of vegetative branches called tillers. Tiller expression has motivated discussions about its yield effect in variable environments, but tiller research is lacking for modern corn genotypes. The objectives of this study were to (a) quantify the relative importance of management, environment, and interactions on the yield effect of tiller expression for two modern genotypes; (b) understand effects of observed tiller density, plant density, and their interaction on yield; and (c) identify key environmental determinants of yield response to tiller density in modern genotypes. In 10 environmentally diverse site-years across Kansas, tiller presence and removal were evaluated in two commercial corn hybrids (P0657AM and P0805AM) across three target plant density levels (25,000, 42,000, and 60,000 plants ha^{-1}). Yields were increased or unaffected by greater plant densities and tiller presence within site-years. Environments varied in yield responsiveness to tiller density, but fine-tuning plant density was needed to maximize yields. Sites with yields most responsive to tiller density were characterized by good soil properties and photothermal quotient values (e.g., soils with high organic matter and climates with greater solar radiation and cooler temperatures). Favorable growing conditions can be exploited by plasticity traits such as tillering in unpredictable

environments with annually variable optimum plant densities while limiting potential yield loss and producer risk due to disproportionate plant density.

2.1 Introduction

From 2008 to 2016, cropland expansion in the United States occurred at a rate of >550,000 ha yr^{-1}, resulting in new cropland that has, on average, lower productivity than the national existing cropland average (Lark et al., 2020). Plant density is an agronomic practice often employed by farmers to match crop demands with anticipated resource availability (Assefa et al., 2016; Schwalbert et al., 2018; van Averbeke & Marais, 1992), typically low precipitation and reduced soil fertility (Khosla et al., 2008; Nielsen et al., 2010). However, sparse plant densities encourage development of secondary vegetative shoots (tillers) when paired with favorable thermal and moisture conditions (Jenkins, 1941; Lyon, 1905). While tillers are generally desirable in other poaceae species such as wheat (*Triticum aestivum* L.) and grain sorghum (*Sorghum bicolor* L. Moench), presence in corn (*Zea mays* L.) has historically raised concerns about resource allocation and yield effects, resulting in the common name "suckers" (Dungan, 1931; Earley et al., 1971).

Long-term selection for yield and yield stability have resulted in a steady increase of optimum plant density over time, particularly in highly productive environments (Assefa et al., 2018; Duvick et al., 2004; Hammer et al., 2009; Russell, 1991; Tokatlidis & Koutroubas, 2004). Optimum plant densities decrease with decreasing resource availability, and low plant populations are typical for corn grown in marginal environments (Berzsenyi & Tokatlidis, 2012; Blumenthal et al., 2003; Mylonas et al., 2020; Ren et al., 2016). Breeders have selected against

tiller expression, but genotypic variation in expression levels of modern germplasm has been identified (Duvick et al., 2004; Major, 1977; Moulia et al., 1999).

Tillering is a form of phenotypic plasticity in corn. Thus, its expression depends on genotype (Hansey & de Leon, 2011; Sangoi, Schmitt, Vieira et al., 2012; Tokatlidis et al., 2005) and the availability of resources (Gardner, 1942). Lower daily average temperatures increase the number of tillers in corn, particularly when combined with higher light intensities (Markham & Stoltenberg, 2010; Stevenson & Goodman, 1972; Tetio-Kagho & Gardner, 1988). Soil fertility and moisture are critical to tiller development in corn (Downey, 1972; Dungan et al., 1959; Jenkins, 1941; Lyon, 1905; Tetio-Kagho & Gardner, 1988). Tiller density is often closely linked to plant density due to the effect of available resources per plant. However, tiller death is commonly observed as plants mature, connecting resource availability to tiller appearance and survival, rather than plant density alone (Major, 1977).

Corn tillers have vascular and root systems that are semi-independent from the main stem (Lyon, 1905). While tillers add competition for plant resources, nutrients and photosynthates can be translocated from tillers to main stalk, depending on tiller sink size (Alofe & Schrader, 1975; Dungan, 1931; Russelle et al., 1984). In previous studies, corn tiller presence has resulted in neutral (Earley et al., 1971; Frank et al., 2013; Sangoi, Schmitt, Vieira et al., 2012), positive (Hansey & de Leon, 2011; Lyon, 1905; Sangoi et al., 2009; Williams, 1912), and negative (Frank et al., 2013; Hansey & de Leon, 2011) effects on yields. In addition, tiller contribution to corn yield has been linked to plant density (Akman, 2002; Hansey & de Leon, 2011), genotype (Akman, 2002; Sangoi et al., 2009), and growing environment (Markham & Stoltenberg, 2010; Williams, 1912). Previous studies were focused on relatively few sites, but without explicitly evaluating the complex interactions of environment and management (E × M).

Research that partials out the effect of corn tillers on yield while accounting for modern genotypes, management, and an array of environments for producers in marginal regions is scarce but needed. The objectives of this study are to (a) quantify the relative importance of management, environment, and interactions on the yield effect of tiller expression for two modern corn genotypes; (b) understand effects of observed tiller density, plant density, and their interaction on yield; and (c) identify key environmental determinants of yield response to tiller density in modern genotypes.

2.2 Materials and Methods

2.2.1 Field experiments

2.2.1.1 Site characteristics and experimental design

Field experiments were conducted at 10 sites across the state of Kansas during the 2019 and 2020 growing seasons. Normal season precipitation and temperature characterization, in addition to annual deviations, are presented for each site-year in Figure 2.1. Field centroids, key dates, irrigation management, apparent seasonal crop water budget, previous crops, and early season soil characterizations are presented in Table 2.1. Apparent season water budget was calculated by subtracting apparent crop water demand—as determined by an estimation of crop evapotranspiration (ETc), calculated as shown in Allen et al. (1998) as the product of the grass reference evapotranspiration (ETr) and crop coefficient (Kc)—from observed water supply for the growing season (considering 1 month prior to planting to physiological maturity). Although large deficits are observed in the water budgets presented, it is key to note that plant-available soil water at planting—measured previously in the evaluated region by Lamm et al. (2017) with an average of 271 mm in a 2.4-m soil profile depth (2011–2012 period) for fields with similar

cropping history—and soil water-holding capacity were not included in this estimation. Accounting for this additional water source, a majority of apparent water budget deficits (mainly occurring from V14 onward) will realistically be negligible. Moreover, as shown in Figure 2.1, seasonal moisture was normal or above normal for all site-years. Weather data were retrieved from the Climate Engine web application (Huntington et al., 2017). Monthly climatic summaries are provided in Table A.1, and apparent crop water budget estimations by development stage are shown in Table A.2.

Six site-years (Manhattan 2019, Keats 2020, Garden City 2020, Goodland 2020, Colby A 2020, and Colby B 2020) were established with a replicated three-way factorial treatment structure in a randomized complete block design (RCBD) with a split-split-plot arrangement. Whole plot factor was target plant density with the three levels of 25,000, 42,000, and 60,000 plants ha^{-1}. These target densities were selected as representative of the range of plant densities commonly utilized by producers with limited or unavailable irrigation resources in the region of interest (Roozeboom et al., 2007). Subplot factor was corn genotype (hybrid) with the two levels of P0657AM and P0805AM. These Pioneer hybrids were selected due to their modern release date, suitability for the region of study, and propensity to express tillering (Corteva Agriscience, Johnston, IA, USA). Sub-subplot factor was tiller presence with the two levels of tillers intact (TI) and removed (TR). Garden City 2019 and Goodland 2019 site-years were also established in a RCBD with a split-split-plot, but with target plant density levels of 25,000 and 42,000 plants ha^{-1}. Buhler 2020 and Greensburg 2020 sites were established with a replicated two-way factorial treatment structure in a RCBD with a split-plot arrangement. Whole-plot and subplot factors and levels were identical to the design mentioned above, but tiller removal was not implemented in the Buhler 2020 and Greensburg 2020 locations. Plant density was selected as

the whole-plot factor across sites to facilitate statistical detection of smaller yield differences in the measurement of genotype and tiller presence effects, when applicable. All sites had at least three replications of each treatment. Plots in all site-years consisted of at least four rows at 0.76-m spacing with final minimum dimensions of 3-m wide by 5-m long. All target plant densities were seeded at double rates, thinned after emergence to ensure even distribution of plants within rows, and confirmed with stand counts. Pesticides were applied as necessary to prevent crop damage and fertilizer was applied to meet crop nutritional requirements.

2.2.1.2 Treatments and measurements

One-time tiller removal treatments were applied to designated plots when the main stalk had reached the V10 growth stage (tenth leaf as described by Ritchie et al., 1997). Tillers were removed from plants by hand to ensure clean, ground-level cuts with no injury to the main stalk. Cut tillers were spread evenly on the ground in respective plots to avoid removing biomass. Development stage V10 was selected to minimize regrowth of tillers as well as tiller effects on ear development and plant resource allocation.

Except for phenological development and tiller appearance notes, all measurements were collected at physiological maturity (R6). To avoid border effects, only the two central-plot rows were measured for data collection and buffer zones were designated on plot row ends. Main stalks and tillers with at least one collared leaf were included in observed stand counts at harvest, and row lengths were measured accounting for the interplant spacing of the nearest removed neighbor on each standing row end. Ears remaining on plants at maturity were harvested and shelled by hand, with ears from tillers and main plants combined for this study. Harvested areas were similar across sites and approximately 4-m long by 1.5-m wide. Yields were calculated based on measured harvest area and adjusted to a 155 g kg^{-1} moisture basis.

2.2.2 Statistical Analyses

A first analysis considered yield data from site-years containing all factor levels in their treatment structure (Manhattan 2019, Keats 2020, Garden City 2020, Goodland 2020, Colby A 2020, and Colby B 2020). A linear mixed effects model was fit using the *lme4* package (Bates et al., 2015) in R (R Core Team, 2022). Site-year, plant density, genotype, tiller presence, and all interactions were set as fixed effects in the model. Random effects included block, whole plot, subplot, and sub-subplot. A significance threshold for all analyses was set at $p \leq 0.05$. Residuals were checked visually for normality, homoscedasticity, and homogeneity of variance. A full description of the statistical model used is given in Equation A.1. The fitted model was subjected to a Type III analysis of variance (ANOVA) for each treatment factor using the *car* package (Fox & Weisberg, 2019). Pairwise comparisons of least-squares means were calculated using the *emmeans* R package (Lenth, 2020) by applying the Tukey method.

A second model was fit to determine the effect of observed tiller and plant densities on yield for all site-years. A linear mixed effects model was fit using the *lme4* package. Site-year, observed tiller and plant densities, and all interactions were set as fixed effects. Random effects were again block, whole plot, subplot, and sub-subplot. A full description of the statistical model used is given in Equation A.2. Residuals were checked visually for normality, homoscedasticity, and homogeneity of variance. The fitted model was subjected to a Type III ANOVA for each treatment factor using the *car* package. Predictions were generated for each site-year using fixed effect coefficient estimates from the fitted model considering plant densities ranging from 20,000 to 70,000 plants ha^{-1} and tiller densities of 0 to 80,000 tillers ha^{-1}. These ranges were selected based on the observed data used to fit the model across sites. To provide realistic tiller density

bounds for results interpretation, a quantile linear regression of 95th percentile tiller density observations was fit for each site using the *quantreg* package (Koenker, 2020).

A third analysis utilized site-years grouped by yield responsiveness to tiller density as defined by the model coefficient estimates (Equation A.2) for the effect of tiller density and the interaction of tiller density and plant density. Groups based on yield responsiveness to tiller density were assigned via the k-means clustering algorithm, and the appropriate number of clusters (three) was determined by the cumulative reduction in total within-cluster sum of squares by additional clusters. Weather variables were partitioned into three time periods and defined for thermal variables as (a) sowing to V4, (b) V4 to V7, and (c) V7 to V14 for each site-year. Soil water supply considered both precipitation and irrigation, when applicable, and extended the early season period to one month pre-sowing to account for soil moisture at planting. As shown in Figure A.1, these stages were selected based on the mean first tiller appearance stage of V5 across site-years. Tillers continued to appear in each site-year following initial appearance, and reproductive components (if present) were fully differentiated by V14. The sowing to V4 time period represents the pre-tillering interval, V4 to V7 represents the tiller appearance interval, and V7 to V14 represents the tiller development interval. In addition to measured temperature variables, the photothermal quotient (PTQ) was considered. The PTQ is defined by Fischer (1985) as the mean daily solar radiation for a selected time period, divided by the difference between the mean temperature for that period and the crop base temperature (10 °C for corn), with final units MJ m^{-2} $°C^{-1}$ d^{-1}. Lastly, a principal component analysis (PCA) was conducted considering available environmental parameters for selected season intervals with the *FactoMineR* package in R (Lê et al., 2008). Dimensions with eigenvalues > 1 were considered,

and variables with the greatest contribution to total variation captured by each dimension were identified. All plots were generated using the R software.

2.3 Results

2.3.1 Yield relation to treatment factors

The factors target plant density (M), genotype (G), site-year (E), E × M, and tiller presence (P) × E were significant in explaining variability in yield (Table 2.2). On average, yields of 7.7, 9.3, and 10.5 Mg ha^{-1} resulted for plant densities of 25,000, 42,000, and 60,000 plants ha^{-1}, respectively (Figure 2.2a). Although the effect of genotype is statistically significant, the effect size is negligible (Figure 2.2b), with means of 9.2 Mg ha^{-1} for both P0657AM and P0805AM. Estimated mean yields by site-year could be clustered in four groups (Figure 2.2c). For the first group, site-years Goodland 2020 and Garden City 2020 produced the greatest yields with respective means of 12.0 and 11.6 Mg ha^{-1}. In the second group, Keats 2020 was significantly lower yielding, with a mean value of 10.4 Mg ha^{-1}. Third, Colby A 2020 was significantly less, with a mean yield of 9.5 Mg ha^{-1}. Finally, Colby B 2020 and Manhattan 2019 yielded the least, both producing an average of 5.8 Mg ha^{-1}.

Mean yields by interaction of factors site-year and plant density were either unaffected or positively influenced by increasing target plant density levels (Figure 2.2d). At site-year Colby A 2020, mean yields of two greatest densities were significantly greater than the lowest density, with mean yields of 8.0, 9.7, and 10.6 Mg ha^{-1} for 25,000, 42,000, and 60,000 plants ha^{-1}, respectively. Yield did not respond to plant density at Colby B 2020, with an average yield of 5.8 Mg ha^{-1}. Garden City 2020 mean yields for the two lower plant densities (average 10.8 Mg ha^{-1}) were significantly less than the highest target density which yielded 13.2 Mg ha^{-1}. Goodland

2020 produced significantly less (9.7 Mg ha^{-1}) in the 25,000 plants ha^{-1} target density than in the two higher densities (averaging 12.5 and 13.9 Mg ha^{-1}). Yields significantly differed for each of the target plant densities at Keats 2020, with yield gains of 3.0 Mg ha^{-1} and 4.9 Mg ha^{-1} for the highest densities relative to the lowest (7.8 Mg ha^{-1}). Mean yields of the highest and lowest target plant densities in Manhattan 2019 were statistically different from each other, with values of 6.8 and 5.0 Mg ha^{-1}, respectively.

Mean yields by interaction of factors site-year and tiller presence were either unaffected or positively affected by the presence of tillers (Figure 2.2e). For site-years Colby A 2020, Colby B 2020, Keats 2020, and Manhattan 2019, tiller removal had no effect on yield. However, yields were reduced 11% (12.2 to 10.9 Mg ha^{-1}) and 13% (12.9 to 11.2 Mg ha^{-1}) at Garden City 2020 and Goodland 2020, respectively, when tillers were removed.

2.3.2 Yield relation to shoot number

All tested factors (i.e., E, observed plant density [D] × E, observed tiller density [T] × E, and D × T × E) were deemed significant (Table 2.3). Model predictions related yield to the observed ranges of tiller and plant densities. Lateral color gradients depict yield response to plant density, vertical color gradients represent yield response to tiller density, and curvature in these contour lines indicates the strength of the interaction term (Figure 2.3).

Site-years Manhattan 2019 (Figure 2.3a), Garden City 2019 (Figure 2.3c), and Colby B 2020 (Figure 2.3f) had visually similar yield responses with minimal effect of tillers on yield at low plant densities. At Manhattan 2019 and Garden City 2019, greatest yields were achieved at high plant densities with minimal tillering, whereas Colby B 2020 yields were mostly independent of plant density and only slightly influenced by tillers in plant densities greater than 30,000 plants ha^{-1}. At Goodland 2019 (Figure 2.3b), Greensburg 2020 (Figure 2.3h), and Keats

2020 (Figure 2.3j), yield responses were similar, being predominantly horizontal and driven by increasing plant densities. Buhler 2020 (Figure 2.3d), Colby A 2020 (Figure 2.3e), Goodland 2020 (Figure 2.3g), and Garden City 2020 (Figure 2.3i) produced similar yield responses to plant density, with strong yield contour curvature primarily centered at low plant densities, but with additional weak centers at high plant densities. At low plant densities, yield gradients were strongly vertical, indicating rapid yield increases with additional tillers. The curvature of yield contours began to flatten and invert across sites as plant density increased, indicating reduced tiller contribution. Considering probable tiller densities (95th percentile tiller density observations for all site-years), the greatest yield was observed in high plant densities with minimal tiller densities in 90% of cases (Figure 2.3). Site-years with yields unaffected by tillers at low plant densities averaged a maximum yield of 8.7 Mg ha^{-1}, and those strongly influenced by tillers at low plant densities averaged 10.2 Mg ha^{-1}.

2.3.3 Environmental influence

The site-year × environment clusters based on model coefficients were as follows: highly tiller responsive – Buhler 2020, Colby A 2020, Garden City 2020, and Goodland 2020; moderately tiller responsive – Garden City 2019, Goodland 2019, and Manhattan 2019; and neutrally tiller responsive – Colby B 2020, Greensburg 2020, and Keats 2020.

Variable vector directions indicate significant positive correlations among soil attributes such as soil organic matter (OM), soil clay, soil cation exchange capacity (CEC), and soil silt. The PTQs for all time points (sowing–V4, V4–V7, V7–V14) were also positively correlated with each other, as are early season water supplies and mid to late vegetative mean minimum temperatures. Negatively correlated variables include soil attributes and soil sand in addition to

soil water supply, as well as PTQ for all season intervals and respective mean minimum temperatures (Figure 2.4a).

In the first dimension of the PCA, 36% of variation was captured, with 4.7% explained by soil clay; 4.3% by soil CEC, soil OM, and soil sand; and 4.0% by soil silt (Figure 4b). In the second dimension, 25% of the variation was captured, with 4.0% explained by both the PTQ of the V7–V14 interval and mean minimum temperature of the V7–V14 interval; 3.75% explained by both the sowing–V4 and V4–V7 interval PTQs; and 3.0% by the mean minimum temperature of the V4–V7 interval. The PTQ variables hold negative *y*-values and named temperature variables hold positive y-values (Figure 4a). The remaining three significant dimensions account for 16% (majorly soil pH and maximum temperatures), 9% (majorly V7–V14 water supply), and 5% (majorly soil phosphorus and V4–V7 water supply) of environment variation (Figure 4b). In summary, the primary sources of environmental variation are soil clay, soil CEC, soil OM, soil sand, and soil silt. Secondary sources of variation are PTQ for all intervals in addition to V7–V14 and V4–V7 interval mean minimum temperatures.

2.4 Discussion

This study quantified effects of genotype (G) × site-year (E) × target plant density (M) and interactions on corn yield effects due to tiller expression, one of few known studies to do so in the last three decades. With eight unique geographical locations in a diverse set of 10 site-years, the dataset used encompasses a greater array of environments (and G × M factors) when considering available scientific literature, particularly regarding the inclusion of cropland areas where drought is a major determinant of yield. Low plant density is an agronomic management practice implemented to tailor resource supply to demand while managing risk associated with

unpredictable growing conditions (Rodriguez et al., 2016; Rotili et al., 2019). Under low plant populations, corn tillers may undermine the goal of matching resource supply to demand, and thus reduce yield (Dungan, 1931; Earley et al., 1971; Lyon, 1905). Dissecting the overall effect of corn tillers under varying G × E × M scenarios is an area of active research (Maddonni et al., 2021; Rotili et al., 2021a). Tiller appearance and development mechanisms were not detailed in the current study, which limits current scope to yield consequences without exploring potential trait expression determinants. This study identified associations between repeatable environmental factors and tiller expression yield effects, providing information to both define adaptive agronomic management practices and guide future studies to understand the physiological determinants of yield. The variable contribution of tillers to yield conditioned to growth environment suggests investigations on within and between plant competition for resources and remobilization potentials and patterns.

Geographical and environmental variation across sites within a moisture regime gradient facilitated collection of an informative dataset to understand management and environmental determinants of tiller expression yield effects. While the two modern corn hybrids studied performed similarly, studies incorporating larger genetic variation in tiller expression could reveal contrasting yield responses to tillers. Sangoi et al. (2009) reported significant differences in tiller-derived grain yield between corn genotypes. Notably in this study however, total yields were not different between these genotypes, as greater tiller yields accompanied reduced main stem yields and vice versa. Consistent with analyses of large datasets of yield response to plant density, increasing plant density was key for yield gain across environments with the exception of lower-yielding sites (Assefa et al., 2016; Prior & Russell, 1975). Similar to our findings in drought-prone environments, Downey (1972) reported no yield gain considering tiller presence

across a range of plant densities (42,000 to 76,300 plants ha^{-1}). From an applied research standpoint, corn tillers had no adverse effects on yields, regardless of all factors evaluated. This agrees with data presented by Earley et al. (1971) and Sangoi, Schmitt, Vieira et al. (2012), who identified tillers as irrelevant to yield outcomes. Similarly, Sangoi et al. (2009) found tiller presence increased yields by 12% (1.1 Mg ha^{-1}) across genotypes and plant densities (40,000 and 70,000 plants ha^{-1}). The interactions plant density × tiller presence and hybrid × tiller presence were not identified as significant in this study, but have been previously reported (Akman, 2002; Sangoi et al., 2009).

Contrary to expectation, tiller density did not affect yields at low plant densities in all environments, even when yields could be increased by adding more plants per hectare. However, this finding supports the proposal that tillers may reduce efficiency in certain scenarios by requiring additional biomass to produce similar or lower amounts of grain (Rotili et al., 2021a; Thapa et al., 2018). This relationship could also be explained by secondary ear expression which has been previously included in corn plasticity and plant density discussions (Mylonas et al., 2020; Tokatlidis et al., 2005). Yields in some environments benefited from tillers at low plant densities but increasing plant density was still most effective in maximizing yield. Hansey and de Leon (2011) reported positive correlations between yield and tillers $plant^{-1}$ at 20,000 plants ha^{-1}, with an inverted relationship at 70,000 plants ha^{-1}. With expected tiller number per plant decreasing as plant number increases (Rotili et al., 2021b; Tetio-Kagho & Gardner, 1988), yield gain is simultaneously more connected to increased plant density. Regardless of environment, yields were maximized by fine-tuning plant density which surpassed tiller compensation capabilities. However, this identification of yield response to tillers in certain scenarios is important, particularly for producer replanting decisions in event of poor emergence or damaged

stands (e.g., early season hail damage). These decisions could be influenced by expected behavior of corn tillers and their ability to compensate a significant portion of yield lost with missing or damaged plants. This potential was previously identified by Sangoi, Schmitt, Silva et al. (2012) as a successful plant mitigation strategy to overcome defoliation in mid-to-late vegetative stages and by Carter (1995) as a compensation mechanism to recover a portion of yield lost due to late frost damage.

Plant density is the significant driver of yield gain, but our results identify a strong influence of environment on tiller contribution to yield. Corn grown in sites with favorable soil properties, for example high organic matter and textures high in clay and silt, higher PTQ values, and lower minimum temperatures in the V7–V14 vegetative stages responded most positively to tillers. Soil properties are key to yield potential in the evaluated region (Lobell & Azzari, 2017), and plant nutrition is key to tiller appearance and survival as demonstrated by Sangoi et al. (2011). The PTQ relationship in corn tillers is novel, and consistent with reports on the link to tiller appearance, tiller number, and productivity in other grasses such as wheat and grain sorghum (Fischer, 1985; Kim et al., 2010; Kumar et al., 2016). A greater PTQ results in a larger potential photosynthate source for the plant at a given timepoint (Nix, 1976). Additional carbohydrates can determine tiller productivity, resulting in tillers able to support themselves and also potentially translocate surplus to the main stem (Alofe & Schrader, 1975; Rotili et al., 2021b). Although water status was not identified as a key environmental classifier, inclusion of more severe water deficit conditions could alter this outcome. Via crop simulation modeling, Rotili et al. (2021a) identified a depressive effect of tiller presence on kernel number m^{-2} at 50% frequency in the driest planting conditions for two probable restrictive moisture environments (approximate yield of 3 to 3.5 Mg ha^{-1} considering a standard of 200 mg $kernel^{-1}$), but positive

effects on kernel number m^{-2} at a 50% frequency even in dry planting conditions for four other less restrictive sites (approximate yield of 4 to 5 Mg ha^{-1} at 200 mg $kernel^{-1}$). The most restrictive environment results were confirmed by a field experiment conducted by Rotili et al. (2021b) at yield levels of 3.3 to 4.3 Mg ha^{-1}, with plant densities of 20,000 and 40,000 plants ha^{-1}. These levels are below the current study's average yield of 9.2 Mg ha^{-1} (ranging from 5.8 to 12.0 Mg ha^{-1}), indicating a discrepancy in the restrictiveness of environments considered. In addition, while Rotili et al. (2021a) considered moisture at planting in presented simulations, the present study considered multiple time periods for sites with varied levels of apparent crop water budgets (including some sites with similar patterns across development stage periods), as indicated in Figure 2.4 and Table A.2. However, sites similar in water budgets performed very differently with regard to yield responsiveness to tiller presence, supporting the finding that water is not a key environmental factor influencing yield responses to tiller presence in less restrictive conditions (when water supply is not a limiting factor). Additional field studies considering more restrictive conditions and various moisture regimes within sites are necessary to fully understand moisture effects on tillering and yield relationships in corn.

Perhaps the most unexpected result was the close association of environments in which yields were most and least influenced by tillers. While sites with yields unresponsive to tillers presented somewhat more favorable soil properties, a trending lower PTQ was also observed. With adequate nutrition, tillers were present, but plants likely produced less photosynthates per tiller and development stage than in sites with a greater PTQ. Assimilate content of the main stem in early vegetative periods has been linked to sorghum tiller grain production given adequate soil fertility and moisture (Lafarge & Hammer, 2002). As with grain sorghum, corn stalks act as storage organs for accumulated carbohydrates until grain filling begins, when

assimilates are translocated from stalk to kernels (Hume & Campbell, 1972; Setter & Meller, 1984). If tillers are able to contribute to carbohydrate reserves in the main stem, these resources are preferentially allocated to grain formed by the main stalk rather than for tiller ears and grain (Alofe & Schrader, 1975). In addition to soil properties, evaluating resource translocation and water-soluble carbohydrate dynamics among corn tillers and main stem has potential to improve our understanding of yield responsiveness to tiller density across environments (Rotili et al., 2021b). This nourishing relationship has been previously documented by Dungan (1931) and specifically identified for phosphorus (P) via relocation from nonreproductive tillers to main stalks by Russelle et al. (1984).

Production risks are typically the most important factor influencing long-term operation success for farmers worldwide (Komarek et al., 2020). According to Mase et al. (2017), 64% of U.S. Midwestern corn producers implement in-field management strategies as their preferred method of adapting to climate-based risk. Most farmers attribute this response to personal perception and experiences with precipitation and temperature variability and trends (Mase et al., 2017). Favorable growing conditions can be exploited by plasticity traits such as tillering in unpredictable environments where optimum plant densities can vary widely, limiting yield loss due to suboptimal densities in favorable seasons while concurrently reducing seed inputs. This can reduce risks associated with lost opportunities in the most productive seasons as a feature of implementing defensive management strategies (Rotili et al., 2021a). With climate change projections indicating more frequent erratic weather events and concerns mounting regarding irrigation resources (Mrad et al., 2020), in-field mitigation options to balance economic and environmental challenges of crop production are of great value (Steiner et al., 2018).

2.5 Conclusions

Regardless of environment or plant density for tested genotypes, tillers had no significant deleterious effects on corn yields. However, environment did play a key role in determining the magnitude of yield response to tillers relative to an increase in plant density. Tillers demonstrated potential to mitigate yield lost due to plant density decreases, but this relationship was only observed in select scenarios. Yield responsiveness to tillers was most influenced by soil properties and favorable PTQ, confirming the importance of source–sink relationships for understanding tiller contribution to corn yields. In all site-years, a fine-tuning of plant density was necessary to maximize yields.

With defensive management strategies becoming increasingly necessary for producers in vulnerable cropping areas affected by climate anomalies, risk-mitigating options are important. Tiller expression in corn may be less reliable than increasing plant density or secondary ear expression to realize yield potential in ideal conditions, but this study presents important evidence on its potential usefulness as a mitigating plasticity trait in unpredictable environments.

Table 2.1 Site-year field experiment coordinates, sowing date, 10th-leaf date (V10); irrigation management; apparent season water budgets; previous crop; and soil pH, organic matter (OM; loss on ignition, LOI), nitrate concentration (NO_3–N), ammonium concentration (NH_4–N), phosphorus (P; via Mehlich III), cation exchange capacity (CEC), and texture. Detailed water budget values are presented in Supplemental Table A.2.

Site-year	Latitude	Longitude	Sowing Date	V10 Date	Irrigation	Apparent Season Water Budget	Previous Crop
	°N	°W				mm	
Manhattan 2019	39.14	96.64	14 May	1 Jul	None	917-411	Corn
Garden City 2019	37.83	100.86	4 May	28 Jun	Subsurface limited	363-549	Corn
Goodland 2019	39.25	101.78	14 May	8 Jul	Subsurface limited	511-605	Soybean
Keats 2020	39.23	96.72	2 May	24 Jun	None	516-466	Soybean
Buhler 2020	38.14	97.73	29 Apr	20 Jun	Subsurface limited	489-562	Soybean
Greensburg 2020	37.58	99.37	5 May	24 Jun	Subsurface limited	478-594	Corn
Garden City 2020	37.83	100.86	18 May	30 Jun	Subsurface limited	501-637	Corn
Goodland 2020	39.25	101.78	7 May	1 Jul	Subsurface limited	398-728	Soybean
Colby A 2020	39.39	101.06	7 May	3 Jul	None	289-669	Wheat
Colby B 2020	39.38	101.06	15 May	3 Jul	None	307-652	Grain sorghum
Site-year	**pH**	**OM**	**NO_3-N**	**NH_4-N**	**P**	**CEC**	**Texture**
		% LOI	mg kg^{-1}	mg kg^{-1}	mg kg^{-1}	meq $100g^{-1}$	
Manhattan 2019	6.3	1.0	1.8	1.3	37.5	5.9	Sandy loam
Garden City 2019	6.6	1.0	2.0	na	42.0	15.8	Sandy loam
Goodland 2019	6.5	2.7	26.8	2.1	52.1	18.2	Silt loam

Keats 2020	7.0	4.5	18.0	4.1	118.0	24.4	Silty clay loam
Buhler 2020	6.4	2.9	17.9	4.8	24.0	23.1	Silty clay loam
Greensburg 2020	5.4	2.6	37.1	13.6	84.9	18.9	Clay loam
Garden City 2020	5.2	1.6	18.4	10.7	55.0	10.6	Sandy loam
Goodland 2020	5.8	3.8	36.9	17.9	106.0	24.0	Silt loam
Colby A 2020	5.4	3.3	19.9	4.3	70.0	21.2	Silt loam
Colby B 2020	6.5	3.2	43.5	36.4	31.0	24.0	Silt loam

Apparent season water budget (ASWB) was calculated as follows: observed water supply (irrigation + precipitation from one month prior to planting through physiological maturity) − apparent crop water demand for the season (crop evapotranspiration, ETc; Allen et al., 1998). The ETc was calculated as the product of grass reference evapotranspiration ETr) and corn crop coefficient (Kc; weighted averages of development stage-specific coefficients provided by the University of Nebraska-Lincoln; (http://nawmn.unl.edu/GrowthStageData). When evaluating the apparent water budget, it is key to note that plant-available soil water at planting (measured in the evaluated region by Lamm et al., 2017, averaging 271 mm in a 2.4-m soil profile depth for the 2011–2012 period for fields with similar cropping history) and soil water-holding capacity are not included in this estimation.

Table 2.2 Analysis of variance results for yield as dependent on experiment treatment factors target plant density, genotype, tiller presence, site-year, and interactions. Tested source of variation (Source), degrees of freedom, degrees of freedom of residuals, F value, and the associated *p* value are presented. Significance levels according to *p* values are denoted in the far-right column, and all sources with *p* values ≤ 0.05 are shown in boldface font. Coefficient of determination values for model fit are presented below.

Source	***df***	**Residual *df***	**F value**	***p* value**
Target Density (M)	**2**	**175.77**	**3.38**	*
Genotype (G)	**1**	**164.61**	**5.42**	*
Tiller Presence (P)	1	163.17	0	ns
Site-Year (E)	**5**	**165.45**	**5.1**	***
G × M	2	164.61	2.16	ns
M × P	2	163.17	0.02	ns
G × P	1	163.17	0.21	ns
E × M	**10**	**165.52**	**3.26**	***
G × E	5	165.31	1.04	ns
E × P	**5**	**163.17**	**4.58**	***
G × M × P	2	163.17	0.04	ns
G × E × M	10	165.26	0.65	ns
E × M × P	10	163.17	1.82	ns
G × E × P	5	163.17	0.35	ns
G × E × M × P	10	163.17	0.44	ns

Marginal $R^2 = 0.88$; Conditional $R^2 = 0.88$; * Significant at the 0.05 probability level; *** Significant at the 0.001 probability level; ns, not significant

Table 2.3 Analysis of variance results for yield and specified interactions of observed predictor variables site-year, observed plant density, and observed tiller density. Tested source of variation (Source), degrees of freedom, degrees of freedom of residuals, F value, and the associated p value are presented. Significance levels according to p values are denoted in the far-right column, and all sources with *p* values ≤ 0.05 are shown in boldface font. Coefficient of determination values for model fit are presented below.

Source	***df***	**Residual *df***	**F value**	***p* value**
Site-year (E)	**10**	**227.95**	**25.79**	*******
Plant density (D) × E	**10**	**207.4**	**35.46**	*******
Tiller density (T) × E	**10**	**284.57**	**10.11**	*******
E × D × T	**10**	**285.02**	**6.43**	*******

Marginal $R^2 = 0.87$; Conditional $R^2 = 0.87$; *** Significant at the 0.001 probability level

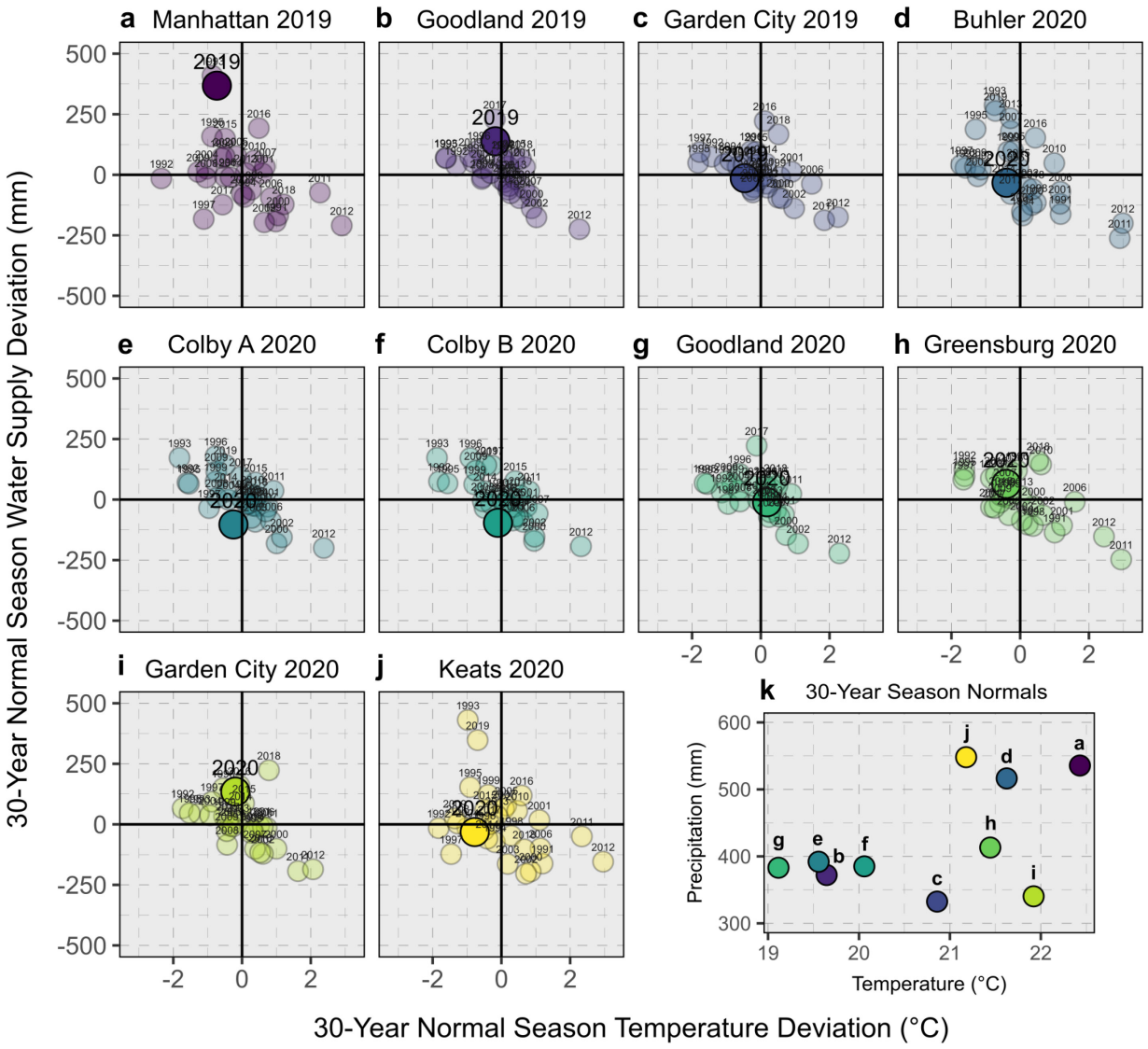

Figure 2.1 Annual season normal precipitation and temperature deviation for 1991–2020 in site-years Manhattan 2019 (a), Goodland 2019 (b), Garden City 2019 (c), Buhler 2020 (d), Colby A 2020 (e), Colby B 2020 (f), Goodland 2020 (g), Greensburg 2020 (h), Garden City 2020 (i), and Keats 2020 (j); and season normal precipitation and temperature characterization by site-year (k). Bold vertical lines indicate normal average temperature for site-year season date ranges, whereas bold horizontal lines indicate normal precipitation accumulation for site-year season date ranges. Year of study for each site-year (a–j) is indicated with a large, opaque point and enlarged text, and considers both precipitation and irrigation in the water supply value (y-axis). All other years in (a–j) are shown with transparent points and smaller text, and water supply (y-axis) includes only precipitation. Base period for all climate normal calculations was 1991—2020.

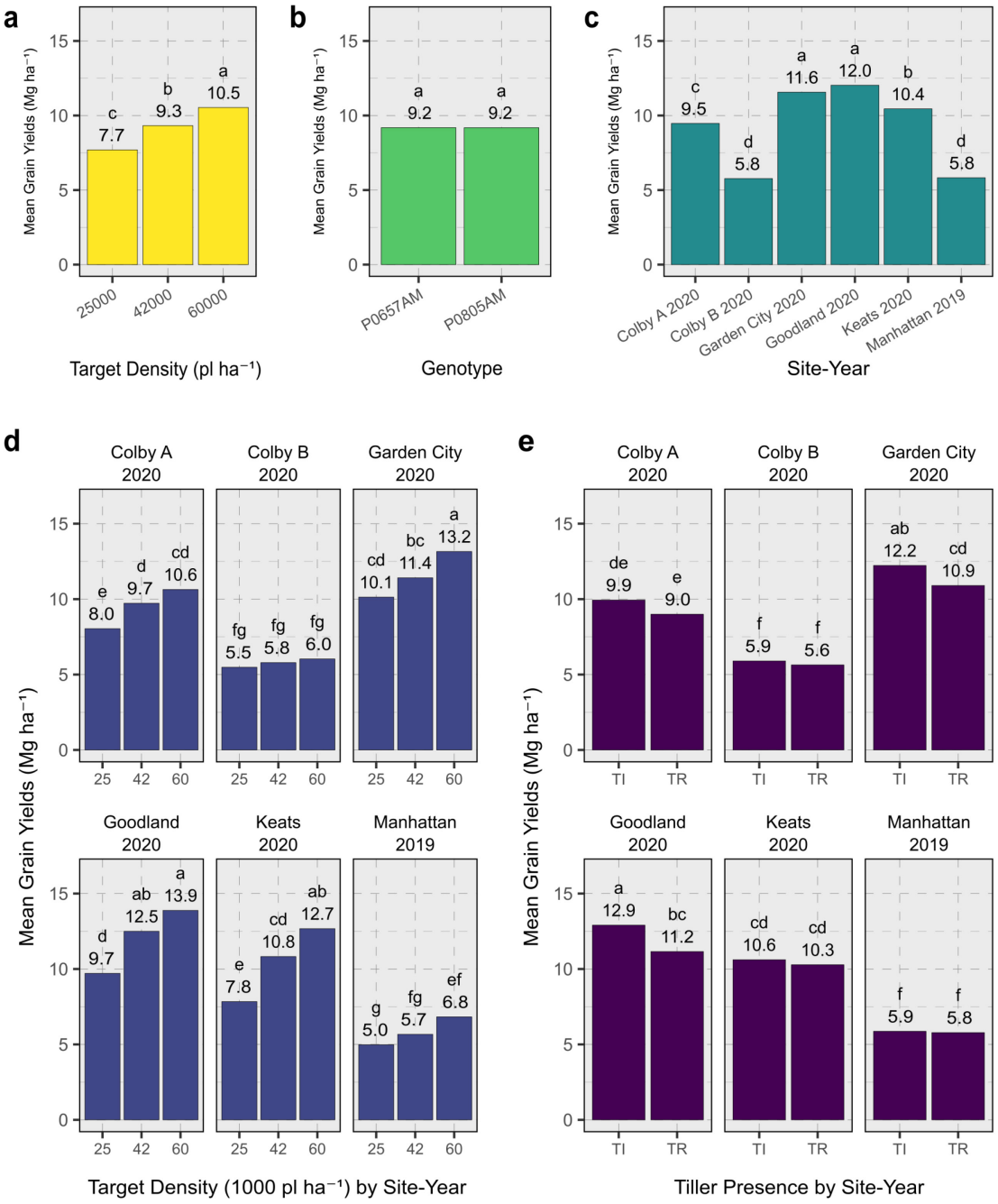

Figure 2.2 Mean yields and pairwise comparisons of each level within factors target plant density (a), genotype (b), site-year (c), target plant density × site-year (d), and tiller presence × site-year (e) as deemed significant by designed experiment analysis of variance results shown in Table 2.1. Means within a panel not sharing a common letter are significantly different at the .05 probability level according to the Tukey method. Tiller presence levels in (e) are denoted by TI (tillers intact) and TR (tillers removed).

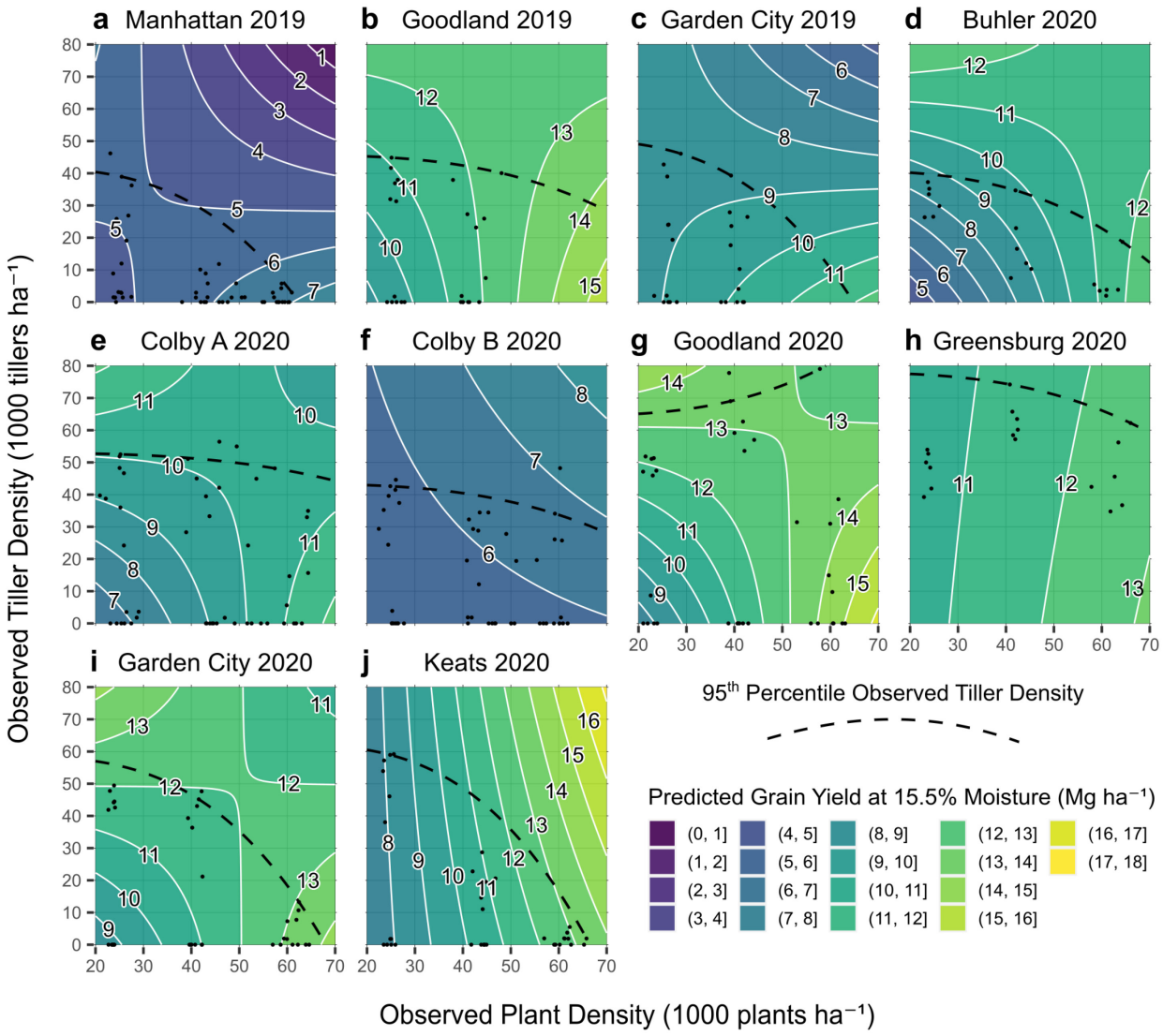

Figure 2.3 Contour plot of predicted grain yields produced by the model described in Equation A.2 for site-years Manhattan 2019 (a), Goodland 2019 (b), Garden City 2019 (c), Buhler 2020 (d), Colby A 2020 (e), Colby B 2020 (f), Goodland 2020 (g), Greensburg 2020 (h), Garden City 2020 (i), and Keats 2020 (j). Contours are shaded and labeled according to 1 Mg ha^{-1} yield intervals. White lines indicate a change in yield interval. Observed plant densities and tiller densities are indicated with black points, and regression lines considering the upper 95% of observed tiller densities are shown with the black dashed line; this line is intended as an indicator of site-year tillering potentials, and extrapolations beyond black points and the dashed black line are shown only for the purpose of comparing site-years on the same density scales.

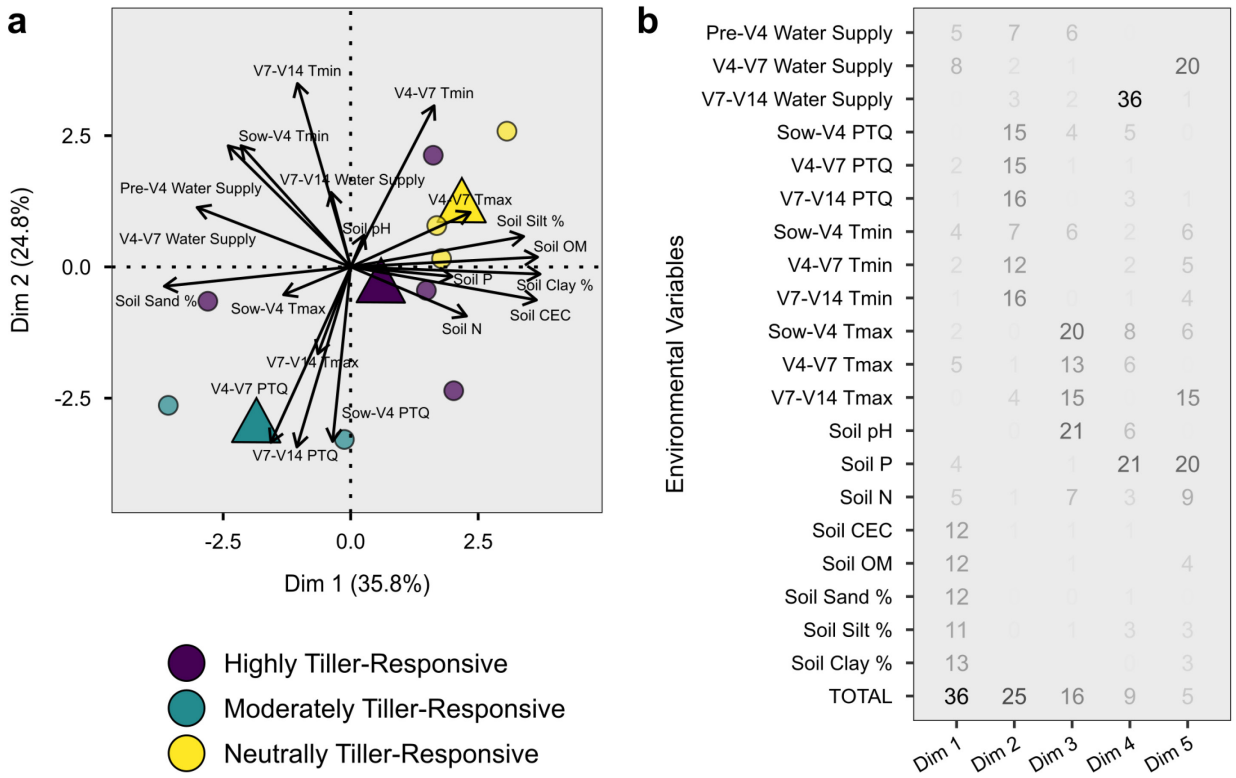

Figure 2.4 Principal component analysis biplot (a) and corresponding variance description summary by dimension and for environmental variables within dimension (b). Biplot (a) points are colored by response cluster, with small circles representing individual sites within each cluster and large triangles indicating cluster centroids. Each black arrow corresponds to the labeled environmental variable, with pointed direction indicating positive correlation and greater length indicating parallelism to the shown two-dimensional plane. Variance values (b) are expressed as percentages, with dimension totals shown at the base ("TOTAL") and individual variables within dimension depicted above. Text opacity indicates the percentage of variance described, with darker values representing greater variance percentages, both for dimension totals and for variables within each dimension. The x-axis variables "Dim 1″ and "Dim 2″ of (b) correspond to the x- and y-axes of (a), respectively.

Chapter 3 - Tillering enhances corn reproductive plasticity by stabilizing yield components across plant densities

**Under review in Frontiers in Plant Science, Plant Abiotic Stress– The Adaptation Strategies of Plants To Alleviate Important Environmental Stresses, Plant Abiotic Stress Special Issue*

Abstract

Crop plasticity is fundamental to sustainability discussions in production agriculture. Modern corn (*Zea mays* L.) genetics can compensate yield determinants to a small degree, but plasticity mechanisms have been masked by breeder selection and plant density management preferences. While tillers are a well-known source of plasticity in cereal crops, the functional trade-offs of tiller expression to the hierarchical yield formation process in corn are unknown. This investigation aimed to further dissect the consequences of tiller expression on corn yield component determination and plasticity in a range of environments from two plant fraction perspectives – i) main stalks only, considering potential functional trade-offs due to tiller expression; and ii) comprehensive (main stalk plus tillers). This multi-seasonal study considered a dataset of 17 site-years across Kansas, United States. Replicated field trials evaluated tiller presence (removed or intact) in two hybrids (P0657AM and P0805AM) at three target plant densities (25000, 42000, and 60000 plants ha^{-1}). Record of ears and kernels per unit area and kernel weight were collected separately for both main stalks and tillers in each plot. Ear number and kernel number per area were less dependent on plant density, but kernel number remained key to yield stability. Although ear number was less related to yield stability, ear source and type were significant yield predictors, with tiller axillary ears as stronger contributors than main stalk secondary ears in high-yielding environments. Such escape from the deterministic hierarchy of

corn yield formation may reduce corn management dependence on a seasonally variable optimum plant density.

3.1 Introduction

Corn (*Zea mays* L.) is of significant global socioeconomic importance, experiencing recent production expansion into stress-prone areas (Lark et al., 2020). In these regions of reduced yield potential, such as the Central High Plains of the United States (US), effective resource use is a key factor considered by farmers as they adapt to variable climatic conditions (Lobell et al., 2011). Phenotypic plasticity (herein termed as crop plasticity) refers to the ability of a genotype to adapt (e.g., express a specific trait) in response to the environment (Laitinen & Nikoloski, 2019). In sub-optimal or otherwise unpredictable growing conditions, exploring crop plasticity mechanisms are a suggested adaptation to maintain yields (Nicotra et al., 2010).

Capitalizing on crop plasticity potential could improve the stability of production in regions with high climatic risk (Berzsenyi & Tokatlidis, 2012; Mylonas et al., 2020). The central US corn belt, where climate is relatively stable year to year, is an important hub of modern corn improvement. In this environment, breeders selected for those plasticity mechanisms conducive to high-yielding environments. Furthermore, as growers have intensified plant density and breeders have enhanced genetic tolerance to increased plant density over time, the expression of corn plasticity may have been constrained (Assefa et al., 2018; Duvick et al., 2004; Russell, 1991).

When corn plants have access to ample resources, tillering is a mechanism of plasticity (Jenkins, 1941; Lyon, 1905). Tillers are secondary vegetative shoots common in Poacea species such as wheat (*Triticum aestivum* L.), rice (*Oryza sativa* L.), and grain sorghum (*Sorghum*

bicolor L. Moench). However, tillers are less common in corn due to historic breeding selection (Duvick et al., 2004; Major, 1977). In spite of this, tiller expression potential has been conserved in modern corn germplasm (Moulia et al., 1999), and breeding program adoption of less restrictive plant densities re-introduces tillering as a plasticity mechanism (Tsaftaris et al., 2008). Tiller expression is highly dependent on genetics (Dungan et al., 1959; Hansey & de Leon, 2011; Tokatlidis et al., 2005), but also strongly influenced by environmental factors such as water, soil fertility, and temperature (Downey, 1972; Gardner, 1942; Stevenson & Goodman, 1972; Tetio-Kagho & Gardner, 1988). Expressed corn tillers may remain vegetative, may abort, or may reach reproductive stages (Alofe & Schrader, 1975; Russelle et al., 1984) – developing into harvestable axillary ears or abnormal, mixed-sex apical inflorescences called "tassel ears" (Bonnett, 1948; Schaffner, 1930).

While previous field studies have considered corn yield as a response to tiller presence (Frank et al., 2013; Massigoge et al., 2022; Sangoi et al., 2009; Veenstra et al., 2021), efforts to understand the mechanisms and flexibility of observed compensatory relationships are lacking, at least in the US. Considering trends in corn genetic selection and agronomic management in the US, plant density is a historic focal point (Duvick et al., 2004) with highly determinate, hierarchical yield components. Yield component plasticity (namely ears and kernels per area and individual kernel weight) in the idealized, single-stalked corn phenotype is marginal relative to the yield gain of additional plants per area (Fernández et al., 2022). For example, kernel number can be adjusted through early grain-filling stages but is limited by the success of a short pollination window (R1, silking per Ritchie et al., 1997) and the number of ears on the main stalk, which is determined in vegetative stages and typically singular (Andrade et al., 1999; Bonnett, 1948). Plastic phenotypes can reduce dependency on precise plant density (Berzsenyi &

Tokatlidis, 2012; Tokatlidis & Koutroubas, 2004) – for instance, by producing more than one ear per plant (Prior & Russell, 1975; Thomison & Jordan, 1995). Tillers, a demonstrated source of plasticity, may facilitate an offset in development from the deterministic, single-stalked hierarchy. Functional trade-offs in resource allocation due to tiller expression are unknown. These relationships may improve or degrade yield stability.

Exploring the impact of tiller expression on yield component plasticity is a novel avenue to understand corn environmental adaptation potential. Although trade-offs in corn yield components are well-known (Sadras & Slafer, 2012; Slafer, 2003) and the concept of tiller-conferred plasticity has been established (Downey, 1972; Rotili et al., 2022; Rotili et al., 2021a; Yamaguchi, 1974), field-based research solidifying the connection between the two is inadequate. Understanding the degree to which tillers impact reproductive plasticity may provide insight for reducing plant density dependence and shed new light on environmental adaptation strategies, particularly as climatic risk intensifies. A range in favorable to negligible yield responses to tiller expression were reported for the first two seasons of this project (Veenstra et al., 2021). Authors hypothesized that tiller expression improved plasticity of yield components, thereby reducing plant density-based yield dependency. Key points to explore in the dissection of observed yield responses included which yield components were most stabilized by tiller expression, if plasticity relationships were adjusted among yield components, and if yield component source (i.e., coming from tillers or main stalk) impacted yield stability and determination. Therefore, the aim of this investigation was to explore the consequences of tiller expression on corn yield component determination and plasticity in a range of environments from two plant fraction perspectives – i) main stalks only, considering potential functional trade-

offs due to tiller expression; and ii) comprehensive (main stalk plus tiller contributions as an overall view of plasticity potential).

3.2 Materials and Methods

3.2.1 Field Experiments

In addition to the ten site-years described in previous work (Veenstra et al., 2021), seven new site-years were evaluated across Kansas, US, during the 2021 growing season. Added site-characterizations are provided in Table B.1 and Figure B.1.

Of the full dataset, ten site-years were implemented using a replicated three-way factorial treatment structure in a randomized complete block design (RCBD) with a split-split-plot arrangement. Plant density was the whole plot factor, with three levels selected as representative of common producer practices in Kansas (25000, 42000, and 60000 plants ha^{-1}; Roozeboom et al., 2007). Corn genotype (hybrid) was the sub-plot factor, with the two levels P0657AM and P0805AM (Corteva Agriscience, Johnston, IA, US), which were selected as suitable for the region of study and conducive to tiller. Tiller presence was the sub-sub-plot factor, with the two levels intact or removed at development stage V10 (tenth leaf per Ritchie et al., 1997). Seven site-years were implemented with a similar RCBD design but missing either partial or total levels of the aforementioned treatment structure. Plots in all site-years were planted at least four rows wide at 0.76-m spacing, resulting in final minimum dimensions of 3 m by 5 m. Plant densities were seeded at double rates and thinned by hand prior to the V3 development stage to ensure accurate and even stands. Plant health was maintained as necessary with pesticides and crop nutritional needs were met with applied fertilizers.

Actual plant density, tiller density, and yield component data were collected at physiological maturity (development stage R6). Only the two central rows in each plot were included in data collection efforts. In addition, buffer zones were established on row ends to minimize edge effects. Tillers with at least one collared leaf were included in tiller density counts. Data rows were measured by carefully accounting for interplant spacing of the nearest buffer-appointed plant on row ends. Intact ears (machine-harvestable and providing > 100 collective kernels $plot^{-1}$) were counted, picked, and shelled by hand at dry maturity (< 200 g kg^{-1} moisture). Data collected were summarized by plot but separated based on plant fraction – main stalk and tillers. Harvested areas across sites were similar in size and approximately 4 m by 1.5 m. Measured yield components included ear number per area, kernel number per area, and weight per kernel. Kernel weights were measured with a representative sample of shelled grain for each plant fraction from each plot. Two sets of 100 kernels were counted and weighed, with values averaged, and final moisture content adjusted to a 155 g kg^{-1} basis. Kernels per area were calculated based on mean kernel weights. Plot averages for yield components were calculated with weighted means of main stalk and tiller data.

3.2.2 Calculations

Yield environment has been previously linked to corn plasticity potential and tiller productivity (Rotili et al., 2021b; Veenstra et al., 2021). Therefore, yield environment clusters were identified and characterized. Site-years were clustered by mean yield using the k-means algorithm. Per the within-cluster sums of squares, the ideal number of yield clusters was visually identified as three – low, moderate, and high. Soil texture and fertility were characterized via early season soil sampling at 15-cm and 60-cm depths. Plasticity was calculated with the methods used by Dingemanse et al. (2010) previously adapted for agronomic applications

(Sadras & Rebetzke, 2013). That is, plasticity of a given response (yield, tiller number, ear number, etc.) was calculated by dividing the variance of the response in a given site-year × hybrid interaction (34 combinations) by the variance of the response considering all observations in the study.

3.2.3 Statistical Analysis

3.2.3.1 Yield component response

All analyses were conducted using program R (R Core Team, 2022). Separate analyses were conducted for each yield component (ears per area, kernels per area, and kernel weight) considering i) main stalks only and ii) comprehensive plants. Initial treatment factor analyses were performed first to discern if yield components responded to tiller presence. These initial analyses considered the ten site years with complete treatment structures. Ears per area, kernels per area, and kernel weight were each considered as a response to treatment factors plant density, genotype, and tiller presence for main stalks (ears and kernels harvested from main stalks only) and comprehensive plants (all ears and kernels harvested). Linear mixed effects models (Equation B.1) were fit to each yield component using the *lme4* package (Bates et al., 2015). All treatment factors and interactions were set as fixed effects. Random effects considered site-year, block, whole plot, and sub-plot. As only 10 of the 17 site years were implemented with a full split-split-plot structure and useful for initial analyses, study-wide yield environment cluster was not included in these models. The fitted models were subjected to a type III analysis of variance (ANOVA) for each treatment factor and resulting interactions with the *car* package (Fox & Weisberg, 2019).

Following analyses considered ears per area, kernels per area, and kernel weight as the response to observed plant density and observed tiller density for main stalks and comprehensive

plants by yield environment, as all 17 sites were included. Linear mixed effects models were fit (Equation B.2). Fixed effects included observed plant density, observed tiller density, yield environment cluster, and all two- and three-way interactions. Random effects considered site-year, block, whole plot, and sub-plot. The fitted models were subjected to a type III ANOVA for each factor and resulting interactions. Ears per area, kernels per area, and kernel weight predictions were generated using the significant fixed effect coefficient estimates from each of the fitted models. Predictive limits were identified based on observed ranges (20000 to 65000 plants ha^{-1} and 0 to 80000 tillers ha^{-1}) and standardized across all environments. To maintain realistic perspective of tiller expression limits within each environment (i.e., not all environments produced similar tiller density trends), a third order polynomial regression was conducted with the 95th percentile of tiller densities for each target plant density in each yield environment. This provides plausible maximum observed tiller densities for prediction interpretation purposes. Error was quantified with the root mean squared error (RMSE).

3.2.3.2 Yield component – yield plasticity relationships

To test correlation of yield plasticity with trait/yield component plasticity, simple linear models ($y = mx + b$) were fit using the *lm* function of the base *stats* package. Tiller number, ear number, and kernel number traits were evaluated by yield environment, as informed by previously mentioned analyses. Only plots without tiller disturbance were considered for this portion of the analysis. Appropriate models were selected separately for each yield environment with a slope parameter threshold of $p \leq 0.05$.

3.2.3.3 Yield response to ear type

To evaluate the relative importance of ear type (as a subset of yield component ear number) to maximizing yields, a linear mixed effects model was fit with grain yield (Mg ha^{-1}) as

the response variable. Fixed effects included observed main stalk primary ears ha^{-1}, observed main stalk secondary ears ha^{-1}, observed tiller axillary ears ha^{-1}, and observed tiller apical ears ("tassel ears") ha^{-1} by yield environment. Random effects considered site-year, block, whole plot, and sub-plot. The fitted model was subjected to a type II ANOVA for each ear type × environment combination. Error was quantified via the RMSE. Resulting yield predictions were generated using the significant fixed effect coefficient estimates. Predictive limits were identified based on observed ranges of ear types for each yield environment (primary, 16000 to 65000 ears ha^{-1}; secondary, 0 to 43000 ears ha^{-1}; tiller axillary, 0 to 43000 ears ha^{-1}; and tiller apical, 0 to 31000 ears ha^{-1}). The 95% confidence intervals were generated for each coefficient to check for similarities and overlaps.

3.3 Results

3.3.1 Yield environments

The three yield environment clusters for all evaluated site-years were as follows: a) Lowest-yielding environments (LYEs) – Manhattan 2019, Colby B 2020, Colby A 2021 (mean 5.6 Mg ha^{-1}); b) Moderate-yielding environments (MYEs) – Garden City 2019 and 2021, Buhler 2020 and 2021, Colby A 2020, Greensburg 2021 (mean 9.2 Mg ha^{-1}); and c) Highest-yielding environments (HYEs) – Goodland 2019 through 2021, Garden City 2020, Greensburg 2020, Keats 2020 and 2021, Selkirk 2021 (mean 11.4 Mg ha^{-1}). Grain yields across environments by treatment factors are shown in Figure 3.1a.

3.3.2 Ears per area

The ANOVA results for models considering ears per area (ears ha^{-1}) as a response are shown in Figure 3.1b and Table B.1. Both ears ha^{-1} responses (main stalks and comprehensive

plants) were influenced by treatment factors plant density, tiller presence, and their interaction (all significant at $p \leq 0.001$). Additionally, both ears ha^{-1} responses were impacted by quantitative factors observed plant density and yield environment ($p \leq 0.001$), observed tiller density ($p \leq 0.001$, main; $p \leq 0.01$, comprehensive), and the interaction between yield environment and observed plant density ($p \leq 0.01$).

Observation-based predictions for ears ha^{-1} are shown in Figure 3.2. Increased tiller densities reduced main stalk ears ha^{-1} in all yield environments, although less sharply at higher plant densities (Fig. 3.1a). Plant density accounted for 50% of the predicted range in main stalk ears ha-1. Comprehensive ears ha^{-1} were more stable than main stalk alone regardless of tiller or plant densities (Fig. 3.1b). Higher tiller densities reduced the plant density-based deficit in comprehensive ears ha^{-1}. Greatest comprehensive ears ha^{-1} was predicted at both i) high observed plant densities with low observed tiller densities (all environments) and ii) low observed plant densities with high observed tiller densities (MYEs and HYEs).

3.3.3 Kernels per area

The ANOVA results for models considering kernels per area (kernels m^{-2}) as a response are shown in Figure 3.1c and Table B.2. Main stalk kernels m^{-2} were influenced by treatment factors plant density and tiller presence ($p \leq 0.001$), and their interaction ($p \leq 0.05$). Comprehensive kernels m^{-2} were only impacted by plant density ($p \leq 0.001$). Main stalk kernels m^{-2} were influenced by quantitative variables tiller density, yield environment, and the interaction between yield environment and observed plant density (all significant at $p \leq 0.001$). Comprehensive kernels m^{-2} were impacted by yield environment and the interaction between yield environment and observed plant density ($p \leq 0.001$), in addition to the interaction between yield environment and observed tiller density ($p \leq 0.05$).

Considering observation-based predictions, increased tiller densities consistently reduced main stalk kernels m^{-2}, regardless of plant density (Fig. 3.3a). Plant density accounted for up to 75% of the range in predicted main stalk kernels m^{-2} when tillers were not present (Fig. 3.3a). Comprehensive kernels m^{-2} were either not impacted by observed plant or tiller densities (LYEs) or independently influenced by both observed plant and tiller densities (MYEs and HYEs; Fig. 3.3b). Greatest kernels per area were predicted at high observed plant densities with high observed tiller densities.

3.3.4 Kernel weights

The ANOVA results for models considering kernel weight (mg $kernel^{-1}$) as a response are shown in Figure 3.1d and Table B.3. Main stalk kernel weight was influenced by treatment factors plant density ($p \leq 0.001$), in addition to genotype and the interaction between plant density and tiller presence ($p \leq 0.05$). Comprehensive kernel weights were impacted by treatment factors plant density ($p \leq 0.001$) and genotype ($p \leq 0.05$). All kernel weight responses were influenced by quantitative factors observed plant density ($p \leq 0.05$) and yield environment ($p \leq 0.001$); predicted trends were similar between the two. Increased plant densities reduced both main stalk and comprehensive kernel weights in all environments, with a 25 to 50 mg $kernel^{-1}$ discrepancy across observed plant densities. Trends were not impacted by tiller density and predictions are therefore not shown.

3.3.5 Trait-yield plasticity relationships

Tillered phenotype trait plasticity correlations with yield plasticity varied by yield environment (Figure 3.4). Tiller number plasticity (i.e., the situational nature of tiller expression in a given environment) reduced yield plasticity in LYEs and MYEs, ultimately acting to stabilize yields (Fig. 3.4a). Greater plasticity of tiller number was associated with greater

plasticity of yield in HYEs, however. Ear number plasticity reduced yield plasticity in HYEs, increased yield plasticity in MYEs, and had no impact on yield plasticity in LYEs (Fig. 3.4b). Kernel number plasticity exhibited the strongest relationship to yield plasticity across environments, with greater plasticity of kernel number increasing yield plasticity (Fig. 3.4c). That is, stable kernel numbers were the yield component most correlated with stable yield values in a given environment.

3.3.6 Ear type relationship to attainable yields

The ANOVA results for yield response to varying ear sources by yield environment are presented in Table B.4. The only ear source not significantly contributing ($p > 0.05$) to yield determination was tiller apical ears. This coefficient estimate was therefore not included in subsequent predictions.

Yield predictions based on various combinations of ear types by yield environment are shown in Figure 3.5. In these ternary plots, each axis depicts the % of attainable ears ha^{-1}. The 95% confidence intervals for coefficient estimates are presented as insets. In LYEs (Fig. 3.5a), predicted yields were greatest with 17 to 67% of attainable primary ears (11050 to 43550 ears ha^{-1}), 0 to 50% of attainable secondary ears (0 to 20500 ears ha^{-1}), and 0 to 50% of attainable tiller axillary ears (0 to 21500 ears ha^{-1}). Confidence intervals overlapped for all ear types in LYEs, indicating one ear type was not more effective in producing yields than others.

In MYEs (Fig. 3.5b), predicted yields were greatest with 37 to 77% of attainable primary ears (24050 to 50050 ears ha^{-1}), 0 to 30% of attainable secondary ears (0 to 12300 ears ha^{-1}), and 0 to 40% of attainable tiller axillary ears (0 to 17200 ears ha^{-1}). The lowest predicted yields in MYEs were most associated with greater than 40% of attainable secondary ears. Confidence

intervals indicated that primary ears exceeded other ear types in producing yield, but secondary and tiller axillary ears remained similar to each other.

In HYEs (Fig. 3.5c), predicted yields were greatest with 37 to 77% of attainable primary ears (24050 to 50050 ears ha^{-1}), 0 to 30% of attainable secondary ears (0 to 12300 ears ha^{-1}), and 0 to 40% of attainable tiller axillary ears (0 to 17200 ears ha^{-1}). The lowest predicted yields in HYEs were most associated with > 40% of attainable secondary ears, > 50% of attainable tiller axillary ears, and > 80% of attainable primary ears ha^{-1}. Considering 95% confidence intervals, a more distinct hierarchy was evident compared to other environments (primary ears > tiller axillary ears > secondary ears) in yield formation.

3.4 Discussion

This study advances corn plasticity discussions by considering the unexplored extent of tiller compensatory relationships across contrasting environments and management practices (particularly plant density). Authors present novel data on yield component determination in tillered corn phenotypes from both main stalk and comprehensive plant perspectives in field-scale trials, the first such study to the extent of our knowledge. Findings from this study apply to a considerable range of environment × management conditions, as the dataset included 17 unique site-years covering typical plant density ranges in the semi-arid US High Plains. Results for tillering-yield relations for 10 of the 17 site-year combinations (Veenstra et al., 2021) motivated extending the study to evaluate yield components, their own plasticities, and how these relate to each other. The tillering element of corn physiology is actively being studied at a global scale, with authors utilizing both simulation and in-field approaches to understand key mechanisms and utility (Rotili et al., 2021b; Veenstra et al., 2021). In agreement with published literature,

evaluated field trials demonstrate that tiller expression facilitates crop plasticity in response to resource availability with favorable genetics (Jenkins, 1941). Tiller appearance and development mechanisms were not explored in the current study, which limits discussion scope to reproductive outcomes (evaluated yield components).

Flexible tiller densities were associated with more stable yield component predictions across all environments. This physiological response is of particular interest when seasonal resources are more abundant early in the growing season (Veenstra et al., 2021) to reduce dependence on plant density (Berzsenyi & Tokatlidis, 2012). Considering the density-dependent nature of yield progress in breeding and management of modern corn hybrids, this result is not surprising in tillered phenotypes (Duvick et al., 2004). An optimized plant density remained critical to maximize ear number, which supports the yield observations in previous tiller response work (Veenstra et al., 2021). However, kernel number was maximized with greater tiller development across plant densities in the present study. The modeled corn tiller expression scenarios of Rotili et al. (2021a) indicated changes in kernels per area due to tillering were determined by yield environment, with marginal environments experiencing reductions in kernel number. In our study, however, tiller density was only neutral or additive to total kernels per area. This difference is perhaps tied to the more marginal environments evaluated by Rotili et al. (2021a), but it should be noted that both studies predicted/observed similar ranges of kernel set (1000 to 3000 kernels m^{-2}).

Although main stalk ears and subsequent kernels per area were reduced in lower plant densities with tiller expression, kernel weights remained relatively stable regardless of tiller expression. While these results may suggest main stalk yield reductions, work by Veenstra and Ciampitti (Veenstra & Ciampitti, 2021) indicated that tiller presence did not significantly reduce

main stalk grain yields in the same environments considered in the present study. The lack of tiller expression impact on main stalk kernel weights also supports the hypothesis of an independent (i.e., grain-bearing tillers in lower plant densities) or nourishing (i.e., non-reproductive tillers in higher plant densities) energy and nutrient remobilization relationship for tillers and main stalk in late-season yield determination (Alofe & Schrader, 1975; Russelle et al., 1984). This point of source-sink relationships in tillered phenotypes requires further investigation.

Kernel number was the most significant component related to yield plasticity across all environments. This result is not surprising, as kernel number is known to be key to corn yield determination (Andrade et al., 1999). In general, situational tiller expression could be associated with non-uniform field features, which is a yield-negating factor for intensively managed corn (Hörbe et al., 2016). Tillering increased corn kernel numbers for shoots with high growth rates in field studies conducted by Rotili et al. (2022). Corn growth rates required to set kernels on primary ears appear to be lower than for tillers, and low growth rates are associated with stressed conditions (Andrade et al., 1999). In this regard, authors note that evaluated conditions in the present study may not have been harsh enough to observe such a response.

Ear number was less significantly related to yield stability than kernel number and varied by environment, which may be due to the potentially abnormal nature of tiller reproductive development (Ortez et al., 2022). A key determinant of tiller contributions to kernel number is successful reproductive development of tillers (i.e., pollination and grain fill of axillary ears). Although tiller apical ears were not found to be significant to corn yields in this study, tiller axillary ears were quite relevant, even when secondary ears were present on the main stalk. While main stalk prolificacy is commonly presented as a source of corn plasticity in

environments where low plant densities are employed, secondary ears were found to be a slightly weaker source of yield than tiller axillary ears in the best-yielding environments. Similar relationships between tiller axillary kernel number and secondary ears kernel number were observed in some cases by Rotili et al. (2022). Such findings indicate value in diversifying yield determination hierarchy with tiller ears in some cases. Additionally, main stalk prolificacy has obvious limits (Mylonas et al., 2020; Tokatlidis et al., 2005), and the presented results identify tiller utility when these limits are realized. Key to note, however, are the low predicted yields when too many tiller axillary ears were present, reaffirming the importance of optimized plant densities in HYEs (Veenstra et al., 2021). Previous studies have suggested that tillering reduces yield efficiency (Kapanigowda et al., 2010; Thapa et al., 2018), but this blanket hypothesis was recently rejected Rotili et al. (2022). Additional exploration of tiller reproductive development (i.e., vegetative, axillary ear, or apical ear) and potential impacts on efficiency metrics is needed.

While continued study is necessary, corn tillers may provide breeders and growers with plasticity trait options to achieve desirable plant density independence in certain environments (Mylonas et al., 2020). By offering additional crop reproductive plasticity when plant-available resources surpass thresholds of selected plant densities, tillers can mitigate management deficits which cannot be remediated mid-season (Massigoge et al., 2022; Rotili et al., 2021b; Veenstra et al., 2021). Future work should evaluate tiller development prediction, specifically driving factors of contrasting levels of expression plasticity, in addition to parameters influencing tiller ear development and resulting reproductive efficiency.

3.5 Conclusions

This study presents new insight on the compensatory extent of tillers as a source of reproductive plasticity in corn (beyond limited main stalk prolificacy). While main stalk yield components determined early in the season were adversely impacted by tiller presence in the lowest plant densities, effects were mitigated and even surpassed by tiller contributions from a comprehensive perspective. Tiller expression, particularly in HYEs, improved stability of ear and kernel yield components while maintaining kernel weights. Mitigation of yield component gradients caused by plant density reductions provides evidence of tiller utility in softening the yield formation hierarchy of conducive corn genotypes. This was evidenced particularly strongly by the superior performance of tiller axillary ears compared to main stalk secondary ears. These conclusions enhance discussion of avenues to reduce dependence on optimized plant density in environments likely to experience volatile seasonal impacts of climate change.

Table 3.1 Site-year field experiment coordinates, sow date, tenth-leaf (V10) date, treatment structure (D, Density; G, Genotype; P, Tiller Presence), irrigation, previous crop, and soil characterization [texture, pH, organic matter (OM – loss on ignition), nitrate concentration (NO3-N), ammonium concentration (NH4-N), phosphorus (P – Mehlich), and cation exchange capacity (CEC)]. Only the 7 additional site-years to the 10 already described in Table 2.1 are shown here.

Site-Year	Latitude	Longitude	Sow Date	V10 Date	Treatment Structure	Irrigation	Previous Crop	Soil Texture
	(°N)	(°W)						
Keats 2021	39.23	96.72	Apr-30	Jun-22	D × G × P	None	Corn	Silt Loam
Buhler 2021	38.14	97.73	May-04	Jun-25	D × G	Subsurface limited	Corn	Silt Loam
Greensburg 2021	37.58	99.37	May-07	Jun-25	D × G	Subsurface limited	Corn	Loam
Selkirk 2021	38.70	101.54	May-06	Jun-30	D × G	Subsurface limited	Field Bean	Loam
Garden City 2021	37.83	100.86	May-13	Jun-28	D × G × P	Subsurface limited	Corn	Sandy Loam
Goodland 2021	39.25	101.78	May-05	Jun-30	D × G × P	Subsurface limited	Soybean	Loam
Colby A 2021	39.39	101.06	Jun-04	Jul-15	D × G × P	None	Wheat	Clay Loam
Site-Year	**pH**	**OM**	**NO_3-N**	**NH_4-N**	**P**	**CEC**		
	(H_20)	% (LOI)	(mg kg^{-1})	(mg kg^{-1})	Mehlich (mg kg^{-1})	(meq 100 g^{-1})		
Keats 2021	6.6	6.2	23.3	12.7	106.4	25.6		
Buhler 2021	6.3	2.6	11.7	7.8	13.3	22.3		
Greensburg 2021	5.6	2.3	33.4	7.4	68.8	20.0		
Selkirk 2021	7.9	2.7	14.0	5.8	90.9	23.2		
Garden City 2021	5.5	1.6	14.2	5.2	52.1	9.7		
Goodland 2021	6.5	2.9	36.9	11.1	65.4	23.2		
Colby A 2021	7.1	2.9	23.8	7.1	93.0	22.2		

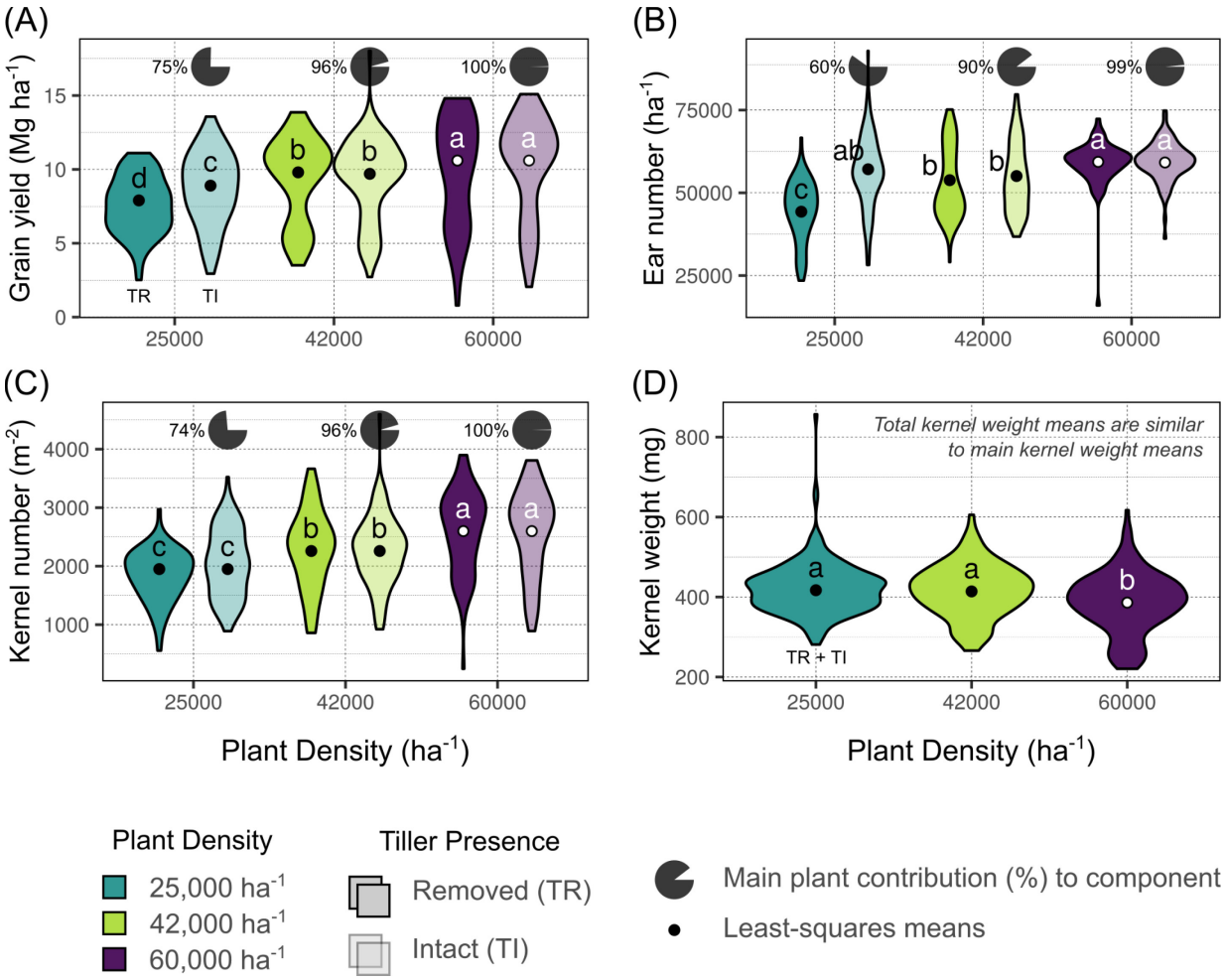

Figure 3.1 Summary of comprehensive yield components based on treatment factors deemed significant by analysis of variance (Tables B.1, B.2, B.3). Colors indicate plant density (blue – 25000 plants ha^{-1}, green – 42000 plants ha^{-1}, purple – 60000 plants ha^{-1}) and transparency indicates tiller presence (removed, TR – opaque; intact, TI – transparent). Data distribution is shown as a violin plot and least-squares means from fitted models are indicated with points. Different letters indicate mean differences within each panel at the 0.05 probability level. Pie charts above TI plots indicate the percent contribution of main shoots to the comprehensive components (e.g., 75% of yield was produced by main shoots in TI plants at the 25000 plants ha^{-1} density, panel A).

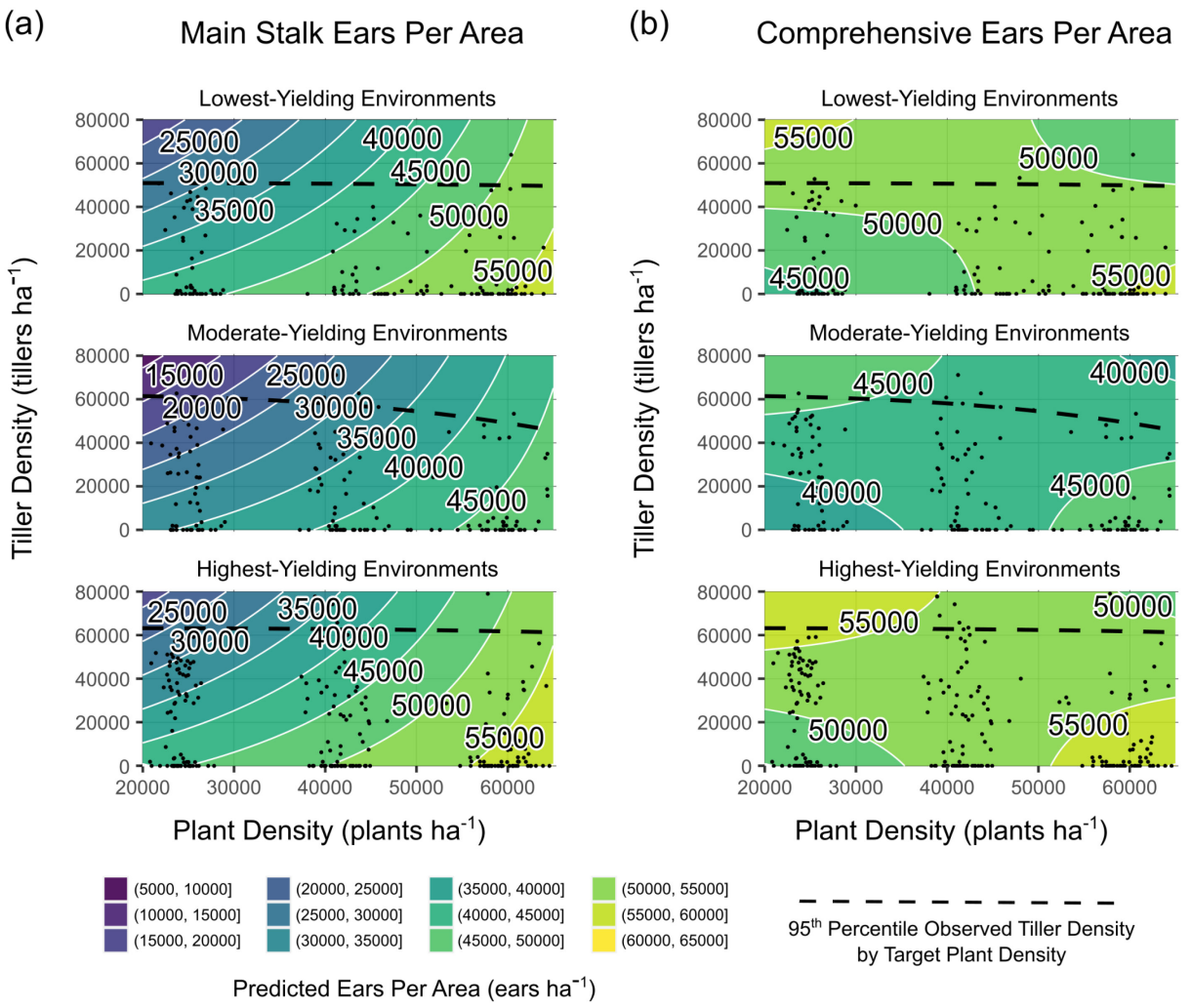

Figure 3.2 Main stalk ears per area (A) and comprehensive ears per area (B) predictions from models of observed plant density, tiller density, and yield environment as determined by analysis shown in Table B.2. Site-years are grouped by realized yield environment. Contours are shaded and labeled according to 5000 ears ha^{-1} density intervals. White lines indicate a change in ear density interval. Observed plant densities and tiller densities are indicated with black points. Black dashed lines are intended as an informal visual indicator of tiller expression potential for each yield environment. Extrapolations beyond black points and dashed black lines are shown for the purpose of comparing environments on the same density scales.

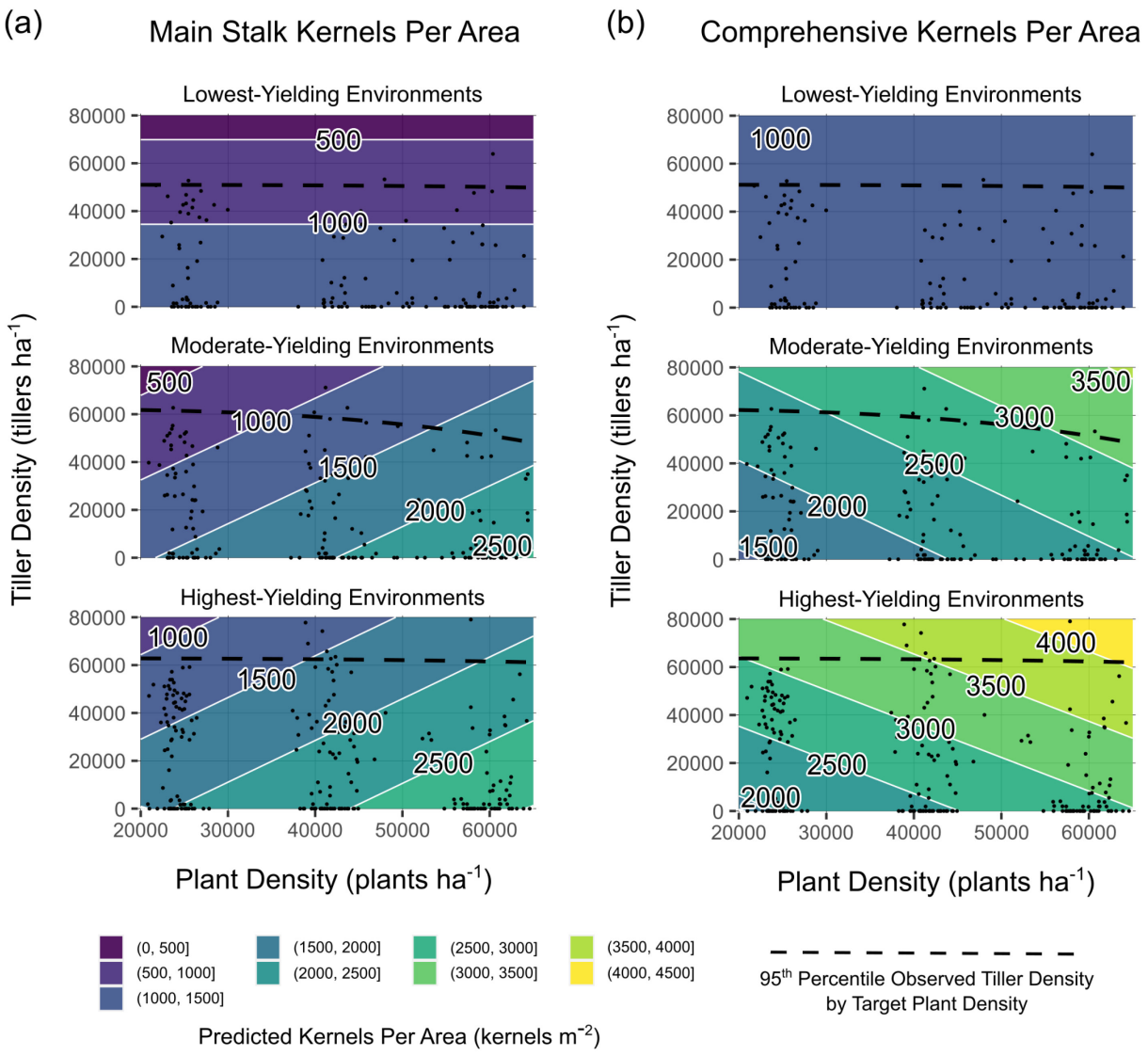

Figure 3.3 Main stalk kernels per area (A) and comprehensive kernels per area (B) predictions from models of observed plant density, tiller density, and yield environment as determined by analysis shown in Supplementary Table 3. Site-years are grouped by realized yield environment. Contours are shaded and labeled according to 500 kernels m^{-2} density intervals. White lines indicate a change in kernel density interval. Observed plant densities and tiller densities are indicated with black points. Black dashed lines are intended as an informal visual indicator of tiller expression potential for each yield environment. Extrapolations beyond black points and dashed black lines are shown for the purpose of comparing environments on the same density scales.

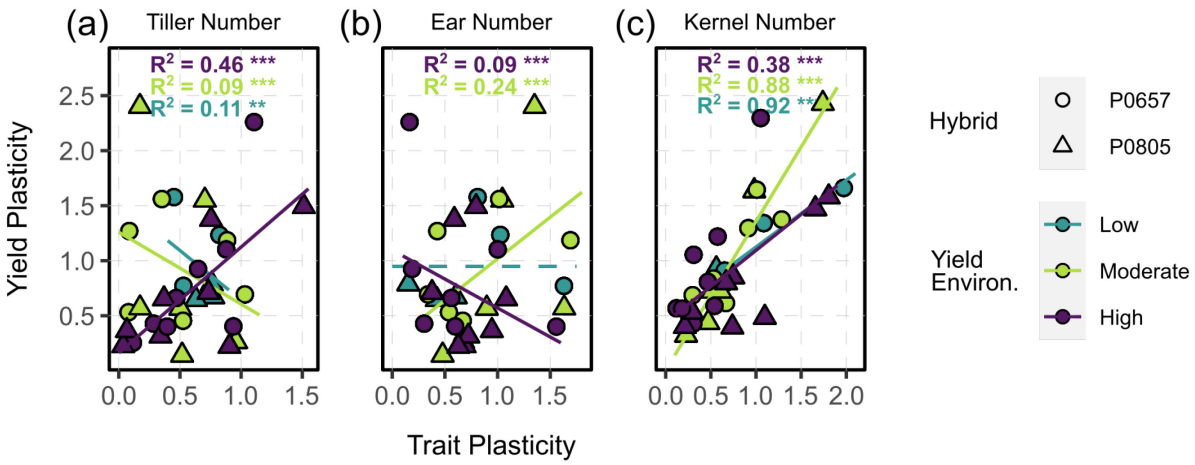

Figure 3.4 Relationships between trait plasticity (A, tiller number; B, ear number; C, kernel number) and yield plasticity (y-axis) of tillered phenotypes. Points are colored by yield environment (blue – low, green – moderate, purple – high); and shaped by hybrid (circle – P0657AM, triangle – P0805AM). Fitted lines and model metrics, when applicable, are colored by yield environment. Dashed lines indicate intercept-only models when other candidates were not significant. Significance symbols are the following: * $p \leq 0.05$, ** $p \leq 0.01$, *** $p \leq 0.001$.

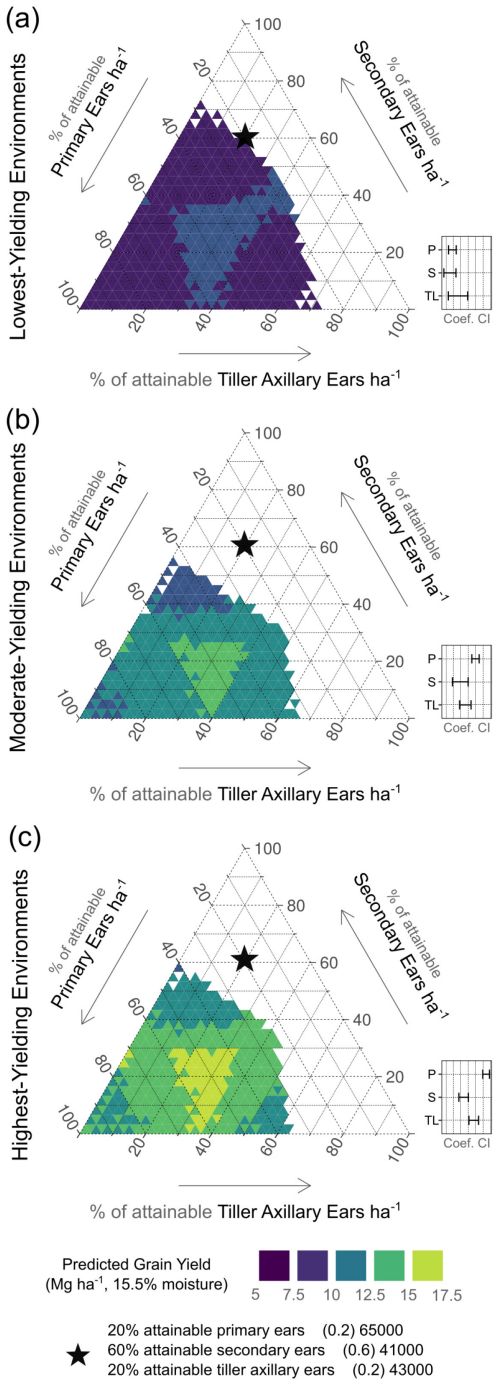

Figure 3.5 Ear type plasticity relationship to predicted yields by yield environment (A, low; B, moderate; C, high). Right axes indicate % of attainable primary ears observed (65000 ears ha^{-1}). Left axes indicate % of attainable secondary ears observed (41000 ear ha^{-1}). Bottom axes indicate % of attainable tiller axillary ears observed (43000 ears ha^{-1}). Contour shades indicate predicted yield level (purple < 7.5 Mg ha^{-1}; lime > 15 Mg ha^{-1}). Black star is shown for reference on each plot, indicating 20%, 60%, and 20% of attainable primary ears, secondary ears, and tiller axillary ears, respectively. Insets show relative 95% confidence intervals for each coefficient estimate (P, primary ears; S, secondary ears; TL, tiller axillary ears).

Chapter 4 - Corn tiller density prediction: Identifying key E × M factors via extensive field studies

Abstract

While globally appreciated for reliable, intensification-friendly phenotypes, modern corn (*Zea mays* L.) genotypes retain crop plasticity potential. For example, weather and heterogeneous field conditions can overcome phenotype uniformity and facilitate tiller expression. No substantial effort has been made to predict tiller presence in field scenarios, which could provide insight on corn plasticity capabilities and drivers. Therefore, the objectives of this investigation are as follows: 1) identify environment, management, or combinations of these factors key to accurately predict tiller density dynamics in corn; and 2) test out-of-season prediction accuracy for identified factors. Replicated field trials were conducted in 17 diverse site-years in Kansas (United States) during the 2019, 2020, and 2021 seasons. Two modern corn genotypes were evaluated with target plant densities of 25000, 42000, and 60000 plants ha^{-1}. Environmental, phenological, and morphological data were recorded. After testing a variety of generalized additive model candidates, plant density interactions with cumulative growing degree days (GDD), photothermal quotient (PTQ), mean minimum and maximum daily temperatures, cumulative vapor pressure deficit (VPD), soil nitrate (NO_3), and soil phosphorus (P) were identified as important predictive factors of tiller density. Many of these factors had stark non-limiting thresholds. Out-of-season prediction errors were seasonally variable, highlighting model limitations due to training datasets. Future studies should expand on tiller density prediction by exploring tiller reproductive development and improving our ability to

more accurately predict the relationship between tiller and main stem resource economy (mainly C).

4.1 Introduction

Corn (*Zea mays* L.) is a key crop in the global food economy, partially due to predictable phenotypes that enable intensive management. For this reason, high plant densities, optimal planting date, and efficient fertility programs are among the key drivers of high-yielding corn (Duvick et al., 2004; Long et al., 2017; Schwalbert et al., 2018). Concurrently, plant uniformity is targeted to an increasing degree by planter technologies improving singulation and seeding depth for timely emergence (Badua et al., 2021). Even when every effort is made to obtain field uniformity, this goal is arguably idealistic. In reality, plant uniformity may be disrupted by plasticity mechanisms which are often masked, but preserved nonetheless, in the corn genome (Moulia et al., 1999).

Crop plasticity is the ability of a crop genotype to express contrasting phenotypes in an array of environmental conditions (Laitinen and Nikoloski, 2019). Broadly, crop plasticity mechanisms include source (carbon capture) and sink (carbon storage and utilization) manipulations (Dingkuhn et al., 2020). Branching is a common plasticity response, for example, increasing both the source (leaf area) and sink (seed set) potential for a crop plant. Although this phenotypic flexibility is beneficial to individual plants, many modern agronomic crop management practices favor intensification and target uniformity (Matesanz and Milla, 2018). These intensively managed, stabilized environments aim to minimize plasticity expression, which may result in both positive and negative outcomes (von Wettberg et al., 2020). Global interest is mounting in crop plasticity mechanisms as breeders anticipate potential impacts of

climate change (Arnold et al., 2019; Schneider and Lynch, 2020). Adaptation to rapidly changing weather patterns and sporadic stress events may be facilitated by plasticity mechanisms conserved in modern crop genetics (Nicotra et al., 2010). The true utility of plasticity is uncertain in modern agronomic settings, as the concept remains mostly theoretical and untested under broad-scale field conditions (Brooker et al., 2022).

Tillers are basal branches of grass crop species, appearing early in plant development for annual crops (Kim et al., 2010b), and continue growing and developing in perennial species. As with any plasticity trait, genotype is a strong regulator of tiller expression (Doust, 2007; Laitinen and Nikoloski, 2019). With conducive genotypes, tiller development is encouraged by an abundance of resources and therefore may vary significantly on an individual plant basis based on light, nutrient, or water availability – commonly associated with plant density (Lafarge and Hammer, 2002; Markham and Stoltenberg, 2010). Nutrients identified as key to tiller development are phosphorus (P) and nitrogen (N), although deficiency may prevent expression (Longnecker et al., 1993; Rodriguez et al., 1999; Thorne and Wood, 1987). When soil factors are not limiting, early-season weather conditions are key to tiller development. Specifically, the relationship between temperature and radiation is commonly quantified via the photothermal quotient (PTQ), which has been correlated to vegetative and reproductive crop mechanisms (Angus et al., 1981; Fischer, 1985; Kim et al., 2010b; Kumar et al., 2016). Within species, genotypes vary in tiller fecundity, even for apparently unrestrictive conditions (Kim et al., 2010a). Tillers can be fertile and develop identically to primary shoots, although delayed in development, usually by a set phyllochron interval (Nemoto et al., 1995). This cumulative age discrepancy sets limitations for the number of tillers able to successfully set seed, as abortion typically occurs in reverse appearance order when resources become limiting over the course of

the growing season (Thorne and Wood, 1987). For tillers emerging at opportune times and surviving through the season, yield contributions can be significant in well-managed grains (Lafarge and Hammer, 2002; Pasuquin et al., 2008).

Modern preferences of farmers and breeders alike commonly mask tiller capacity in corn fields, although this plasticity mechanism is conserved and situationally expressed (Duvick et al., 2004; Moulia et al., 1999). Common factors promoting tiller expression in corn are linked to plant density and are seasonal in nature (Downey, 1972; Markham and Stoltenberg, 2010). Interplant competition is minimized when plant density is reduced. Intentional plant density reductions are employed by farmers to match crop needs with limited resource availability, a pervasive component of dryland crop production (Roozeboom et al., 2007; Rotili et al., 2019). Unintentional plant density reductions include poor plant establishment or early season plant losses. In these situations, corn tillers may be expressed in row gaps or as a response to the released apical dominance of a damaged primary shoot (Carter, 1995; Thapa et al., 2018). Tillering in corn has historically lent itself to the theory that expression ("suckering") reduced yields (Dungan, 1931; Earley et al., 1971). More recent studies have challenged this blanket opinion (Rotili et al., 2022; Veenstra et al., 2021).

While past work has quantified the impact of tillers on corn yield (Sangoi et al., 2009; Veenstra et al., 2021), plastic capacity (Rotili et al., 2022, 2021b), and resource use (Rotili et al., 2022; Thapa et al., 2018), no substantial effort has been made to quantify the predictability of tiller presence in field scenarios. Corn yields responded to varying levels of tiller density (i.e., tillers ha^{-1}) in previous work from this database (Veenstra et al., 2021) and others (Massigoge et al., 2022). Therefore, accurately predicting this plasticity behavior is relevant in the evaluation of corn tillering utility. Plasticity quantification remains a broad research gap, particularly in light

of agronomic applications (Sadras et al., 2013). Because environmental drivers were strongly correlated with yield responsiveness to tiller formation in Veenstra et al. (2021) and Massigoge et al. (2022) and similar variables have been proposed in a mechanistic framework for understanding this trait in corn (Rotili et al., 2021b), it follows that such data should be useful in describing tiller densities at the field scale. Authors hypothesized that corn tiller densities in tiller-prone genotypes could be reliably predicted within 25% of the target plant density using variables related to crop management and environment. Therefore, the objectives of this study were as follows: 1) identify key environment, management, or combinations of these variables useful for predicting tiller density dynamics in corn; and 2) test out-of-season prediction accuracy for identified variables.

4.2 Materials and Methods

4.2.1 Field Experiments

This study utilized unanalyzed data from 17 site-years of field experiments across the state of Kansas in the 2019 to 2021 seasons, as previously described in Veenstra et al. (2021) and Table B.1. At each site, treatments were applied in a split-split-plot arrangement with a randomized complete block design (RCBD) and replicated three or four times depending on the site-year, as field space allowed. Whole plot was assigned as plant density, with target levels 25000, 42000, and 60000 plants ha^{-1}. Sub-plot was assigned as genotype, with levels P0805AM and P0657AM (Corteva Agriscience, Johnston, IA, USA). These genotypes were selected for their modern release date, suitability for the region and limited moisture production systems targeted, and high propensity to tiller. Sub-sub-plot was assigned as tiller presence, with levels

intact or removed. For the current study, only plots with undisturbed tillers were evaluated. Additional information on plot care and size can be found in the aforementioned article.

Plant counts per area, tiller counts per area, and average crop phenology were recorded in unique sections (at least 1.2 m^2) of buffered central plot rows at various times throughout the season in each study. Data were collected at target development stages V5 (fifth leaf; Ritchie et al., 1997), V10 (tenth leaf), and R6 (physiological maturity) in all years, and additionally at V16 (sixteenth leaf) and R3 (kernel milk stage) in 2019 and 2021. Counts were scaled to plants ha^{-1} and tillers ha^{-1}.

4.2.2 Environmental Data and Calculations

Soil type and fertility were characterized for each site-year via early-season soil sampling at 60-cm (NO_3 and NH_4) and 15-cm depths (all others). Weather data were obtained from the Climate Engine web application for all desired geographic locations and date ranges (Huntington et al., 2017). Soil bulk density data were downloaded from the Web Soil Survey application (Soil Survey Staff et al., 2022) and used to calculate nutrient values in kg ha^{-1}. In total, 16 environmental variables were available for study, which were grouped into 15 categories based on previous knowledge of importance to tiller response (Veenstra et al., 2021), ease of producer manipulation (i.e., management factors – including plant density, amendable soil variables, and water as irrigation), and field observations. All calculations, data transformation, and analyses were conducted using program R (R Core Team, 2022).

All climate data considered the time period from planting to date of observation, regardless of plant development stage. While previous work has indicated critical periods for tiller appearance (Moulia et al., 1999; Rotili et al., 2021b), authors wished to capture seasonal trends that could impact tiller density through abortion as well. Mechanistic relationships are not

well-defined in this regard (e.g., tiller abortion has been related to phenological progression, but this could be more influenced by seasonal stress or soil water depletion than plant development alone). Cumulative values (additive from planting to field observation date) included growing degree days (GDD), vapor pressure deficit (VPD), and soil water supply. Daily GDD was calculated as the difference between mean daily temperature and the crop base temperature of 10 °C, with a forced daily maximum of 30 °C. The VPD was provided in kilopascals (kPa) and added over the specified date range. Soil water supply included both precipitation and irrigation, when applicable, with the season extended one month pre-sowing to estimate soil moisture at planting. Daily minimum temperature, daily maximum temperature, daily thermal amplitude, and photothermal quotient (PTQ) were averaged over the assigned period (planting to field observation). The PTQ is defined by Fischer (1985) as the mean daily solar radiation for a selected time period, divided by the difference between the mean temperature for that period and the crop base temperature (10 °C), with final units megajoules (MJ) m^{-2} $°C^{-1}$ day^{-1}.

4.2.3 Statistical Analysis

4.2.3.1 Model specification, fit, and selection

In preparation for model fitting and evaluation, the complete dataset (multiple sites, seasons, and development stages) was divided into training and testing sets – 80% and 20% (4:1), respectively. This split was selected as a compromise between maximizing the training dataset and maintaining the integrity of both training and testing sets (Gholamy et al., 2018). These initial sets had similar representation of all site-years, potential predictor variables, and observed tiller densities (Figure 4.1). The training set (80%) was utilized for model fitting (e.g., estimation of regression coefficients). The testing set (20%) was sacrificed for model testing only

and reserved to evaluate the predictive accuracy and adequacy of the model fit to the training set. This 4:1 model is henceforth referred to as the "cross-season" fit.

The 15 different variable combinations selected as potential predictors of tiller density are presented in Table 4.1. To facilitate useful interpretation of interactions among non-categorical variables, observed plant density was categorized into three clusters based on target plant densities of 25000, 42000, and 60000 plants ha^{-1}, of which realized densities were representative (Figure C.1). These factor levels were utilized when plant density was involved in interactions with at least one other continuous variable. As generalized additive models (GAMs) require a distribution representative of the response variable, we selected a Binomial distribution for realization of tillers ha^{-1}. Essentially, this assumption allowed us to determine the probability (ranging from 0 to 1) of attaining a maximum potential tiller density ha^{-1} as the response variable. The assumed maximum achievable tiller expression at a field scale was based on findings of others (3 tillers $plant^{-1}$; Major, 1977; Rotili et al., 2021a), and a realistic maximized plant density of 100000 plants ha^{-1}, as utilized in previous plant density studies in the US (Assefa et al., 2016). The potential tiller density in our model was therefore $0 \leq y \leq 300000$ tillers ha^{-1}, where y is the predicted tiller density expressed as $m \times 300000$ tillers ha^{-1}, with m being the modeled probability of attaining a maximized tiller density per area. Such a tiller density has never been reported in the literature and is arguably not achievable. The highest observed tiller density in this study was 152842 tillers ha^{-1} (mean of 0.8 tillers $plant^{-1}$, with 2% of individual observations > 3 tillers $plant^{-1}$). The mean plant density in the current study was 41295 plants ha^{-1}, ranging from 17514 to 73807 (Figure C.1). A maximum tiller density at the field level determined independently of present observations minimizes assumptions of tiller responses to plant density, for example. Such responses have been reported at the tillers $plant^{-1}$ scale

(Downey, 1972; Hansey and de Leon, 2011; Sangoi et al., 2009; Tetio-Kagho and Gardner, 1988), but authors believe tiller density drivers at the field scale (tillers ha^{-1}) are too uncertain (Downey, 1972) to necessitate constraints based on specific variables. All GAMs were fit to the training set using the *mgcv* package with all continuous variables set as flexible smoothed effects via thin-plate regression splines (Wood, 2017). Limiting thresholds for each of the selected variables were defined based on a 0.50 probability.

Predictive accuracy was evaluated by the mean absolute error (MAE) and mean bias error (MBE) of out-of-sample predictions in the test set. Smaller values of MAE indicate increased predictive accuracy. The flexible smooth effects (i.e., probability of achieving maximum tiller densities) for predictor variables in the most accurate model were independently plotted across the range of corresponding observations.

4.2.3.2 Out-of-season evaluation

After the most accurate predictive model was identified for the cross-season dataset, the same model structure was evaluated for out-of-season predictive accuracy. The goal of such tests was to determine strengths and weaknesses of the predictive model for in-field agronomic applications. To test the predictive accuracy of the model for one year (2019, for example), the training dataset included only observations from the other two years (in this case, 2020 and 2021). The splits for these sets (percent train / percent test) were 80/20, 62/38, and 58/42 for 2019, 2020, and 2021, respectively. These fits are henceforth referred to as “out-of-season” models.

To evaluate out-of-season model performance, predictive accuracy for each site-year was determined as the difference between the true tiller density and the corresponding point

prediction at the mean target plant density of 42000 plants ha^{-1} (representative of the true observed mean, 41295 plants ha^{-1}). To explore predictive error causation in each site-year, out-of-season coefficient estimates were independently set to zero. Resulting prediction MAE was calculated for each exclusion. The excluded coefficient that most drastically reduced MAE for a given site-year was identified as the variable too heavily weighted for the observed conditions in a given out-of-season fit.

4.3 Results

4.3.1 Model Training and Selection

Observation distributions in model training/testing splits for cross-season and out-of-season datasets are shown in Figure 4.1. Observations were relatively similar for all sets with regard to cumulative GDD (Fig. 4.1a), seasonal PTQ (Fig. 4.1b), mean minimum and maximum temperatures (Fig. 4.1 c-d), cumulative VPD (Fig. 4.1e), and tiller density (Fig. 4.1h). Although NO_3 (Fig. 1f) and P (Fig. 1g) observations were similar between the cross-season sets, as expected, seasonal variation was evident in the out-of-season sets.

The mean observed tiller density in the full dataset was 28781 tillers ha^{-1} and the mean observed plant density was 41295 plants ha^{-1}. Therefore, an acceptable error range across the dataset (< 25% of the plant density) was < 10324 tillers ha^{-1}. Considering the 15 variable combinations, out-of-sample prediction MAE is presented for each model fit in Table 4.2. Models including weather-based factors were consistently below the targeted error threshold. The three most accurate models were the simplified E × M (MAE = 7776 tillers ha^{-1}; MBE = -38 tillers ha^{-1}), the simplified G + E + M (MAE = 9050 tillers ha^{-1}), and the full model (MAE = 9051 tillers ha^{-1} MAE). The simplified E × M model was selected as the most appropriate

(Equation C.1). Plant density was the key management factor identified, and the most relevant environmental factors were temperature- (GDD, PTQ, VPD, mean minimum and maximum daily temperatures) and soil fertility-related (NO_3 and P).

4.3.2 Independent Predictor Effects

Smoothed effects of predictor variables on maximum tiller density probability are presented independently in Figure 4.2. It is key to note that the greatest tiller density observed in the present study was 152842 tillers ha^{-1}. That is, even when a variable was apparently non-limiting, other limiting variables prevented the observed density from reaching the set theoretical maximum of 300000 tillers ha^{-1}. Cumulative GDD had a consistent impact on tiller probabilities across plant densities, with a clear threshold of > 200 °C day identified as non-limiting (Fig. 4.2a). The effect of seasonal PTQ was clear as well across plant densities, with a non-limiting threshold of > 1 MJ m^{-2} C^{-1} day^{-1} (Fig. 4.2b). Non-limiting mean minimum temperature thresholds were > 8 °C for the 25000 plants ha^{-1} target, < 9 °C for 42000 plants ha^{-1}, and < 17.5 but > 11 °C for 60000 plants ha^{-1} (Fig. 4.2c). Mean maximum temperature was consistently non-limiting > 22 °C for 25000 and 42000 pl ha^{-1} and > 26 °C for 60000 pl ha^{-1} (Fig. 4.2d). Cumulative VPD was limiting below 20-30 kPa for all plant densities, but was also limiting to some degree at higher values for the 42000 (200 kPa) and 60000 (150 kPa) plants ha^{-1} targets (Fig. 4.2e). Soil fertility impacts were less consistent overall (Fig. 4.2f-g). At 25000 pl ha^{-1}, increasing kg NO_3 ha^{-1} appeared to have detrimental impacts on tiller expression beyond 200 kg ha^{-1}, whereas P had a clear minimum threshold of 100 kg ha^{-1}. Tiller response was fairly stable across nutrient gradients for both NO_3 and P at 42000 pl ha^{-1}. Highest values of NO_3 and P were the most limiting at 60000 pl ha^{-1}, with the apparent NO_3 threshold at 230 kg ha^{-1} and the P threshold at 150 kg ha^{-1}.

In summary, highest tiller densities in a 25000 plants ha^{-1} density would be observed with cumulative GDD > 200 °C day, PTQ > 1 MJ m^{-2} C^{-1} day^{-1}, mean minimum temperature > 8 °C, mean maximum temperature > 22 °C, cumulative VPD > 30 kPa, soil NO_3 < 200 kg ha^{-1}, and soil P > 100 kg ha^{-1}. Highest tiller densities in a 42000 plants ha^{-1} density would be observed with cumulative GDD > 200 °C day, PTQ > 1 MJ m^{-2} C^{-1} day^{-1}, mean minimum temperature < 9 °C, mean maximum temperature > 22 °C, and a cumulative VPD > 30 kPa but < 200 kPa, with minimal direct impact of soil nutrients. Highest tiller densities in a 60000 plants ha^{-1} density would be observed with cumulative GDD > 200 °C day, PTQ > 1 MJ m^{-2} C^{-1} day^{-1}, mean minimum temperature > 11 but < 17.5 °C, mean maximum temperature > 26 °C, cumulative VPD > 30 kPa but < 150 kPa, soil NO_3 < 230 kg ha^{-1}, and soil P < 150 kg ha^{-1}. These independently presented variables are correlated with each other (Figure C.2). For example, the most correlated associations (with r > 0.7) were cumulative VPD with cumulative GDD, mean maximum with mean minimum temperature, mean maximum temperature with cumulative VPD, and mean temperatures with cumulative GDD.

4.3.3 Out-of-season Predictive Accuracy

Out-of-season predictions and resulting accuracy are presented in Figure 4.3. Overall, predictions for the -2021 and -2019 trained models were most accurate. When calculated via the -2019 coefficient estimates, 2019 tiller density predictions ranged in absolute error from 7211 to 23795 tillers ha^{-1}, and averaged -16003 tillers ha^{-1} (Fig. 4.3a). When calculated via the -2020 coefficient estimates, 2020 tiller density predictions ranged in absolute error from 19574 to 280461 tillers ha^{-1}, and averaged +125553 tillers ha^{-1} (Fig. 4.3b). When calculated via the -2021 coefficient estimates, 2021 tiller density predictions ranged in absolute error from 2564 to 40372 tillers ha^{-1}, and averaged -1544 tillers ha^{-1} (Fig. 4.3b).

4.3.4 Out-of-season Error Evaluation

Prediction accuracy impacts of independent out-of-season coefficient estimate removal are presented in Table 4.3. When select out-of-season coefficient estimates were excluded, 59% of site-years dropped below the reasonable error threshold of 10500 tillers ha^{-1} (25% of 42000 plants ha^{-1} target). The 2020 predictions were responsible for 71% of the unacceptable error. Coefficients most improperly weighted for 2019 sites were soil NO_3 and mean maximum temperatures. Coefficients most improperly weighted for 2020 sites were GDD, soil P, soil NO_3, and PTQ. The site-years most over-predicted by the full model in 2020 had the highest and lowest observed NO_3 and P kg ha^{-1} in the collected dataset. Predictions for two 2020 sites were most accurate with all coefficient estimates. Coefficients most improperly weighted for 2021 sites were temporal and temperature-related (VPD, GDD, minimum temperature, and maximum temperature).

4.4 Discussion

From a diverse dataset of field experiments, this study presents novel conclusions on the predictability of tiller densities in selected modern corn genotypes. While recently published literature has explored the general yield and reproductive outcomes of corn tiller presence in modern farm management systems (Rotili et al., 2022, 2021a; Veenstra et al., 2021), no substantial effort has been made to explore appearance and survival factors for corn tiller densities. In an effort to fill this knowledge gap, G, E, and M variables were evaluated in replicated, multi-season, state-wide field trials in Kansas, US. These 17 site-years comprise an expansive tiller-focused database which has offered numerous yield and reproductive plasticity insights for corn management in the US Central High Plains region (Veenstra et al., 2021). The

expanse of this dataset facilitates unique modelling approaches (e.g., GAMs) not typically possible in traditional field experiments evaluated via ANOVA and mixed models. The current study provides perspective of tiller density drivers and out-of-season tiller density predictability for selected corn genotypes in a range of environments, management practices, and crop stages.

Corn tiller expression was heavily facilitated by environmental factors, as evidenced by model testing parameters in Table 4.2. Identified by previous work for corn and other crop species, season timing, the PTQ, and thermal variables were crucial predictive components for tiller densities. Corn tiller initiation was found to follow the typical grass species delay of one phyllochron from main shoot development by Moulia et al. (1999) and to follow thermal time by Rotili et al. (2021b). Rotili et al. presented data from Maddonni et al. (2002), which began measurements at 500 °C days. Tillers plant^{-1} were as high as 0.5 for some initial values, indicating the limiting value was < 500 °C days. The red to far-red light ratio was also key to tiller development in this study by Maddonni et al. (2002). Kim et al. (2010) indicated that grain sorghum tiller appearance started between 150 and 250 °C days and PTQ was a useful indicator of tillering potential. These observations correspond with the threshold of 200 °C days identified here for corn, as well as the importance of PTQ as a potentially limiting factor in tiller expression. Related to the PTQ, C assimilates are commonly associated with tiller appearance, and reduced tiller densities in grain sorghum were not necessarily an indicator of C depletion (Lafarge and Hammer, 2002). These reductions may actually be more related to red:far-red light quality linked to changes in plant density (Markham and Stoltenberg, 2010). Plant density was the key management factor significantly altering the outcome of tiller densities in the current study, as previously reported for corn at the plant scale (Hansey and de Leon, 2011; Major, 1977; Rotili et al., 2021b; Tetio-Kagho and Gardner, 1988) and field scale (Downey, 1972). Thorne

and Wood (1987) observed reduced tiller number with high temperatures in pre-kernel set periods of wheat (a C3 species). In addition, greater radiation encouraged tiller development, although onset of heat treatments canceled out this effect at harvest (Thorne and Wood, 1987). The current study identified a base threshold for high temperature rather than an upper threshold (potentially attributed to the C4 nature of corn) and a base threshold for low temperatures, but correlation between temperatures and other factors reducing corn tiller density probability is apparent (Figure C.1). Cumulative VPD was associated with tiller expression as a base threshold, likely due to the temporal nature of how this variable was calculated. Considered as a stress index for this study, however, high cumulative VPD captured tiller abortion responses not attributed to GDD alone at 42000 and 60000 plants ha^{-1} densities. The VPD is associated with heterogeneity in corn phenology and yield, which could facilitate plasticity in certain environments (Lobell and Azzari, 2017). Higher VPD is related to lower growth, necessitating a lower maximum for higher plant populations to maintain growth per plant. Soil fertility, specifically NO_3 and P, were significant to predictive accuracy, as expected based on precedent in wheat (Rodriguez et al., 1999; Thorne and Wood, 1987), rice (Alam et al., 2009), and grain sorghum (van Oosterom et al., 2010). Adequate P levels are crucial to hormonal branching responses in plants, mitigating the apical dominance conferred by strigalactones and promoting production of cytokinins (Yan et al., 2020). Relationships and thresholds for soil fertility variables in tiller expression probability were less apparent than for weather factors, but these parameters are certainly important. Continued corn tiller field studies should include fertility as a dosed treatment factor to evaluate this response more formally with a factorial design approach.

A key component for selected predictor variables is the Sprengel-Liebig Law of the Minimum (van der Ploeg et al., 1999). This foundation discloses that none of the insignificant

parameters were obviously limiting in any of the evaluated trials. If this assumption is not met, model predictive accuracy may be degraded. Moisture supply was not a significant factor, likely because no evaluated environments were critically water-restricted. Previous simulation work has indicated tiller productivity response to water supply (Rotili et al., 2021a). Diverse, field-based data sets for model training are imperative, as evidenced by the out-of-season predictions and resulting error margins in the current study. Maximum temperature, temporal, and fertility coefficients were most commonly overweighted in the out-of-season training data sets, solidifying the observation that these factors are better classified as benchmark indicators (e.g., minimum or maximum for expression) than as tiller density drivers. Studies by Rodriguez et al. (1999) indicated that P deficiency altered the wheat phyllochron and subsequently reduced tiller emergence rate. In addition, a greater diversity of genotypes could uncover alternate tiller expression responses, as supported by previous work (Hansey and de Leon, 2011).

Although weather factors appear to be reliable tiller density predictors, the utility of models dependent on future observations is an important caveat. However, out-of-season data forecasting (i.e., weather) is the common scapegoat for prediction challenges. This study clearly demonstrates the power of predictive distribution uncertainty, as out-of-season prediction intervals for some site-years were quite wide. Even if "reliable" data is available (i.e., observed in-season weather and soil data), uncertainty remains high in our attempt to replicate reality in biological systems. A diverse dataset is required to properly train such prediction models. This is demonstrated by the error of an appropriately trained model (Fig. 4.3c) and the error reduction following removal of certain coefficients (Table 4.3).

From a farm decision standpoint, the key challenge moving forward in such studies is making useful recommendations with the model-limited clarity (Gneiting and Katzfuss, 2014;

Raftery, 2016). Introducing risk-reward perspectives of economics, environment, etc. may aid in generating such actionable decisions, but such ideals are difficult to quantify and vary by individual (Komarek et al., 2020; Mase et al., 2017; Williams and Hooten, 2016). For example, model predictions are likely not useful to assist farmers with plant density selection based on tiller expression expectations for an upcoming season. However, in potential replant situations, increased certainty may generate a more actionable prediction of tiller compensation potential. Outcomes of this study are useful for in-season diagnostics addressing farmer questions and concerns of year-to-year variation in tiller densities.

Knowledge of factors contributing to tiller productivity remains limited. Kernels from ears on tillers are key to yield compensation of tillered corn phenotypes (Massigoge et al., 2022; Rotili et al., 2022), but tiller reproductive development is not well understood. Not all tillers may equally contribute to plant productivity (Alofe and Schrader, 1975; Bonnett, 1948; Russelle et al., 1984; Schaffner, 1930). Future work should identify drivers of successful tiller reproductive development (i.e., tiller axillary ear) and expand on the overall plant C economy conclusions of Alofe and Schrader (1975).

4.5 Conclusions

The hypothesis put forth for this study "*that tiller densities can be reasonably predicted (i.e., within 25% of the target plant density) via environmental factors*" appears to be supported by our results. Plant density, thermal parameters, and soil fertility were critical components to achieving the lowest error in tiller density prediction. The cross-season predictive accuracy of identified models fell within the reasonable benchmark of < 25% observed plants ha^{-1}, although not all out-of-season fits performed equally. Critical non-limiting thresholds for select

environmental parameters were apparent in coefficient estimates. Wide prediction intervals highlighted the volatile nature of tiller expression and model assumptions, but point predictions were relatively good with sufficiently diverse training data. While useful for early season diagnostic purposes, these models are limited in forecast utility and should be coupled with appropriate decision theory and risk assessments. Future studies should expand on tiller density prediction by exploring how those tillers develop through the season.

Table 4.1 Predictive factors included in tiller density model candidates. G, genotype; E, environment; M, management; GDD, cumulative growing degree days; PTQ, growing period photothermal quotient; T_{min}, mean daily minimum growing period temperature; T_{max}, mean daily maximum growing period temperature; T_{amp}, mean daily growing period thermal amplitude; CM, cumulative seasonal moisture (precipitation + irrigation, when applicable); VPD, cumulative vapor pressure deficit; PD, observed plant density; pH, soil test pH; OM, soil test organic matter (percent loss on ignition); NO_3, soil nitrate; NH_4, soil ammonium; P, soil phosphorus; CEC, soil test cation exchange capacity; Sand, percent soil sand; Silt, percent soil silt; Clay, percent soil clay.

Model Candidate	**GDD**	**PTQ**	**T_{min}**	**T_{max}**	**T_{amp}**	**CM**	**VPD**	**PD**	**G**
	°C day	MJ m^{-2} $°C^{-1}$ d^{-1}	°C	°C	°C	mm	kPa	pl ha^{-1}	
Full	●	●	●	●	●	●	●	●	●
Temporal	●	●							
Weather	●	●	●	●	●	●	●		
Soil									
E	●		●	●	●	●	●		
M	●					●		●	●
Stress			●	●		●	●		
G + E	●	●	●	●			●		●
G × E	●	●	●	●			●		●
E + M	●	●	●	●			●	●	
E × M	●	●	●	●			●	●*	
G + M								●	●
G × M								●	●
G + E + M	●	●	●	●			●	●	●
G × E × M	●	●	●	●			●	●*	●

Model Candidate	**pH**	**OM**	**NO3**	**NH4**	**P**	**CEC**	**Sand**	**Silt**	**Clay**
		% LOI	kg ha^{-1}	kg ha^{-1}	kg ha^{-1}	meq $100g^{-1}$	%	%	%
Full	●	●	●	●	●	●	●	●	●
Temporal									
Weather									
Soil	●	●	●	●	●	●	●	●	●
E	●	●	●	●	●	●	●	●	●
M	●		●	●	●				
Stress			●		●				
G + E			●		●				

G × E	●	●
E + M	●	●
E × M	●	●
G + M		
G × M		
G + E + M	●	●
G × E × M	●	●

* PD classified into three factor levels (A, 25000 plants ha^{-1}; B, 42000; C, 60000)

Table 4.2 Prediction accuracy metrics for tiller density model candidates. Lowest values for each distribution are shown in boldface type. MAE, mean absolute error of cross-season, out-of-sample predictions for test data set (80% train, 20% test); E, environment; M, management; G, genotype.

Model Candidate	MAE (tillers ha^{-1})
Full	9051
Temporal	13908
Weather	9362
Soil	19560
E	9362
M	11377
Stress	10605
G + E *	9116
G × E *	9736
E + M *	9066
E × M *	7776
G + M *	22764
G × M *	23131
G + E + M *	9050
G × E × M *	10371

Table 4.3 Out-of-season error evaluation resulting from independent coefficient eliminations by site-year. VPD, cumulative vapor pressure deficit; GDD, cumulative growing degree days; PTQ, growing period photothermal quotient; T_{max}, mean daily maximum growing period temperature; T_{min}, mean daily minimum growing period temperature; NO_3, soil nitrate; P, soil phosphorus.

Model	Location	Full Error	Lowest Error	Zeroed Coefficient
-2019 Train, 2019 Test	Manhattan	7211	4099	VPD
	Goodland	15003	5963	NO_3
	Garden City	23795	13366	T_{min}
-2020 Train, 2020 Test	Keats	280461	10283	P
	Greensburg	236793	56352	NO_3
	Goodland	39840	39840	
	Garden City	19574	19574	
	Colby B	272656	27344	PTQ
	Colby A	42732	27631	P
	Buhler	191106	1653	P
-2021 Train, 2021 Test	Selkirk	40372	9770	VPD
	Keats	9477	7280	GDD
	Greensburg	25012	11851	T_{min}
	Goodland	12594	6547	GDD
	Garden City	12847	1058	T_{max}
	Colby A	19507	8579	GDD
	Buhler	2564	912	VPD

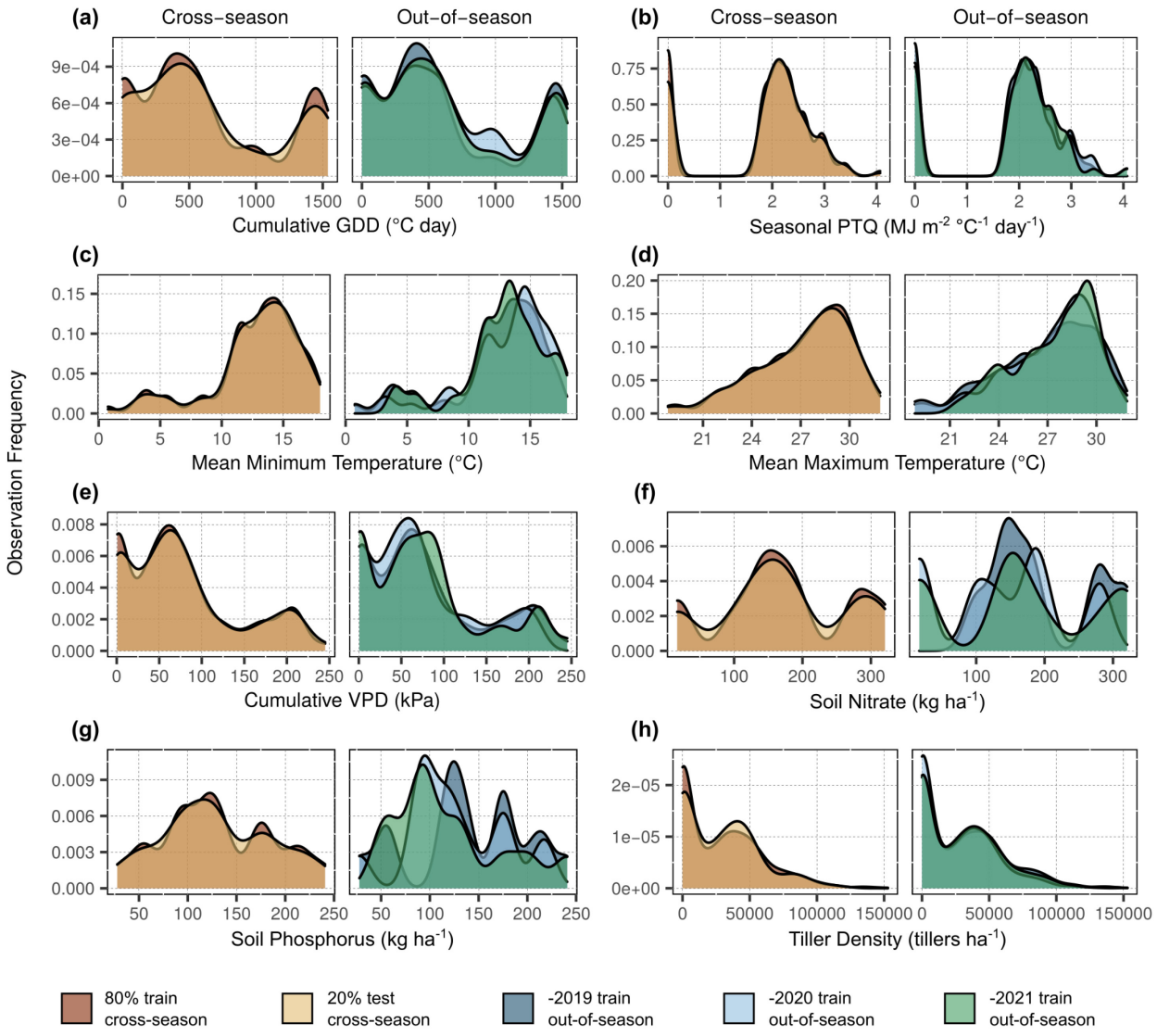

Figure 4.1 Observation frequency for key factors in dataset model splits. Y-axes indicate the observation frequency for each factor within a given dataset split. Factors shown are based on the selected model structure (Equation C.1) and include cumulative growing degree days (GDD; panel a), seasonal photothermal quotient (PTQ; panel b), mean minimum and maximum temperatures (panels c-d), cumulative vapor pressure deficit (VPD; panel e), soil nitrate (panel f), soil phosphorus (panel g), and response variable tiller density (panel h). The left side of each panel demonstrates the cross-season 80% train (rust), 20% test (gold) dataset split. The right side of each panel demonstrates the seasonal variation of the out-of-season (-2019, dark blue; -2020, pale blue; -2021, green) dataset splits.

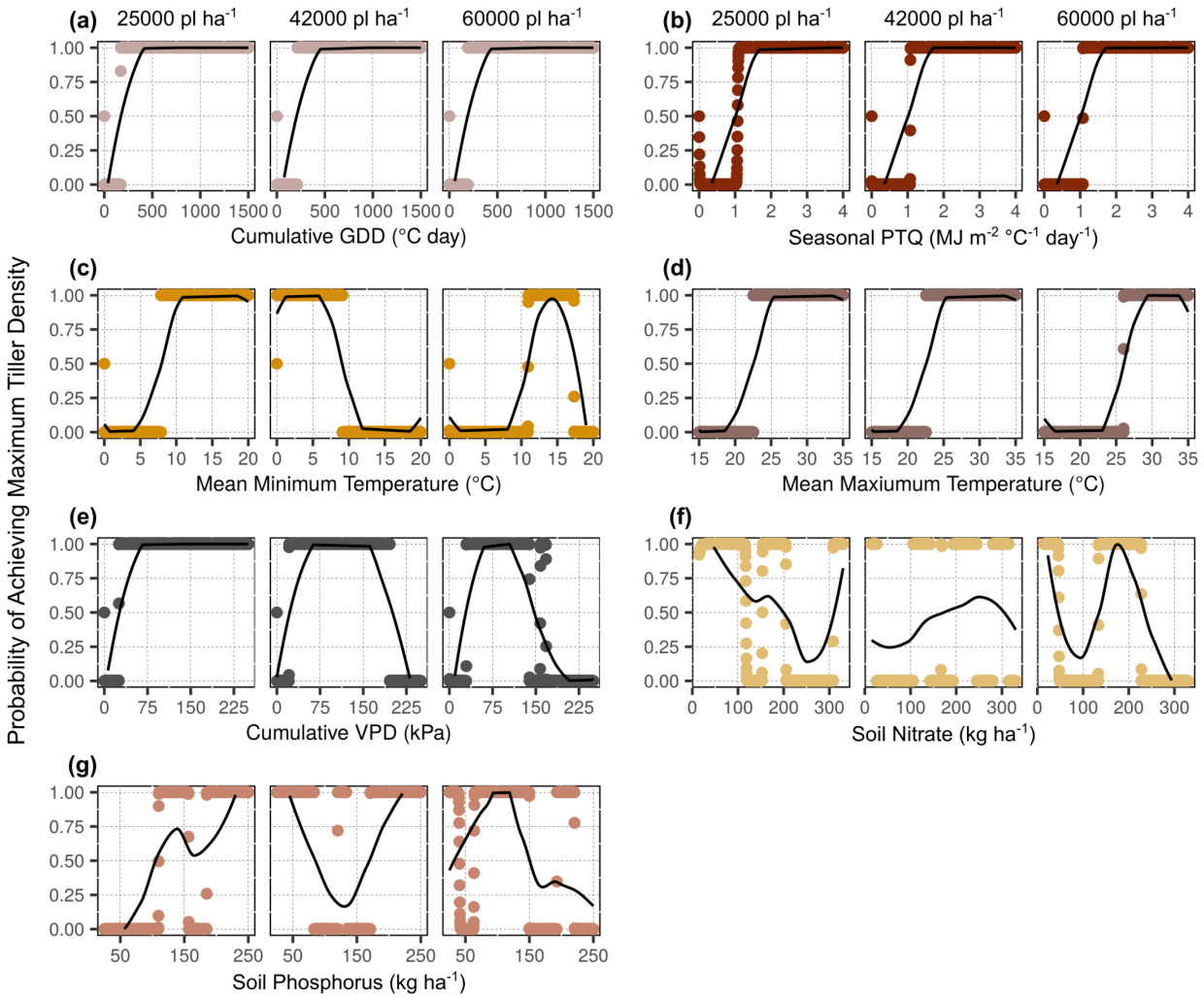

Figure 4.2 Independent smooth functions fitted to key environmental factors by target plant density. Y-axes indicate the model-generated probability of a maximum tiller density observation (300000 tillers ha^{-1}) across a range of potential factor levels. Probabilities for each variable level are shown with solid points, and moving averages are indicated with solid black lines. Factors shown include cumulative growing degree days (GDD; panel a), seasonal photothermal quotient (PTQ; panel b), mean minimum and maximum temperatures (panels c-d), cumulative vapor pressure deficit (VPD; panel e), soil nitrate (panel f), and soil phosphorus (panel g).

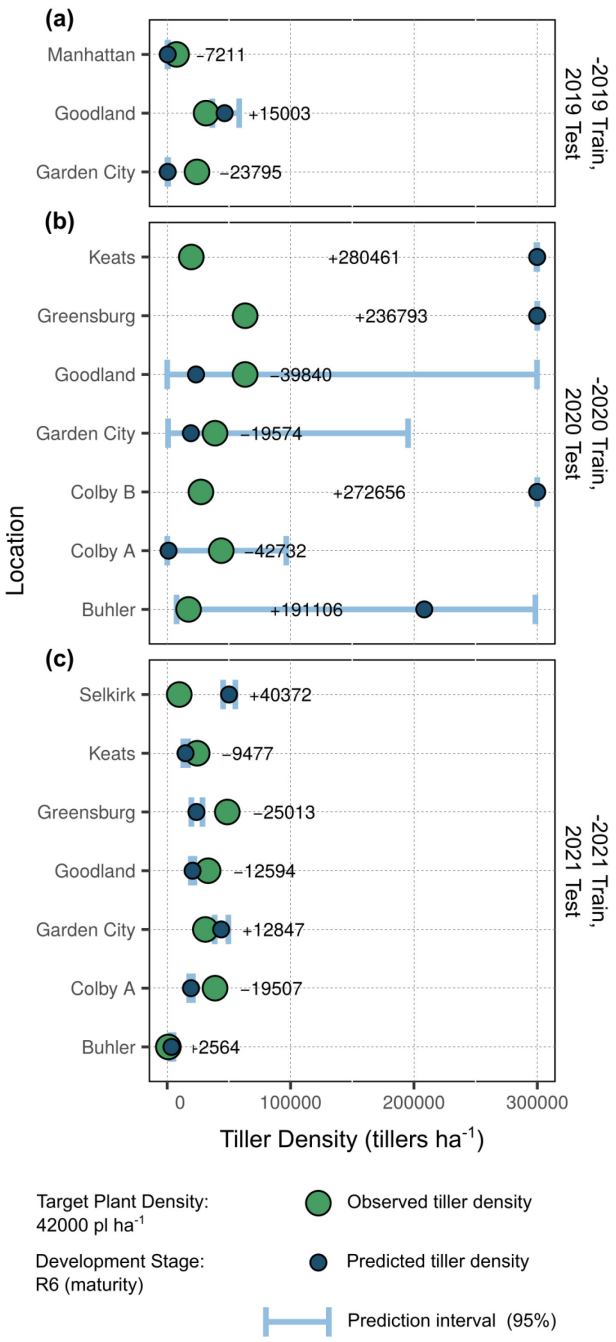

Figure 4.3 Predictions and predictive accuracy of out-of-season model fits (-2019, panel a; -2020, panel b; -2021, panel c) by site-year. Large green points indicate true tiller density observations for a plant density of 42000 plants ha^{-1} at development stage R6 (physiological maturity). Small dark blue points indicate model-generated predictions for tiller density (also 42000 plants ha^{-1} at stage R6). Pale blue bars indicate the 0.95 quantile prediction interval. In-row text indicates the error of the point prediction compared to the observed value for a given site-year.

Chapter 5 - Tiller biomass in low plant-density corn enhances transient C sink without direct harvest index detriment

**Under review in Field Crops Research*

Abstract

Tillering allows grass crops to adapt to their environment by increasing leaf area (source) and grain set (sink). Efficient translocation of water-soluble carbohydrates (WSCs) from tiller biomass is key to match the carbon (C) demand of ears. This ability is still commonly disputed, particularly in corn (*Zea mays* L.) when tillers are barren. Clarifying these points is imperative to determine tillering usefulness to corn growers, particularly when low plant densities are employed to manage restrictive environmental conditions with lower yield potential. Therefore, the objectives of the current study are to determine the following: 1) the impact of plant density and tiller presence on corn biomass accumulation, 2) the reproductive efficiency of tillered corn phenotypes considering the harvest index (grain to aboveground biomass ratio), and 3) the changes in stem C storage capacity and remobilization capabilities across tested E × M scenarios. The database used to accomplish these objectives included six site-years across Kansas, United States, three plant densities (25000, 42000, and 60000 plants ha^{-1}), two genotypes (P0657AM and P0805AM), and two tiller scenarios (intact or removed at stage V10). At these site-years, aboveground plant biomass and stem samples for WSC were collected at five unique timepoints throughout the season. Tiller presence stabilized aboveground biomass across plant densities and increased the WSC storage capacity in the lowest plant density. Comprehensive harvest index, for all treatments, was maintained at approximately 0.49 regardless of tiller biomass. Results indicate the tillers enhance WSC storage and augment main stem WSC remobilization during

grain fill. Findings support conclusions of previous yield-related publications from this database, but additional work is needed to specify the carbon economy in tillered corn plants.

5.1 Introduction

Branching, a plasticity mechanism employed by many crop species, facilitates crop adaption to the immediate environment (Laitinen and Nikoloski, 2019). Branching expression is therefore related to the quantity and quality of available resources and the need for such resources to produce plant biomass as additional leaf area and grain set. Intra-plant source-sink relationships are also critical, as the plant allocates photosynthates from leaves (source) to developing tissues, storage organs, and ultimately, grain (sink; Smith et al., 2018). Basal vegetative branches in grass crops such as grain sorghum (*Sorghum bicolor* L. Moench), wheat (*Triticum aestivum* L.), and corn (*Zea mays* L.) are known as tillers and appear from the crown region of the stem (Kim et al., 2010). Little is known about how tillers contribute to yield determination in corn, which is particularly relevant in the western US corn belt. In such environments, tillering is more commonly observed by corn growers.

A key function of tillers is increasing leaf area and aboveground biomass, thus enhancing the source of energy through photosynthates and grain set potential (Lafarge and Hammer, 2002). Essentially, tillers may 1) contribute to yield directly, 2) increase the rate of light interception and growth, and/or 3) store remobilizable carbon and nitrogen. Conversion efficiency is key to tiller effectiveness – both in converting environmental resources to biomass and biomass to grain. In environments with resource limitations requiring plant density reductions, efficient input use is crucial to maintain yield potential (Mylonas et al., 2020; Rotili et al., 2019). Tiller biomass not accounted for in the selection of a plant density may upset the

intended balance of environmental resources, which may be fragile in restrictive conditions. For example, alternative planting geometries (skip-row, clump, etc.) in environments with limited water supply aim to reduce tillering as a key prerogative (Haag, 2013; Kapanigowda et al., 2010; Thapa et al., 2020, 2018). Metrics such as radiation use efficiency (RUE; aboveground biomass increase per unit intercepted radiation), nitrogen (N) use efficiency (NUE; grain yield increase per unit N uptake), and water use efficiency (WUE; grain yield per unit water uptake) are generally unexplored for corn phenotypes expressing tillers. Rotili et al. (2021b) hypothesized WUE would be enhanced or maintained in tillered corn phenotypes, dependent on seasonality of precipitation. Similarly, if tillers develop and are barren, NUE is hypothesized to decrease (Rotili et al., 2021b), but more extensive N studies are needed to confirm these claims. Ear number plasticity (impacted directly by tiller expression) has been correlated with RUE and WUE plasticity in wheat (Sadras and Rebetzke, 2013). Tiller leaf area is strongly linked to water use in various grain crops (Jones and Kirby, 1977; Xue et al., 2013), but grain yield and reproductive efficiency are ultimately an indicator of WUE in such cases that moisture becomes limiting (George-Jaeggli et al., 2017). This is particularly true when moisture is supplied and utilized at key grain development stages. In summary, tiller barrenness can have repercussions for efficiency metrics across various grass crops. Reproductive efficiency is commonly quantified via the harvest index (HI), which is the ratio of grain to aboveground plant biomass. HI has remained relatively stable in modern corn genotypes at optimal plant densities, with yield potential largely reliant on increased biomass production (Hay, 1995). If tillers are barren, as commonly observed in corn, a reduced HI may be likely. Thapa et al. (2018) presented a negative correlation between tiller presence and crop HI using alternative planting geometries in restrictive growing environments, with all of the observed tillers barren. Rotili et al. (2021b)

presented an unusually high total HI for a tiller-prone corn genotype (HI 0.57) relative to a non-tillered counterpart (HI 0.49) in well-watered conditions. To the extent of authors' knowledge, targeted measurement of fertile corn tiller HI has not been documented.

Over cycles of selection, source and sinks were optimized iteratively to increase corn yields. The utility of corn tillers may be more subtle than direct grain set (Veenstra et al., 2021). Enhanced by tiller formation, the allocation of water-soluble carbohydrates (WSCs) in grass stem tissues (Bihmidine et al., 2013) can provide a larger reservoir of non-structural C for tillered relative to non-tillered counterparts. The usefulness of this ability hinges on tiller capability to accomplish one of the following: 1) directly set and fill grain using the WSC stored in their own stems, or 2) efficiently translocate the WSC stored in their stems to ears set on the main stalk. These two points were key in foundational work executed by Alofe and Schrader (1975), in which WSC movement from tillers to main stalks was documented and characterized by relative shoot sink strengths. In addition to WSC, mobile nutrients like phosphorus (P) have been shown to relocate from tiller to main stalk tissues in reproductive stages, particularly when tillers are small and barren (Russelle et al., 1984). Such a relationship has been proposed for nitrogen (N), but remains untested to current knowledge (Rotili et al., 2021b).

Past work revealed yields were not deleteriously impacted by tiller presence and greater tiller densities could compensate for plant density deficits in favorable environments (Veenstra et al., 2021). Considering that plant density remained a key management practice to maximize yield regardless of tiller development in Veenstra et al. (2021) and main stalk yields were not reduced by tiller presence in the same experiments (Veenstra and Ciampitti, 2021), tiller source-sink economies appear to be supportive or mostly independent of main stalk counterparts. A deeper exploration of the reproductive efficiency and source-sink dynamics of tillered corn phenotypes

is warranted. Authors hypothesize that tiller presence increased plant biomass and improved plant C capture and reproductive efficiency – but this is dependent on tiller barrenness. Therefore, the objectives of the current study are to determine 1) the impact of plant density and tiller presence on corn biomass accumulation, 2) the reproductive efficiency of tillered corn phenotypes considering the harvest index, and 3) the changes in stem C storage capacity and remobilization capabilities across tested E × M scenarios.

5.2 Materials and Methods

5.2.1 Field Experiments

This study explored a large field database collected across Kansas, USA, in the 2019-2021 growing seasons. These field trials considered three plant densities (lowest, 25000; moderate, 42000; and highest, 60000 plants ha^{-1}), two genotypes (P0657AM and P0805AM; Corteva Agriscience, Johnston, IA), and two tiller scenarios (intact or removed at development stage V10; tenth leaf, Ritchie et al., 1997). Detailed experimental site descriptions are available in Tables 2.1 and 3.1 (Veenstra et al., 2021). Data for the present study included six of the site-years described in these past studies – Manhattan 2019, Garden City 2019 and 2021, Goodland 2019 and 2021, and Keats 2021. These site-years were the only six trials where intensive biomass samplings were conducted, due to the effort required to accomplish such samplings. In light of this, the selected site-years were located in far corners of the state, capturing the highest degree of environmental variation possible.

5.2.2 Data Collection and Calculations

Aboveground fresh biomass was collected in buffered 1-row, 1.5-m sampling zones at five pre-determined time points throughout the season in each site-year. Data were collected at

target development stages V5 (fifth leaf), V10 (tenth leaf), V16 (sixteenth leaf), R3 (kernel milk stage), and R6 (physiological maturity). After the initial fresh weight was recorded for the appointed sampling zone (two to seven plants, dependent on plant density), two representative plants were selected from each sample. Representative plants were partitioned into stems (stems + leaf sheaths), leaves (green + senescent blades), reproductive (husks + silks + cobs + tassels, if present), and grain (kernels, if present). This was done separately for main shoots and tiller shoots, if present. Fresh weights of each partition were used to calculate the percentage of total fresh weight attributed to each organ class, which was then multiplied by the total sampling zone biomass. Partitions were dried in an air-forced oven at 60 °C until constant weight to achieve moisture content for each organ class. Resulting dry matter calculations were scaled to a kg ha^{-1} basis.

Stem partitions were ground using a 0.25-mm sieve and analyzed for water-soluble carbohydrate (WSC) concentration. All 2019-collected samples were analyzed by sequential extractions in water followed by colorimetric reaction via the anthrone reagent method (Galicia et al., 2009). WSC concentrations of 2021 samples were estimated through near-infrared (NIR) spectroscopy (DA 7250, Perten Instruments, Sweden), using the 2019 samples for instrument calibration. WSC concentrations were multiplied by stem dry biomass to obtain WSC content, which was scaled to a g m^{-2} basis. WSC content was used in all data analyses.

The central two plot rows were reserved for grain harvest (harvested area of approximately 6 m^2). Ears remaining on plants at dry maturity were picked and shelled by hand. Yields were calculated based on actual harvested area and a 155 g kg^{-1} grain moisture. Grains from tillers and main shoots were handled separately. Harvest index (HI) was calculated as dry

grain weight ha^{-1} divided by total aboveground dry biomass ha^{-1} for the main and tiller shoot fractions individually, as well as the total (all shoots).

Seasonal growing degree days (GDD) were calculated using weather data downloaded from the Climate Engine web application (Huntington et al., 2017). GDD was calculated as the cumulative sum of the difference between mean daily temperature and the crop base temperature of 10 °C, with a forced daily maximum of 30 °C.

5.2.3 Statistical Analyses

5.2.3.1 Seasonal dynamics

Initial analyses considered additive organ biomass (leaves only, leaves + stem, leaves + stem + reproductive + grain; where reproductive considered husks, silks, cobs, and tassels, if present) and carbohydrate content as responses to treatment factors and time of sampling. All data analyses were performed in program R (R Core Team, 2022). Linear mixed effects models were fit using the *lme4* package (Bates et al., 2015). Fixed effects included plant density, genotype, tiller presence, and target sampling stage, with site-year, block, whole-plot, and sub-plot set as random intercept effects. The fitted models were subjected to a Type III analysis of variance (ANOVA) for each fixed effect using the *car* package (Fox and Weisberg, 2019). Least squares means were calculated using the *emmeans* package (Lenth, 2020). These initial ANOVA results are available in Table D.1 (aboveground biomass by organ) and Table D.2 (WSC content).

Seasonal dynamics of biomass and WSC accumulation (for both $plant^{-1}$ and ha^{-1} scales) and relative shoot contributions to each (for both main stalks and tillers) were visualized as flexible smoothed effects of cumulative GDD. These models were applied via smoothing cubic splines with the *smooth.spline()* function in the base *stats* package, with cumulative GDD as the

predictor variable for each plant density × tiller presence interaction. Seasonal dynamics of full crop biomass (leaves + stem + reproductive + grain) are known to produce a logistic curve, and were thus fitted to the following equation for each plant density × tiller presence interaction:

$$b = \alpha/1 + e(p - g)/s, \qquad \textbf{Eq (5.1)}$$

where b is the total aboveground biomass, α is the asymptote, p is the curve inflection point, g is the cumulative GDD, and s is the scale parameter. Logistic models were fit using the *getInitial()* and *SSlogis()* functions in the base *stats* package to generate starting values and estimate model parameters.

5.2.3.2 Plant fraction relationships

Simple linear models ($y = mx + b$) were fit using the *lm()* function of the base *stats* R package to explore plant fraction (i.e., tiller and main stalk) relationships for HI and WSC. Models were selected as more appropriate than the mean ($y = b$) based on the threshold $p \leq 0.05$. The coefficient of determination (R^2) was calculated for each.

5.3 Results

5.3.1 Environmental Characterization

Environmental characterizations are available for the six evaluated site-years in Figure D.1. Normal seasonal precipitation for these site-years ranged from 355 to 547 mm, with half of the evaluated site-years wetter than normal. Normal seasonal mean temperature ranged from 19.2 to 22.4 °C, with 67% of site-years cooler than normal. Yields ranged from 5.8 to 12.6 Mg ha^{-1}.

5.3.2 Biomass Dynamics

Least squares means and seasonal progression curves for aboveground biomass by organ are shown in Figure 5.1. Maximum mean leaf biomass ha^{-1} was observed at R3. Leaf biomass ha^{-}

^{1} was greater with tillers present in the lowest plant density after stage V10 (Fig. 5.1a) and from flowering to R3 in the moderate plant density (Fig. 5.1b). Maximum leaf and stem biomass ha^{-1} was also observed at R3. Stem and leaf biomass ha^{-1} was greater with tillers present in the lowest plant density after stage V10 (Fig. 5.1a) and in the moderate plant density in early grain-filling stages (Fig. 5.1b). Stem biomass contributed the most to increased biomass with tillers present in the lowest plant density (up to 1939 kg ha^{-1}). Maximum total (leaf + stem + reproductive + grain) biomass ha^{-1} was observed at R6. Total biomass was only greater with tillers present in the lowest plant density at maturity (Fig. 5.1a), where total biomass with tillers intact was not significantly different from the higher plant densities (Fig. 5.1b-c).

Leaf biomass pl^{-1} was only significantly different due to tiller presence in the lowest plant density after V10 (Fig. 5.1d) and at R3 in the moderate plant density (Fig. 5.1e). Maximum leaf and stem biomass pl^{-1} was significantly different between tiller treatments in the lowest plant density after stage V10 (Fig. 5.1d) and in the moderate plant density in early grain-filling stages (Fig. 5.1e). Stem biomass contributed the most to increased biomass with tiller presence in the lowest plant density (up to 0.08 kg pl^{-1}). Total biomass pl^{-1} was only different due to tiller presence in the lowest plant density after flowering (Fig. 5.1d).

Main shoots were responsible for a majority of aboveground biomass production (Fig. 5.1g). Tiller contributions to biomass were inversely related to plant density, with the 25000, 42000, and 60000 pl ha^{-1} densities maximized at 33%, 15%, and 4% tiller biomass, respectively. All plant densities declined in tiller biomass proportion in late grain-filling stages (Fig. 5.1g).

5.3.3 Harvest Index

Main shoot HI values ranged from 0.15 to 0.67 (mean 0.51). Tiller shoot harvest index values ranged from 0 (no grain produced) to 0.66 (mean 0.22). For both tiller and main shoot

fractions, greater biomass was positively correlated with greater HI (Figure 5.2). Tiller fractions exhibited a steeper slope, but total (main + tiller shoots) HI values (mean 0.49) were not correlated with tiller shoot biomass.

5.3.4 Water-soluble Carbohydrate Dynamics

Least squares means and seasonal progression curves for stem WSC content are shown in Figure 5.3. Maximum mean WSC content m^{-2} was observed at R3. Stem WSC content m^{-2} was only significantly higher with tillers present in the lowest plant density after flowering (Fig. 5.3a). Mean stem WSC content m^{-2} at maturity was greatest (99 g) in the lowest plant density with tillers intact (Fig. 5.3a), and the least (49 g) in the same plant density but with tillers removed (Fig. 5.3a).

Maximum mean WSC content pl^{-1} was also observed at R3, greatest (50 g) in the lowest plant density (Fig. 5.3d), and least (25 g) in the highest plant density (Fig. 5.3f), both with tillers intact. Stem WSC content pl^{-1} was only significantly greater with tillers present than tillers removed in the lowest plant density after flowering (Fig. 5.3a). Mean stem WSC content pl^{-1} at maturity was greatest (41 g) in the lowest plant density with tillers intact (Fig. 5.3d), and the least (11.4 g) in the highest plant density with tillers removed (Fig. 5.3f).

Main shoots were responsible for a majority of WSC content (Fig. 5.3g), averaging 91% across all plant densities and sampling stages. Tiller contributions to WSC content were inversely related to plant density, with the 25000, 42000, and 60000 pl ha^{-1} densities maximized at 44%, 17%, and 6% tiller WSC content, respectively. All plant densities declined in tiller WSC content proportion in late grain-filling stages (Fig. 5.3g).

5.3.5 Water-soluble Carbohydrates and Grain Fill

Main stem WSC (g m^{-2}) relationships to sink strength during grain fill are shown in Figure 5.4. Comparing tillered to non-tillered phenotypes at stage R3, main stalks with barren tillers behaved most similarly to plants without tillers (Fig. 5.4a, b). That is, greater main stem WSC was strongly associated with greater grain production (R^2 of 0.39 and 0.42 for non-tillered and tillered plants with barren tillers, respectively). Non-tillered phenotypes maintained the relationship with main stem WSC observed at R3 through stage R6, with greater main stem WSC associated with higher grain production (Fig. 5.4b, d). However, mature grain production of tillered phenotypes was not associated with main stem WSC (Fig. 5.4c). Tillered phenotypes with barren tillers produced 1.5 Mg ha^{-1} more dry grain on average than phenotypes with grain-bearing tillers. Comparing tillered and non-tillered phenotypes, minimum and achievable yields were similar (approximately 2.5 to 15 Mg ha^{-1}; Fig. 5.4c, d).

5.4 Discussion

As a complement to explorations of tiller impact on corn yield (Veenstra et al., 2021; Veenstra and Ciampitti, 2021), this study presents new insights on seasonal dynamics of aboveground biomass, reproductive efficiency, and source-sink relationships of tillered corn phenotypes. Tiller impact on biomass and energy relationships in corn is less explored relative to other crops, but this knowledge is foundational to understanding yield and development observations reported previously (Massigoge et al., 2022; Rotili et al., 2021b, 2021a). While labeled WSC work in tillered corn phenotypes was done nearly 50 years ago (Alofe and Schrader, 1975), this study fills a modern research gap by quantifying season-long dynamics of aboveground biomass and WSC movement in both main shoots and tiller shoots in field environments.

As expected, tiller development increased plant biomass, but this was plant density-based as in previous studies (Rotili et al., 2021b; Tetio-Kagho and Gardner, 1988). In effect, tillered phenotypes were able to produce similar aboveground biomass with less than half of the plant density. Main shoots remained the main contributor of biomass, likely due to reproductive preference and apical dominance (Doebley et al., 1997). In agreement with the plant density-based observations of (Duvick et al. (2004), increased shoot biomass was accompanied with a greater HI regardless of shoot type (i.e., main or tiller). Because HI is relatively stable, gains in modern corn grain yields are driven by shoot biomass (Lorenz et al., 2010). Conversely, Thapa et al. (2020) demonstrated a reduced HI was possible when plants were unable to sustain grain production with additional shoot biomass in water-limited environments, but these outcomes were identified in alternative planting geometries (i.e., skip-row, clump, etc.). The efficiency of tillers in converting biomass to grain was more dynamic across biomass accumulations than the efficiency of main plants. Both main and tiller had similar maximum HI values. In this light, greater tiller biomass was not correlated with comprehensive (main + tiller shoots) HI, which was potentially more related to yield environment and post-flowering stresses (Rotili et al., 2022). Specifically, tiller reproductive efficiency compared to main stalk counterparts appears dependent on plant growth rate, an indicator of plant health and stress. Tiller-influenced HI ranges in the present study were representative of the high values (0.57) reported in well-watered conditions of other studies (Rotili et al., 2021b) and even lower values (0.33) reported in more restrictive conditions (Thapa et al., 2020). Ultimately however, as the achievable tiller HI in the present study was represented by well-watered scenarios in the literature (Rotili et al., 2021b), and tiller HI was strongly tied to biomass production, this study perhaps failed to capture

scenarios where moisture was truly limiting to tiller development. More restrictive scenarios could therefore reduce tiller efficacy as previously hypothesized (Stewart, 2009).

Tillered phenotypes appeared quite effective at converting their own shoot biomass to grain or supporting grain fill elsewhere on the plant. In previous studies, tillers were able to overcome the strongly limited WSC storage capacity per plant across plant densities (Cazetta and Revoredo, 2018) by providing additional transient sinks. In the current study, such a relationship was only observed at the lowest plant density (10000 pl ha^{-1}), presumably due to reduced tiller number per plant and tiller biomass as plant density increased (Hansey and de Leon, 2011; Rotili et al., 2021b; Tetio-Kagho and Gardner, 1988).

Strong evidence for tiller nourishment of main stalks has been demonstrated in this study by tillered phenotypes, regardless of sink capacity, as previously reported (Alofe and Schrader, 1975; Dungan, 1931; Russelle et al., 1984). Alofe and Schrader (1975) used targeted $^{14}CO_2$ labeling of tillered corn phenotypes at grain fill to determine that fixed C remained in the labeled plant fraction (tiller or main stalk) unless barren tillers were labeled, in which case a majority of the ^{14}C was recovered in main stalk grains. In the current study, the relationship between main stem WSC and grain production was interrupted at maturity by tillered phenotypes. The utility of transient sink alternatives (i.e., main stem versus tiller stems) is important when considering restrictive growing environments. While tiller sink strength (barren or grain-bearing) did not change the general relationship between main stem WSC and grain production, plants with barren tillers yielded significantly more on average. This suggests that tillered corn phenotypes may be more productive overall when grain is not set directly on the tillers and tillers are instead used as buffered WSC reserves. This WSC buffering is agronomically significant for several reasons, including standability and stabilized kernel weights (Campbell, 1964; Esechie, 1985;

Slewinski, 2012). Two caveats for this generalization, however, are 1) the correlation between tiller productivity and plant density (i.e., tillers in high plant densities are less likely to set grain due to increased competition), and 2) the nature of the grain-bearing inflorescences observed on tillers. Tillers may produce no ear (barren), a grain-bearing axillary ear, or a grain-bearing apical ear (Bonnett, 1948; Schaffner, 1930). Both ear types are considered sinks, but only axillary ears are reliably harvestable. That is, the generalization of tiller productivity may be altered if the target plant density is not achieved or if only productive sinks (axillary ears) are considered. More intensive samplings of tillered corn phenotypes (and a non-tillered check) through grain fill with contrasting tiller ear development would be useful to explore this point of WSC (and overall plant C) economy.

Potential bottlenecks in this study are linked to the lack of quantification of other resource use efficiencies (NUE, WUE, RUE). Tillered corn phenotypes have been suggested as both detrimental (additional leaf area) and beneficial (additional grain set) to these metrics. Because WUE was impacted by unusual planting geometry (which subsequently reduced tiller number) in Thapa et al. (2020, 2018) and Kapanigowda et al. (2010), WUE conclusions of tillered versus non-tillered phenotypes are unclear from these studies. The lack of correlation between tiller productivity and tiller density to water factors suggests this study did not include levels of water deficit severe enough to impact tiller development (Veenstra et al., 2021; Figure D.1). Massigoge et al. (2022) presented tillered phenotypes as a potential source of yield and efficiency enhancement, with environments similar in productivity (approximately 3 to 12 Mg ha^{-1}) to the sites of Thapa et al. (2020) and Kapanigowda et al. (2010). Beyond efficiency metrics, an economic analysis of tillering as a plasticity mechanism in low-density corn should

also be explored. Doing so is imperative to advance climate-smart management decisions in light of crop plasticity utility (Brooker et al., 2022).

5.5 Conclusions

The proposed hypothesis "*that tiller presence increased plant biomass and improved plant C capture and reproductive efficiency dependent on tiller barrenness*" is partially supported by our results. Tiller presence did indeed enhance plant biomass production, but only meaningfully in the 10000 pl ha^{-1} density. Because a majority of additional biomass from tillers was stem tissue, additional carbon storage was provided. This reserve allowed plants to escape the per-plant cap on WSC accumulation at low plant densities, which is typically managed by increasing plant density. Within the range of productivity environments in this study, tillers alone did not impact reproductive efficiency, regardless of sink size or biomass allocation. In addition, authors propose that tiller-accumulated WSC acts to augment main stem WSC reserves. These additional transient sinks are proposed as a contributor to the yield stability observed across environments.

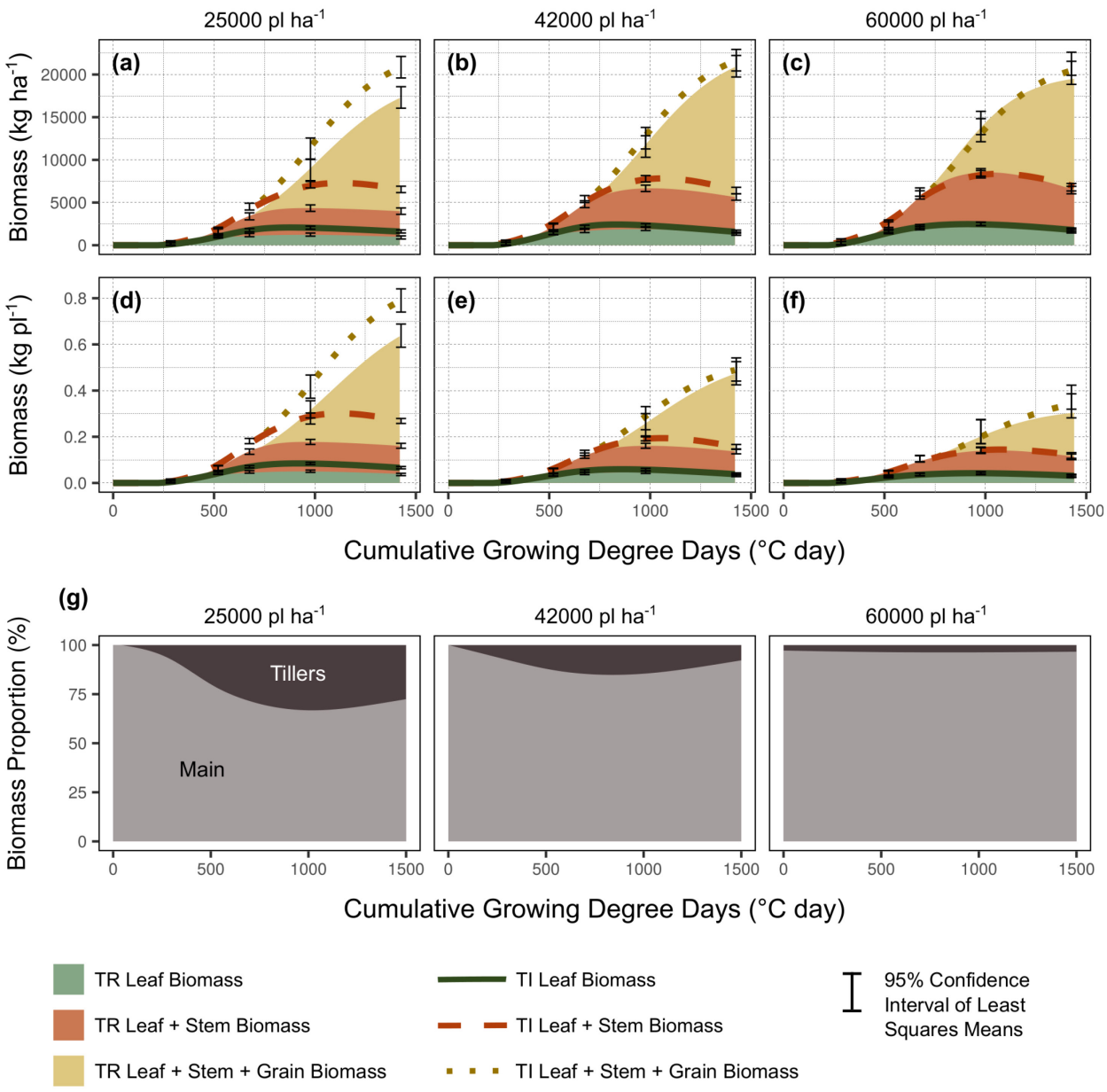

Figure 5.1 Seasonal aboveground biomass accumulation from both hectare and individual perspectives by plant fraction. Panels a-f depict total aboveground biomass accumulation of each organ (leaf, green; leaf + stem, orange; leaf + stem + reproductive, yellow) by plant density (25000, 42000, and 60000 pl ha^{-1}) for both kg ha^{-1} and kg pl^{-1} perspectives. Biomass of plants with tillers removed is shown as an area plot (pale colors), while biomass of plants with tillers intact is indicated with lines (vibrant colors). Whisker bars indicate the 95% confidence interval of the least squares means for each of five sampling observations (V5, V10, V16, R3, and R6). Panel g depicts the relative proportion of tillered phenotype biomass attributed to main shoots (light area) and tiller shoots (dark area) for each plant density throughout the season.

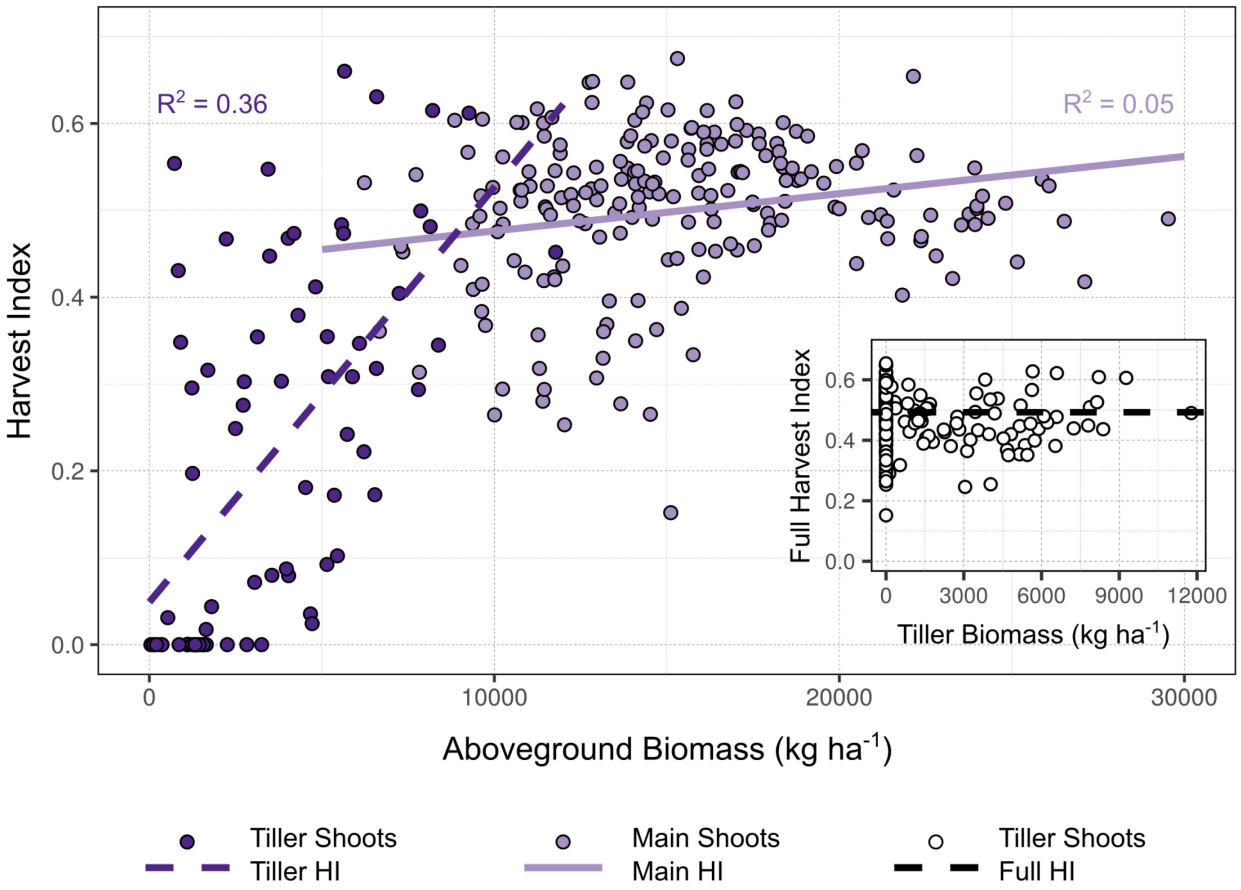

Figure 5.2 Mature aboveground biomass (x-axis) and harvest index (y-axis) by plant fraction. Dark circles and dark, dashed lines indicate tiller shoot biomass and tiller shoot harvest indices (HI); pale circles and pale, solid lines indicate main shoot biomass and main shoot harvest indices. Inset – relationship between tiller mature biomass (x-axis) and full shoot harvest index (y-axis).

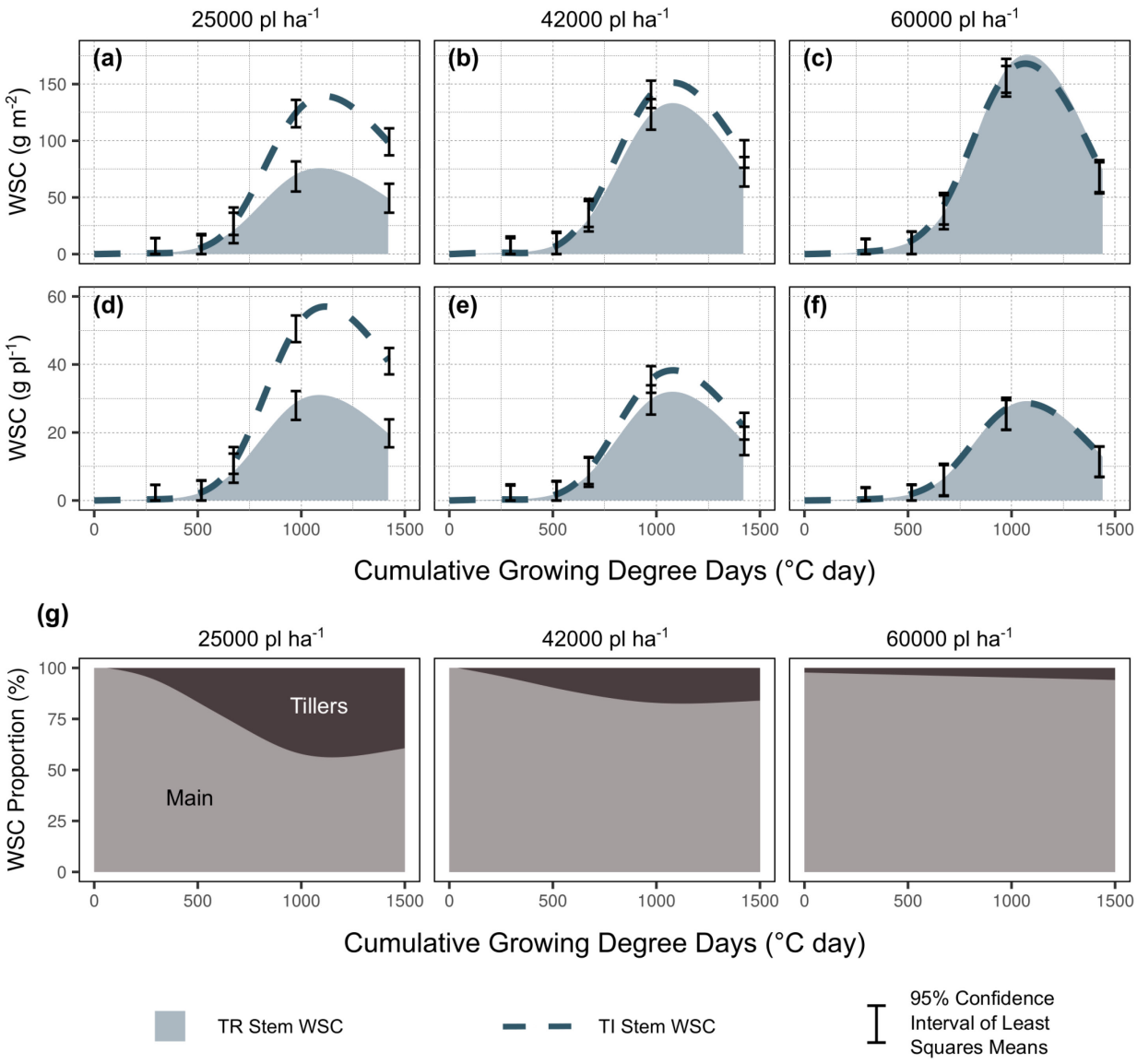

Figure 5.3 Seasonal stem water soluble carbohydrate (WSC) accumulation from both hectare and individual perspectives by plant fraction. Panels a-f depict total stem WSC accumulation by plant density (25000, 42000, and 60000 pl ha^{-1}) for both g m^{-2} and g pl^{-1} perspectives. WSC content of plants with tillers removed (TR) is shown in pale blue areas, while biomass of plants with tillers intact (TI) is indicated with dark blue dashed lines. Whisker bars indicate the 95% confidence interval of the least squares means for each of five sampling observations (V5, V10, V16, R3, and R6). Panel g depicts the relative proportion of tillered phenotype WSC found in main stems (light area) and tiller stems (dark area) for each plant density throughout the season.

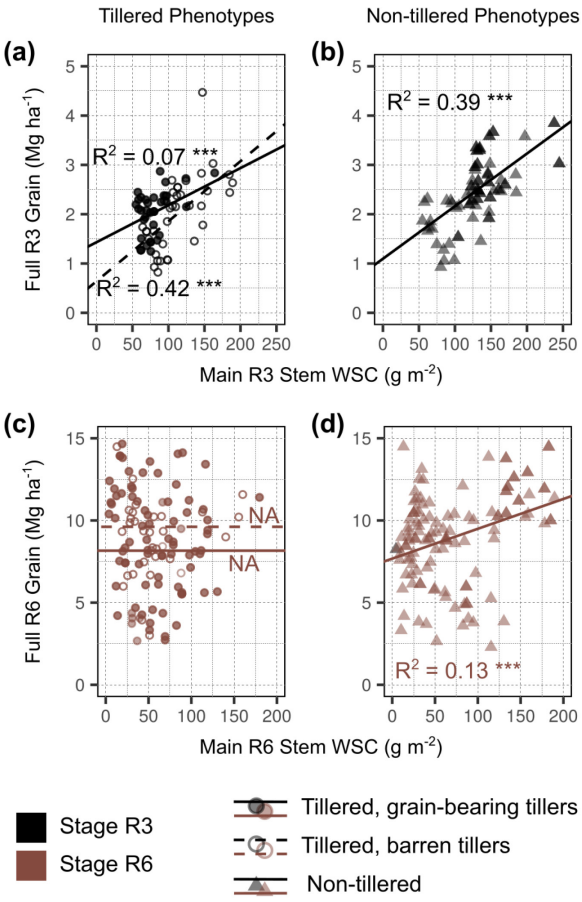

Figure 5.4 Main stem water-soluble carbohydrate (WSC) sink (grain) relationships by development stage (R3 – black, R6 – rust). Tillered phenotypes (panels a, c) are grouped by sink strength – barren tillers indicated by empty circles and short-dashed lines, grain-bearing tillers indicated by filled circles and solid lines. Non-tillered phenotypes (panels b, d) are indicated by triangles and solid lines. Linear relationships between x and y variables are paired with either coefficient of determination (R^2) and *p*-value (where *** indicates $p \leq 0.001$) or "NA" if only the intercept was significant.

Chapter 6 - Conclusions

This dissertation sought to quantify, characterize, and adequately describe the usefulness of a generally unstudied plasticity mechanism in dent corn – tillering, to plants and corn growers. Research and actionable information regarding tillering in corn production are largely unavailable. This area of study is particularly relevant in environments where crops are resource-limited or environments in which the target plant density is not properly achieved. This study utilized two tillered corn phenotypes in a range of environment (E) × management (M) scenarios across the state of Kansas, United States (US), to progress the objectives listed below.

6.1 Determine impact of tiller development on corn yields (Chapter 2)

With the hypothesis that tiller expression would alter corn yields, intermediate objectives to evaluate this hypothesis were as follows: 1) quantify the relative importance of E, M, and their interactions on the yield effect of tiller expression for two modern corn genotypes; 2) understand effects of observed tiller density, plant density, and their interaction on yield; and 3) identify key environmental determinants of yield response to tiller density in modern corn genotypes.

Results in Chapter 2 demonstrated that tillers did not reduce corn yields in any of the evaluated environments with the tested genotypes. Favorable environments (most notably, high PTQ and desirable soil properties) facilitated increased yields when tillers were present. This response, however, was coupled with a sub-optimal plant density, and was cancelled out when plant density was ameliorated. While tiller production reliability was not explored, this chapter presented critical evidence of the potential usefulness of tiller expression as a corn plasticity trait. Subsequent chapters built upon this groundwork.

6.2 Determine the plastic extent and relative importance of yield components (Chapter 3)

With the hypothesis that "*that tiller expression improved plasticity of yield components, thereby reducing plant density-based yield dependency*", intermediate objectives to evaluate this hypothesis were to explore the consequences of tiller expression on corn yield component determination and plasticity in a range of environments from two plant fraction perspectives – 1) main stalks only, considering potential functional trade-offs due to tiller expression; and 2) comprehensive (main stalk plus tiller contributions as an overall view of plasticity potential).

Results in Chapter 3 demonstrated that tiller contributions to reproductive plasticity facilitated mitigation for reduced plant densities. This tiller capability surpassed secondary ear grain contributions in the best environments, in fact. The softened hierarchy of yield formation in such a deterministic crop can perhaps enhance plasticity usefulness in climate-smart management and phenotypic progression as breeders work to adapt to volatile seasonal impacts of climate change.

6.3 Determine the drivers and predictability of corn tiller development (Chapter 4)

With the hypothesis that "*corn tiller densities in tiller-prone genotypes could be reliably predicted within 25% of the target plant density using variables related to crop management and environmen*t", intermediate objectives to evaluate this hypothesis were as follows: 1) identify key environment, management, or combinations of these variables useful for predicting tiller density dynamics in corn; and 2) test out-of-season prediction accuracy for identified variables.

Results in Chapter 4 demonstrated that tiller expression was predictable within realistic and useful error ranges. Based on conclusions from previous chapters, tiller density (tillers ha^{-1}) can play an important role in yield formation (yield components) and realization (harvested grain). If plasticity expression (in this case, tillering in corn) can be predicted, it follows that producer incorporation into decision-making strategies is feasible. Understanding the seasonal behavior of this particular corn trait could benefit producers facing challenges related to field uniformity, climate, or other unforeseen mid-season circumstances.

6.4 Determine the effect of tiller expression on biomass accumulation, carbon economy, and subsequent reproductive efficiency (Chapter 5)

With the hypothesis that "*tiller presence increased plant biomass and improved plant C capture and reproductive efficiency – but this is dependent on tiller barrenness*", intermediate objectives to evaluate this idea were to determine the following: 1) the impact of plant density and tiller presence on corn biomass accumulation, 2) the reproductive efficiency of tillered corn phenotypes considering the harvest index, and 3) the changes in stem C storage capacity and remobilization capabilities across tested E × M scenarios.

Results in Chapter 5 demonstrated that tillered phenotypes were able to escape the plant density-regulated biomass and carbohydrate accumulation patterns. The additional biomass produced when tillers were expressed was not associated with plant harvest index. This indicates tillers may not be directly responsible for efficiency reductions generally assumed in expressing phenotypes. Certainly, more restrictive environments (with fewer resources) could alter this outcome. Harvest index neutrality was accompanied by altered dynamics of C reserves during grain filling, with tillers augmenting main stem remobilization during this period. This final

chapter solidified the findings of previous chapters, indicating that internal plant dynamics support yield-based theories.

6.6 Future work and outstanding questions

A great deal of interest and conversation about plasticity in a historically non-plastic crop (corn) has stemmed from the writing and dissemination of the work presented here. While study components presented useful and opportune conclusions regarding drivers, development, and impact of corn tillers on yield stability across the state of Kansas, much work remains to be done. Such wonderings and future directions are outlined below.

6.6.1 Reproductive development of corn tillers

A common theme presented throughout the chapters of this dissertation is the dependency of tiller productivity on development – both appearance and ultimate ear type (or barrenness). Although reproductive development does not appear to have a significant deleterious impact on yield, successful development of tiller axillary ears seems to increase yield potential in environments without an optimized plant density (Chapter 3). Chapter 5 presented the case of source-sink relationships, which are certainly impacted by reproductive development of tiller shoots. While Chapter 4 provided insight on tiller numbers, tiller reproductive development has yet to be explored. The dataset collected for this dissertation includes information needed to expand on this point and should be evaluated to understand these relationships.

6.6.2 Risk-reward of plasticity mechanisms in defensive production systems

Although the chapters presented here provide useful insight of tiller potential in corn production systems, a key question commonly raised by producers is the economic value of such information. Certainly, as discussed in the introduction, implementation at the farm level of

results from plasticity studies is far from achieved. The utility of such traits and related mechanisms (corn tillers, for example) is highly subjective and changes seasonally. Incorporating this information into decision tools is a daunting task.

Risk-reward analysis is a key part of producer decision-making processes. Production systems in harsher growing environments (such as those more commonly impacted by volatile weather patterns) are forced to implement defensive strategies to remain viable and profitable. With climate change projections and other challenges related to water availability (e.g., Ogallala aquifer depletion in southwest Kansas), supply chain disruptions, etc., balancing the strategic use of available resources and maintaining profit may become more difficult. Development of tools related to environmental adaptation must include economic and social perspectives as a foundational component of their structure to be useful or successful in this regard.

6.7 Data Availability Statement

The data used to generate the results and support the conclusions of this dissertation will be made publicly available following publication of these chapters. In addition, Ciampitti Lab will gladly provide this data upon request.

References

Abdelrahman, M., Burritt, D. J., Gupta, A., Tsujimoto, H., & Tran, L.-S. P. (2020). Heat stress effects on source–sink relationships and metabolome dynamics in wheat. *Journal of Experimental Botany*, *71*(2), 543–554. https://doi.org/10.1093/jxb/erz296

Adriani, D. E., Lafarge, T., Dardou, A., Fabro, A., Clément-Vidal, A., Yahya, S., Dingkuhn, M., & Luquet, D. (2016). The qTSN positive effect on panicle and flag leaf size of rice is associated with an early down-regulation of tillering. *Frontiers in Plant Science*, *6*. https://doi.org/10.3389/fpls.2015.01197

Aguilar, J. J., Moore, M., Johnson, L., Greenhut, R. F., Rogers, E., Walker, D., O'Neil, F., Edwards, J. L., Thystrup, J., Farrow, S., Windle, J. B., & Benfey, P. N. (2021). Capturing in-field root system dynamics with RootTracker. *Plant Physiology*, *187*(3), 1117–1130. https://doi.org/10.1093/plphys/kiab352

Ajal, J., Kiær, L. P., Pakeman, R. J., Scherber, C., & Weih, M. (2022). Intercropping drives plant phenotypic plasticity and changes in functional trait space. *Basic and Applied Ecology*. https://doi.org/10.1016/j.baae.2022.03.009

Akman, Z. (2002). Effect of tiller removing and plant density on ear yield of sweet corn (Zea mays saccharata Sturt). *Pakistan Journal of Biological Sciences*, *5*(9), 906–908.

Alam, M. M., Hasanuzzaman, M., & Nahar, K. (2009). Tiller dynamics of three irrigated rice varieties under varying phosphorus levels. *American-Eurasian Journal of Agronomy*, *2*(2), 89–94.

Allen, R. G., Pereira, L. S., Raes, D., & Smith, M. (1998). *Crop evapotranspiration-Guidelines for computing crop water requirements*. FAO.

Alofe, C. O., & Schrader, L. E. (1975). Photosynthate translocation in tillered Zea mays following 14 CO2 assimilation. *Canadian Journal of Plant Science*, *55*(2), 407–414. https://doi.org/10.4141/cjps75-064

Andrade, F. H., Vega, C., Uhart, S., Cirilo, A., Cantarero, M., & Valentinuz, O. (1999). Kernel number determination in maize. *Crop Science*, *39*(2), 453–459. https://doi.org/10.2135/cropsci1999.0011183X0039000200026x

Angus, J. F., Mackenzie, D. H., Morton, R., & Schafer, C. A. (1981). Phasic development in field crops II. Thermal and photoperiodic responses of spring wheat. *Field Crops Research*, *4*, 269–283. https://doi.org/10.1016/0378-4290(81)90078-2

Arnold, P. A., Kruuk, L. E. B., & Nicotra, A. B. (2019). How to analyse plant phenotypic plasticity in response to a changing climate. *New Phytologist*, *222*(3), 1235–1241. https://doi.org/10.1111/nph.15656

Assefa, Y., Carter, P., Hinds, M., Bhalla, G., Schon, R., Jeschke, M., Paszkiewicz, S., Smith, S., & Ciampitti, I. A. (2018). Analysis of long term study indicates both agronomic optimal plant density and increase maize yield per plant contributed to yield gain. *Scientific Reports*, *8*(1), 4937. https://doi.org/10.1038/s41598-018-23362-x

Assefa, Y., Vara Prasad, P. V., Carter, P., Hinds, M., Bhalla, G., Schon, R., Jeschke, M., Paszkiewicz, S., & Ciampitti, I. A. (2016). Yield responses to planting density for US modern corn hybrids: a synthesis-analysis. *Crop Science*, *56*(5), 2802–2817. https://doi.org/10.2135/cropsci2016.04.0215

Badua, S. A., Sharda, A., Strasser, R., & Ciampitti, I. (2021). Ground speed and planter downforce influence on corn seed spacing and depth. *Precision Agriculture*, *22*(4), 1154–1170. https://doi.org/10.1007/s11119-020-09775-7

Bates, D., Mächler, M., Bolker, B., & Walker, S. (2015). Fitting linear mixed-effects models using {lme4}. *Journal of Statistical Software*, *67*(1), 1–48. https://doi.org/10.18637/jss.v067.i01

Berzsenyi, Z., & Tokatlidis, I. S. (2012). Density dependence rather than maturity determines hybrid selection in dryland maize production. *Agronomy Journal*, *104*(2), 331–336. https://doi.org/10.2134/agronj2011.0205

Bihmidine, S., Hunter, C. T., Johns, C. E., Koch, K. E., & Braun, D. M. (2013). Regulation of assimilate import into sink organs: update on molecular drivers of sink strength. *Frontiers in Plant Science*, *4*. https://doi.org/10.3389/fpls.2013.00177

Blumenthal, J. M., Lyon, D. J., & Stroup, W. W. (2003). Optimal plant population and nitrogen fertility for dryland corn in western Nebraska. *Agronomy Journal*, *95*(4), 878–883. https://doi.org/10.2134/agronj2003.8780

Bonnett, O. T. (1948). Ear and tassel development in maize. *Annals of the Missouri Botanical Garden*, *35*(4), 269–287. https://doi.org/https://doi.org/10.2307/2394693

Brooker, R., Brown, L. K., George, T. S., Pakeman, R. J., Palmer, S., Ramsay, L., Schöb, C., Schurch, N., & Wilkinson, M. J. (2022). Active and adaptive plasticity in a changing climate. *Trends in Plant Science*. https://doi.org/10.1016/j.tplants.2022.02.004

Campbell, C. M. (1964). Influence of seed formation of corn on accumulation of vegetative dry matter and stalk strength 1. *Crop Science*, *4*(1), 31–34. https://doi.org/10.2135/cropsci1964.0011183X000400010011x

Cao, Y., Zhong, Z., Wang, H., & Shen, R. (2022). Leaf angle: a target of genetic improvement in cereal crops tailored for high-density planting. *Plant Biotechnology Journal*, *20*(3), 426–436. https://doi.org/10.1111/pbi.13780

Carter, P. R. (1995). Late Spring Frost and Postfrost Clipping Effect on Corn Growth and Yield. *Journal of Production Agriculture*, *8*(2), 203–209. https://doi.org/10.2134/jpa1995.0203

Cazetta, J., & Revoredo, M. (2018). Non-structural carbohydrate metabolism, growth, and productivity of maize by increasing plant density. *Agronomy*, *8*(11), 243. https://doi.org/10.3390/agronomy8110243

Chen, L., Luo, W., Huang, J., Peng, S., & Xiong, D. (2021). Leaf photosynthetic plasticity does not predict biomass responses to growth irradiance in rice. *Physiologia Plantarum*, *173*(4), 2155–2165. https://doi.org/10.1111/ppl.13564

Choi, W.-J., Lee, M.-S., Choi, J.-E., Yoon, S., & Kim, H.-Y. (2013). How do weather extremes affect rice productivity in a changing climate? An answer to episodic lack of sunshine. *Global Change Biology*, *19*(4), 1300–1310. https://doi.org/10.1111/gcb.12110

Dingemanse, N. J., Kazem, A. J. N., Réale, D., & Wright, J. (2010). Behavioural reaction norms: animal personality meets individual plasticity. *Trends in Ecology & Evolution*, *25*(2), 81–89. https://doi.org/10.1016/j.tree.2009.07.013

Dingkuhn, M., Luquet, D., Fabre, D., Muller, B., Yin, X., & Paul, M. J. (2020). The case for improving crop carbon sink strength or plasticity for a CO2-rich future. *Current Opinion in Plant Biology*, *56*, 259–272. https://doi.org/10.1016/j.pbi.2020.05.012

Doebley, J., Stec, A., & Hubbard, L. (1997). The evolution of apical dominance in maize. *Nature*, *386*(6624), 485–488. https://doi.org/10.1038/386485a0

Doust, A. (2007). Architectural evolution and its implications for domestication in grasses. *Annals of Botany*, *100*(5), 941–950. https://doi.org/10.1093/aob/mcm040

Downey, L. A. (1972). Effect of varying plant density on a tillering variety of maize. *Experimental Agriculture*, *8*(1), 25–32. https://doi.org/10.1017/S0014479700023462

Dungan, G. H. (1931). An indication that corn tillers may nourish the main stalk under some conditions 1. *Agronomy Journal*, *23*(8), 662–670. https://doi.org/10.2134/agronj1931.00021962002300080007x

Dungan, G. H., Lang, A. L., & Pendleton, J. W. (1959). Corn plant population in relation to soil productivity. In *Advances in Agronomy* (pp. 435–473). https://doi.org/10.1016/S0065-2113(08)60072-3

Duvick, D. N. (2005). Genetic progress in yield of United States maize (Zea mays L.). *Maydica*, 50(3/4), 193.

Duvick, D. N., Smith, J. S. C., & Cooper, M. (2004). Long-term selection in a commercial hybrid maize breeding program. In *Plant Breeding Reviews* (pp. 109–151). John Wiley & Sons, Inc. https://doi.org/10.1002/9780470650288.ch4

Earley, E. B., Seif, R. D., & Bensley, F. A. (1971). Relation of tillers to yield of dent corn (Zea mays L.). *Agronomy Journal*, *63*(3), 472–474. https://doi.org/10.2134/agronj1971.00021962006300030037x

Esechie, H. A. (1985). Relationship of stalk morphology and chemical composition to lodging resistance in maize (Zea mays L.) in a rainforest zone. *The Journal of Agricultural Science*, *104*(2), 429–433. https://doi.org/10.1017/S0021859600044130

Fatiukha, A., Deblieck, M., Klymiuk, V., Merchuk-Ovnat, L., Peleg, Z., Ordon, F., Fahima, T., Korol, A., Saranga, Y., & Krugman, T. (2021). Genomic architecture of phenotypic plasticity in response to water stress in tetraploid wheat. *International Journal of Molecular Sciences*, *22*(4), 1723. https://doi.org/10.3390/ijms22041723

Faye, J. M., Maina, F., Hu, Z., Fonceka, D., Cisse, N., & Morris, G. P. (2019). Genomic signatures of adaptation to Sahelian and Soudanian climates in sorghum landraces of Senegal. *Ecology and Evolution*, *9*(10), 6038–6051. https://doi.org/10.1002/ece3.5187

Fernández, J. A., Messina, C. D., Salinas, A., Prasad, P. V. V., Nippert, J. B., & Ciampitti, I. A. (2022). Kernel weight contribution to yield genetic gain of maize: a global review and US case studies. *Journal of Experimental Botany*, *73*(11), 3597–3609. https://doi.org/10.1093/jxb/erac103

Finlay, K., & Wilkinson, G. (1963). The analysis of adaptation in a plant-breeding programme. *Australian Journal of Agricultural Research*, 14(6), 742. https://doi.org/10.1071/AR9630742

Fischer, R. A. (1985). Number of kernels in wheat crops and the influence of solar radiation and temperature. *The Journal of Agricultural Science*, *105*(2), 447–461. https://doi.org/10.1017/S0021859600056495

Fox, J., & Weisberg, S. (2019). *An {R} companion to applied regression* (Third). Sage. https://socialsciences.mcmaster.ca/jfox/Books/Companion/

Frank, B. J., Schlegel, A. J., Stone, L. R., & Kirkham, M. B. (2013). Grain yield and plant characteristics of corn hybrids in the Great Plains. *Agronomy Journal*, *105*(2), 383–394. https://doi.org/10.2134/agronj2012.0330

Galicia, L., Nurit, E., Rosales, A., & Palacios-Rojas, N. (2009). *Maize nutrition quality and plant tissue analysis laboratory: laboratory protocols 2008*. CIMMYT.

Gambín, B. L., & Borrás, L. (2007). Plasticity of sorghum kernel weight to increased assimilate availability. *Field Crops Research*, *100*(2–3), 272–284. https://doi.org/10.1016/j.fcr.2006.08.002

Gambín, B. L., Borrás, L., & Otegui, M. E. (2008). Kernel weight dependence upon plant growth at different grain-filling stages in maize and sorghum. *Australian Journal of Agricultural Research*, *59*(3), 280. https://doi.org/10.1071/AR07275

Gardner, J. L. (1942). Studies in tillering. *Ecology*, *23*(2), 162–174. https://doi.org/10.2307/1931083

George-Jaeggli, B., Mortlock, M. Y., & Borrell, A. K. (2017). Bigger is not always better: Reducing leaf area helps stay-green sorghum use soil water more slowly. *Environmental and Experimental Botany*, *138*, 119–129. https://doi.org/10.1016/j.envexpbot.2017.03.002

Ghatak, A., Chaturvedi, P., Bachmann, G., Valledor, L., Ramšak, Ž., Bazargani, M. M., Bajaj, P., Jegadeesan, S., Li, W., Sun, X., Gruden, K., Varshney, R. K., & Weckwerth, W. (2021). Physiological and proteomic signatures reveal mechanisms of superior drought resilience in pearl millet compared to wheat. *Frontiers in Plant Science*, *11*. https://doi.org/10.3389/fpls.2020.600278

Gholamy, A., Kreinovich, V., & Kosheleva, O. (2018). Why 70/30 or 80/20 relation between training and testing Sets: A pedagogical explanation. *Departmental Technical Reports (CS)*, *1209*. https://scholarworks.utep.edu/cs_techrep/1209?utm_source=scholarworks.utep.edu%2Fcs_techrep%2F1209&utm_medium=PDF&utm_campaign=PDFCoverPages

Gneiting, T., & Katzfuss, M. (2014). Probabilistic forecasting. *Annual Review of Statistics and Its Application*, *1*(1), 125–151. https://doi.org/10.1146/annurev-statistics-062713-085831

Haag, L. A. (2013). *Ecophysiology of dryland corn and grain sorghum as affected by alternative planting geometries and seeding rates* [Kansas State University]. http://hdl.handle.net/2097/16277

Hammer, G. L., Dong, Z., McLean, G., Doherty, A., Messina, C., Schussler, J., Zinselmeier, C., Paszkiewicz, S., & Cooper, M. (2009). Can changes in canopy and/or root system architecture explain historical maize yield trends in the U.S. corn belt? *Crop Science*, *49*(1), 299–312. https://doi.org/10.2135/cropsci2008.03.0152

Hansey, C. N., & de Leon, N. (2011). Biomass yield and cell wall composition of corn with alternative morphologies planted at variable densities. *Crop Science*, *51*(3), 1005–1015. https://doi.org/10.2135/cropsci2010.08.0490

Hay, R. K. M. (1995). Harvest index: a review of its use in plant breeding and crop physiology. *Annals of Applied Biology*, *126*(1), 197–216. https://doi.org/10.1111/j.1744-7348.1995.tb05015.x

Hörbe, T. A. N., Amado, T. J. C., Reimche, G. B., Schwalbert, R. A., Santi, A. L., & Nienow, C. (2016). Optimization of within-row plant spacing increases nutritional status and corn yield: A comparative study. *Agronomy Journal*, *108*(5), 1962–1971. https://doi.org/10.2134/agronj2016.03.0156

Hughes, T. P., Linares, C., Dakos, V., van de Leemput, I. A., & van Nes, E. H. (2013). Living dangerously on borrowed time during slow, unrecognized regime shifts. *Trends in Ecology & Evolution*, *28*(3), 149–155. https://doi.org/10.1016/j.tree.2012.08.022

Hume, D. J., & Campbell, D. K. (1972). Accumulation and translocation of soluble solids in corn stalks. *Canadian Journal of Plant Science*, *52*(3), 363–368. https://doi.org/10.4141/cjps72-056

Huntington, J. L., Hegewisch, K. C., Daudert, B., Morton, C. G., Abatzoglou, J. T., McEvoy, D. J., & Erickson, T. (2017). Climate engine: cloud computing and visualization of climate and remote sensing data for advanced natural resource monitoring and process understanding. *Bulletin of the American Meteorological Society*, *98*(11), 2397–2410. https://doi.org/10.1175/BAMS-D-15-00324.1

Jacott, C. N., & Boden, S. A. (2020). Feeling the heat: developmental and molecular responses of wheat and barley to high ambient temperatures. *Journal of Experimental Botany*, *71*(19), 5740–5751. https://doi.org/10.1093/jxb/eraa326

Jenkins, M. T. (1941). Influence of climate and weather on growth of corn. In *Yearbook of Agriculture*. United States Department of Agriculture.

Jones, H. G., & Kirby, E. J. M. (1977). Effects of manipulation of number of tillers and water supply on grain yield in barley. *The Journal of Agricultural Science*, *88*(2), 391–397. https://doi.org/10.1017/S0021859600034882

Kamiji, Y., Yoshida, H., Palta, J. A., Sakuratani, T., & Shiraiwa, T. (2011). N applications that increase plant N during panicle development are highly effective in increasing spikelet number in rice. *Field Crops Research*, *122*(3), 242–247. https://doi.org/10.1016/j.fcr.2011.03.016

Kapanigowda, M., Stewart, B. A., Howell, T. A., Kadasrivenkata, H., & Baumhardt, R. L. (2010). Growing maize in clumps as a strategy for marginal climatic conditions. *Field Crops Research*, *118*(2), 115–125. https://doi.org/10.1016/j.fcr.2010.04.012

Karlova, R., Boer, D., Hayes, S., & Testerink, C. (2021). Root plasticity under abiotic stress. *Plant Physiology*, *187*(3), 1057–1070. https://doi.org/10.1093/plphys/kiab392

Khosla, R., Inman, D., Westfall, D. G., Reich, R. M., Frasier, M., Mzuku, M., Koch, B., & Hornung, A. (2008). A synthesis of multi-disciplinary research in precision agriculture: site-specific management zones in the semi-arid western Great Plains of the USA. *Precision Agriculture*, *9*(1–2), 85–100. https://doi.org/10.1007/s11119-008-9057-1

Kim, H. K., Luquet, D., van Oosterom, E., Dingkuhn, M., & Hammer, G. (2010). Regulation of tillering in sorghum: genotypic effects. *Annals of Botany*, *106*(1), 69–78. https://doi.org/10.1093/aob/mcq080

Kim, H. K., van Oosterom, E., Dingkuhn, M., Luquet, D., & Hammer, G. (2010). Regulation of tillering in sorghum: environmental effects. *Annals of Botany*, *106*(1), 57–67. https://doi.org/10.1093/aob/mcq079

Koenker, R. (2020). *quantreg: quantile regression*. https://cran.r-project.org/package=quantreg

Komarek, A. M., De Pinto, A., & Smith, V. H. (2020). A review of types of risks in agriculture: what we know and what we need to know. *Agricultural Systems*, *178*, 102738. https://doi.org/10.1016/j.agsy.2019.102738

Kumar, P. V., Rao, V. U. M., Bhavani, O., Dubey, A. P., & Singh, C. B. (2016). Effect of temperature and photothermal quotient on the yield components of wheat (Triticum aestivum L .) in Indo-Gangetic Plains of India. *Experimental Agriculture*, *52*(1), 14–35. https://doi.org/10.1017/S0014479714000532

Kumar, R. R., Goswami, S., Shamim, M., Mishra, U., Jain, M., Singh, K., Singh, J. P., Dubey, K., Singh, S., Rai, G. K., Singh, G. P., Pathak, H., Chinnusamy, V., & Praveen, S. (2017). Biochemical defense response: Characterizing the plasticity of source and sink in spring wheat under terminal heat stress. *Frontiers in Plant Science*, *8*. https://doi.org/10.3389/fpls.2017.01603

Kumar, U., Laza, M. R., Soulié, J.-C., Pasco, R., Mendez, K. V. S., & Dingkuhn, M. (2017). Analysis and simulation of phenotypic plasticity for traits contributing to yield potential in twelve rice genotypes. *Field Crops Research*, *202*, 94–107. https://doi.org/10.1016/j.fcr.2016.04.037

Lafarge, T. A., & Hammer, G. L. (2002). Tillering in grain sorghum over a wide range of population densities: modelling dynamics of tiller fertility. *Annals of Botany*, *90*(1), 99–110. https://doi.org/10.1093/aob/mcf153

Lafarge, T., Seassau, Ć., Martin, M., Bueno, C., CÍment-Vidal, A., Schreck, E., & Luquet, D. (2010). Regulation and recovery of sink strength in rice plants grown under changes in light intensity. *Functional Plant Biology*, *37*(5), 413–428. https://doi.org/10.1071/FP09137

Laitinen, R. A. E., & Nikoloski, Z. (2019). Genetic basis of plasticity in plants. *Journal of Experimental Botany*, *70*(3), 739–745. https://doi.org/10.1093/jxb/ery404

Lamm, F. R., Rogers, D. H., Schlegel, A. J., Lin, X., Aiken, R. M., Klocke, N. L., Stone, L. R., & Shaw, L. K. (2017). Trends in plant available soil water on producer fields of western Kansas. *Applied Engineering in Agriculture*, *33*(6), 859–868. https://doi.org/10.13031/aea.12452

Lark, T. J., Spawn, S. A., Bougie, M., & Gibbs, H. K. (2020). Cropland expansion in the United States produces marginal yields at high costs to wildlife. *Nature Communications*, *11*(1), 4295. https://doi.org/10.1038/s41467-020-18045-z

Lê, S., Josse, J., & Husson, F. (2008). {FactoMineR}: a package for multivariate analysis. *Journal of Statistical Software*, *25*(1), 1–18. https://doi.org/10.18637/jss.v025.i01

Lenth, R. (2020). *emmeans: estimated marginal means, aka least-squares means*. https://cran.r-project.org/package=emmeans

Liang, X., Erickson, J. E., Vermerris, W., Rowland, D. L., Sollenberger, L. E., & Silveira, M. L. (2017). Root architecture of sorghum genotypes differing in root angles under different water regimes. *Journal of Crop Improvement*, *31*(1), 39–55. https://doi.org/10.1080/15427528.2016.1258603

Liu, Y., Zhang, P., Li, M., Chang, L., Cheng, H., Chai, S., & Yang, D. (2020). Dynamic responses of accumulation and remobilization of water soluble carbohydrates in wheat stem to drought stress. *Plant Physiology and Biochemistry*, *155*, 262–270. https://doi.org/10.1016/j.plaphy.2020.07.024

Lobell, D. B., Schlenker, W., & Costa-Roberts, J. (2011). Climate trends and global crop production since 1980. *Science*, *333*(6042), 616–620. https://doi.org/10.1126/science.1204531

Lobell, David B, & Azzari, G. (2017). Satellite detection of rising maize yield heterogeneity in the U.S. Midwest. *Environmental Research Letters*, *12*(1), 014014. https://doi.org/10.1088/1748-9326/aa5371

Long, N. V., Assefa, Y., Schwalbert, R., & Ciampitti, I. A. (2017). Maize yield and planting date relationship: A synthesis-analysis for US high-yielding contest-winner and field research data. *Frontiers in Plant Science*, *8*. https://doi.org/10.3389/fpls.2017.02106

Longnecker, N., Kirby, E. J. M., & Robson, A. (1993). Leaf emergence, tiller growth, and apical development of nitrogen-deficient spring wheat. *Crop Science*, *33*(1), 154–160. https://doi.org/10.2135/cropsci1993.0011183X003300010028x

Loomis, R. S., & Connor, D. J. (1992). Crop Ecology. Cambridge University Press. https://doi.org/10.1017/CBO9781139170161

Lorenz, A. J., Gustafson, T. J., Coors, J. G., & de Leon, N. (2010). Breeding maize for a bioeconomy: A literature survey examining harvest index and stover yield and their relationship to grain yield. *Crop Science*, *50*(1), 1–12. https://doi.org/10.2135/cropsci2009.02.0086

Lyon, T. L. (1905). Experiments with corn. *Bulletin of the Agricultural Experiment Station of Nebraska*, *91*(18), 2.

Maddonni, G. A., Otegui, M. E., Andrieu, B., Chelle, M., & Casal, J. J. (2002). Maize leaves turn away from neighbors. *Plant Physiology*, *130*(3), 1181–1189. https://doi.org/10.1104/pp.009738

Maddonni, G., Rodriguez, D., Giorno, A., Ciampitti, I. A., Martinez Rueda, C., & Ferreyra, J. M. (2021). *Grupo de estudio y trabajo "red de ultra baja densidad de maiz."* https://www.agro.uba.ar/GET/reduba-demaiz/divulgacion

Major, D. J. (1977). Seasonal dry-weight distribution of single-stalked and multi-tillered corn hybrids grown at three population densities in southern Alberta. *Canadian Journal of Plant Science*, *57*(4), 1041–1047. https://doi.org/10.4141/cjps77-155

Markham, M. Y., & Stoltenberg, D. E. (2010). Corn morphology, mass, and grain yield as affected by early-season red: far-red light environments. *Crop Science*, *50*(1), 273–280. https://doi.org/10.2135/cropsci2008.10.0614

Mase, A. S., Gramig, B. M., & Prokopy, L. S. (2017). Climate change beliefs, risk perceptions, and adaptation behavior among Midwestern U.S. crop farmers. *Climate Risk Management*, *15*, 8–17. https://doi.org/10.1016/j.crm.2016.11.004

Massigoge, I., Ross, F., Fernández, J. A., Echarte, L., Ciampitti, I. A., & Cerrudo, A. (2022). Contribution of tillers to maize yield stability at low plant density. *Crop Science*. https://doi.org/10.1002/csc2.20827

Matesanz, S., & Milla, R. (2018). Differential plasticity to water and nutrients between crops and their wild progenitors. *Environmental and Experimental Botany*, *145*, 54–63. https://doi.org/10.1016/j.envexpbot.2017.10.014

Messina, C., McDonald, D., Poffenbarger, H., Clark, R., Salinas, A., Fang, Y., Gho, C., Tang, T., Graham, G., Hammer, G. L., & Cooper, M. (2021). Reproductive resilience but not root architecture underpins yield improvement under drought in maize. *Journal of Experimental Botany*, 72(14), 5235–5245. https://doi.org/10.1093/jxb/erab231

Moulia, B., Loup, C., Chartier, M., Allirand, J. M., & Edelin, C. (1999). Dynamics of architectural development of isolated plants of maize (Zea mays L.), in a non-limiting environment: The branching potential of modern maize. *Annals of Botany*, *84*(5), 645–656. https://doi.org/10.1006/anbo.1999.0960

Mrad, A., Katul, G. G., Levia, D. F., Guswa, A. J., Boyer, E. W., Bruen, M., Carlyle-Moses, D. E., Coyte, R., Creed, I. F., van de Giesen, N., Grasso, D., Hannah, D. M., Hudson, J. E., Humphrey, V., Iida, S., Jackson, R. B., Kumagai, T., Llorens, P., Michalzik, B., … Scanlon, B. R. (2020). Peak grain forecasts for the US High Plains amid withering waters. *Proceedings of the National Academy of Sciences*, *117*(42), 26145–26150. https://doi.org/10.1073/pnas.2008383117

Mylonas, I., Sinapidou, E., Remountakis, E., Sistanis, I., Pankou, C., Ninou, E., Papadopoulos, I., Papathanasiou, F., Lithourgidis, A., Gekas, F., Dordas, C., Tzantarmas, C., Kargiotidou, A., Tokamani, M., Sandaltzopoulos, R., & Tokatlidis, I. S. (2020). Improved plant yield efficiency alleviates the erratic optimum density in maize. *Agronomy Journal*, *112*(3), 1690–1701. https://doi.org/10.1002/agj2.20187

Nemoto, K., Morita, S., & Baba, T. (1995). Shoot and root development in rice related to the phyllochron. *Crop Science*, *35*(1), 24–29. https://doi.org/10.2135/cropsci1995.0011183X003500010005x

Nicotra, A. B., Atkin, O. K., Bonser, S. P., Davidson, A. M., Finnegan, E. J., Mathesius, U., Poot, P., Purugganan, M. D., Richards, C. L., Valladares, F., & van Kleunen, M. (2010). Plant phenotypic plasticity in a changing climate. *Trends in Plant Science*, *15*(12), 684–692. https://doi.org/10.1016/j.tplants.2010.09.008

Nicotra, A. B., & Davidson, A. (2010). Adaptive phenotypic plasticity and plant water use. *Functional Plant Biology*, *37*(2), 117. https://doi.org/10.1071/FP09139

Nielsen, D. C., Halvorson, A. D., & Vigil, M. F. (2010). Critical precipitation period for dryland maize production. *Field Crops Research*, *118*(3), 259–263. https://doi.org/10.1016/j.fcr.2010.06.004

Nix, H. A. (1976). Climate and crop productivity in Australia. In *Climate and rice* (pp. 495–507). IRRI.

Ortez, O. A., McMechan, A. J., Hoegemeyer, T., Ciampitti, I. A., Nielsen, R., Thomison, P. R., & Elmore, R. W. (2022). Abnormal ear development in corn: A review. *Agronomy Journal*, *114*(2), 1168–1183. https://doi.org/10.1002/agj2.20986

Passioura, J. B. (1977). Grain yield, harvest index, and water use of wheat. *J. Aust. Inst. Agric. Sci.*, 43, 117–120.

Passioura, J. B. (2006). Increasing crop productivity when water is scarce—from breeding to field management. *Agricultural Water Management*, 80(1–3), 176–196. https://doi.org/10.1016/j.agwat.2005.07.012

Pasuquin, E., Lafarge, T., & Tubana, B. (2008). Transplanting young seedlings in irrigated rice fields: early and high tiller production enhanced grain yield. *Field Crops Research*, *105*(1–2), 141–155. https://doi.org/10.1016/j.fcr.2007.09.001

Pfeiffer, B. K., Pietsch, D., Schnell, R. W., & Rooney, W. L. (2019). Long-term selection in hybrid sorghum breeding programs. *Crop Science*, *59*(1), 150–164. https://doi.org/10.2135/cropsci2018.05.0345

Pierik, R., Fankhauser, C., Strader, L. C., & Sinha, N. (2021). Architecture and plasticity: optimizing plant performance in dynamic environments. *Plant Physiology*, *187*(3), 1029–1032. https://doi.org/10.1093/plphys/kiab402

Prior, C. L., & Russell, W. A. (1975). Yield performance of nonprolific and prolific maize hybrids at six plant densities 1. *Crop Science*, *15*(4), 482–486. https://doi.org/10.2135/cropsci1975.0011183X001500040010x

R Core Team. (2022). *R: a language and environment for statistical computing*. https://www.r-project.org/

Raftery, A. E. (2016). Use and communication of probabilistic forecasts. *Statistical Analysis and Data Mining: The ASA Data Science Journal*, *9*(6), 397–410. https://doi.org/10.1002/sam.11302

Ren, X., Sun, D., & Wang, Q. (2016). Modeling the effects of plant density on maize productivity and water balance in the Loess Plateau of China. *Agricultural Water Management*, *171*, 40–48. https://doi.org/10.1016/j.agwat.2016.03.014

Ritchie, S. W., Hanway, J. J., & Benson, G. O. (1997). How a corn plant develops. *Iowa State University Coop. Ext. Serv.*, *48*.

Rodriguez, D, Andrade, F., & Goudriaan, J. (1999). Effects of phosphorus nutrition on tiller emergence in wheat. *Plant and Soil*, *209*, 283–295. https://doi.org/10.1023/A:1004690404870

Rodriguez, Daniel, de Voil, P., & Power, B. (2016). Modelling dryland agricultural systems. In *Innovations in Dryland Agriculture* (pp. 239–256). Springer International Publishing. https://doi.org/10.1007/978-3-319-47928-6_9

Roozeboom, K., Devlin, D., Duncan, S., Janssen, K., Olson, B., & Thompson, C. (2007). Optimum planting practices. In *Corn Production Handbook* (pp. 10–14). Kansas Agricultural Experiment Station, Kansas State University.

Rostamza, M., Richards, R. A., & Watt, M. (2013). Response of millet and sorghum to a varying water supply around the primary and nodal roots. *Annals of Botany*, *112*(2), 439–446. https://doi.org/10.1093/aob/mct099

Rotili, D. H., Abeledo, L. G., DeVoil, P., Rodríguez, D., & Maddonni, G. Á. (2021a). Exploring the effect of tillers on the water economy, plant growth and kernel set of low-density maize crops. *Agricultural Water Management*, *243*, 106424. https://doi.org/10.1016/j.agwat.2020.106424

Rotili, D. H., Abeledo, L. G., Martínez Larrea, S., & Maddonni, G. Á. (2022). Grain yield and kernel setting of multiple-shoot and/or multiple-ear maize hybrids. *Field Crops Research*, *279*, 108471. https://doi.org/10.1016/j.fcr.2022.108471

Rotili, D. H., Giorno, A., Tognetti, P. M., & Maddonni, G. Á. (2019). Expansion of maize production in a semi-arid region of Argentina: climatic and edaphic constraints and their implications on crop management. *Agricultural Water Management*, *226*, 105761. https://doi.org/10.1016/j.agwat.2019.105761

Rotili, D. H., Sadras, V. O., Abeledo, L. G., Ferreyra, J. M., Micheloud, J. R., Duarte, G., Girón, P., Ermácora, M., & Maddonni, G. Á. (2021b). Impacts of vegetative and reproductive plasticity associated with tillering in maize crops in low-yielding environments: A physiological framework. *Field Crops Research*, *265*, 108107. https://doi.org/10.1016/j.fcr.2021.108107

Russell, W. A. (1991). Genetic improvement of maize yields. In *Advances in Agronomy* (pp. 245–298). https://doi.org/10.1016/S0065-2113(08)60582-9

Russelle, M. P., Schild, J. A., & Olson, R. A. (1984). Phosphorus translocation between small, non-reproductive tillers and the main plant of maize 1. *Agronomy Journal*, *76*(1), 1–4. https://doi.org/10.2134/agronj1984.00021962007600010001x

Sadras, V. O., & Rebetzke, G. J. (2013). Plasticity of wheat grain yield is associated with plasticity of ear number. *Crop and Pasture Science*, *64*(3), 234. https://doi.org/10.1071/CP13117

Sadras, V.O., Rebetzke, G. J., & Edmeades, G. O. (2013). The phenotype and the components of phenotypic variance of crop traits. *Field Crops Research*, *154*, 255–259. https://doi.org/10.1016/j.fcr.2013.10.001

Sadras, Victor O., & Slafer, G. A. (2012). Environmental modulation of yield components in cereals: Heritabilities reveal a hierarchy of phenotypic plasticities. *Field Crops Research*, *127*, 215–224. https://doi.org/10.1016/j.fcr.2011.11.014

Sangoi, L., Schmitt, A., Saldanha, A., Fiorentin, C. F., Pletsch, A. J., Vieria, J., & Gattelli, M. A. (2009). Grain yield of maize hybrids at two plant densities with and without tillers removal. *Ciencia Rural*, *39*, 325–331.

Sangoi, L., Schmitt, A., Silva, P. R. F. da, Vargas, V. P., Zoldan, S. R., Viera, J., Souza, C. A. de, Picoli Junior, G. J., & Bianchet, P. (2012). Perfilhamento como característica mitigadora dos

prejuízos ocasionados ao milho pela desfolha do colmo principal. *Pesquisa Agropecuária Brasileira*, *47*(11), 1605–1612. https://doi.org/10.1590/S0100-204X2012001100007

Sangoi, L., Schmitt, A., Vieira, J., Vargas, V. P., Girardi, D., & Zoldan, S. R. (2012). A remoção dos perfilhos não aumenta o rendimento de grãos do milho, independentemente da época de semeadura. *Ciência Rural*, *42*(8), 1354–1359. https://doi.org/10.1590/S0103-84782012000800004

Sangoi, L., Vargas, V. P., Schimitt, A., Pletsch, A. J., Vieira, J., Saldanha, A., Siega, E., Carniel, G., Mengarda, R. T., & Picoli Junior, G. J. (2011, February). Disponibilidade de nitrogênio, sobrevivência e contribuição dos perfilhos ao rendimento de grãos do milho. *Revista Brasileira de Ciência Do Solo*, *35*(1), 183–191. https://doi.org/10.1590/S0100-06832011000100017

Schaffner, J. H. (1930). Sex reversal and the experimental production of neutral tassels in Zea mays. *Botanical Gazette*, *90*(3), 279–298. https://doi.org/10.1086/334101

Schneider, H. M., & Lynch, J. P. (2020). Should root plasticity be a crop breeding target? *Frontiers in Plant Science*, *11*. https://doi.org/10.3389/fpls.2020.00546

Schwalbert, R., Amado, T. J. C., Horbe, T. A. N., Stefanello, L. O., Assefa, Y., Prasad, P. V. V., Rice, C. W., & Ciampitti, I. A. (2018). Corn yield response to plant density and nitrogen: spatial models and yield distribution. *Agronomy Journal*, *110*(3), 970–982. https://doi.org/10.2134/agronj2017.07.0425

Setter, T. L., & Meller, V. H. (1984). Reserve carbohydrate in maize stem. *Plant Physiology*, *75*(3), 617–622. https://doi.org/10.1104/pp.75.3.617

Slafer, G. A. (2003). Genetic basis of yield as viewed from a crop physiologist's perspective. *Annals of Applied Biology*, *142*(2), 117–128. https://doi.org/10.1111/j.1744-7348.2003.tb00237.x

Slewinski, T. L. (2012). Non-structural carbohydrate partitioning in grass stems: a target to increase yield stability, stress tolerance, and biofuel production. *Journal of Experimental Botany*, *63*(13), 4647–4670. https://doi.org/10.1093/jxb/ers124

Smith, M. R., Rao, I. M., & Merchant, A. (2018). Source-sink relationships in crop plants and their influence on yield development and nutritional quality. *Frontiers in Plant Science*, *9*. https://doi.org/10.3389/fpls.2018.01889

Staff, S. S., Service, N. R. C., & Agriculture, U. S. D. of. (2022). *Web soil survey*. http://websoilsurvey.sc.egov.usda.gov/

Steiner, J. L., Briske, D. D., Brown, D. P., & Rottler, C. M. (2018). Vulnerability of Southern Plains agriculture to climate change. *Climatic Change*, *146*(1–2), 201–218. https://doi.org/10.1007/s10584-017-1965-5

Stevenson, J. C., & Goodman, M. M. (1972). Ecology of exotic races of maize. I. Leaf number and tillering of 16 races under four temperatures and two photoperiods 1. *Crop Science*, *12*(6), 864–868. https://doi.org/10.2135/cropsci1972.0011183X001200060045x

Stewart, B. A. (2009). Manipulating tillage to increase stored soil water and manipulating plant geometry to increase water-use efficiency in dryland areas. *Journal of Crop Improvement*, *23*(1), 71–82. https://doi.org/10.1080/15427520802418319

Suneja, Y., Gupta, A. K., & Bains, N. S. (2019). Stress adaptive plasticity: Aegilops tauschii and Triticum dicoccoides as potential donors of drought associated morpho-physiological traits in wheat. *Frontiers in Plant Science*, *10*. https://doi.org/10.3389/fpls.2019.00211

Tetio-Kagho, F., & Gardner, F. P. (1988). Responses of maize to plant population density. I. Canopy development, light relationships, and vegetative growth. *Agronomy Journal*, *80*(6), 930–935. https://doi.org/10.2134/agronj1988.00021962008000060018x

Thapa, S., Stewart, B. A., Xue, Q., Rhoades, M. B., Angira, B., & Reznik, J. (2018). Canopy temperature, yield, and harvest index of corn as affected by planting geometry in a semi-arid environment. *Field Crops Research*, *227*, 110–118. https://doi.org/10.1016/j.fcr.2018.08.009

Thapa, S., Xue, Q., & Stewart, B. A. (2020). Alternative planting geometries reduce production risk in corn and sorghum in water-limited environments. *Agronomy Journal*, *112*(5), 3322–3334. https://doi.org/10.1002/agj2.20347

Thomison, P. R., & Jordan, D. M. (1995). Plant population effects on corn hybrids differing in ear growth habit and prolificacy. *Journal of Production Agriculture*, *8*(3), 394–400. https://doi.org/10.2134/jpa1995.0394

Thorne, G. N., & Wood, D. W. (1987). Effects of radiation and temperature on tiller survival, grain number and grain yield in winter wheat. *Annals of Botany*, *59*(4), 413–426. https://doi.org/10.1093/oxfordjournals.aob.a087330

Tokatlidis, I. ., & Koutroubas, S. . (2004). A review of maize hybrids' dependence on high plant populations and its implications for crop yield stability. *Field Crops Research*, *88*(2–3), 103–114. https://doi.org/10.1016/j.fcr.2003.11.013

Tokatlidis, I. ., Koutsika-Sotiriou, M., & Tamoutsidis, E. (2005). Benefits from using maize density-independent hybrids. *Maydica*, *50*, 9–17.

Tsaftaris, A. S., Polidoros, A. N., Kapazoglou, A., Tani, E., & Kovačević, N. M. (2008). Epigenetics and plant breeding. In *Plant Breeding Reviews* (pp. 49–177). John Wiley & Sons, Inc. https://doi.org/10.1002/9780470380130.ch2

van Averbeke, W., & Marais, J. N. (1992). Maize response to plant population and soil water supply: I. yield of grain and total above-ground biomass. *South African Journal of Plant and Soil*, *9*(4), 186–192. https://doi.org/10.1080/02571862.1992.10634627

van der Ploeg, R. R., Böhm, W., & Kirkham, M. B. (1999). On the origin of the theory of mineral nutrition of plants and the law of the minimum. *Soil Science Society of America Journal*, *63*(5), 1055–1062. https://doi.org/10.2136/sssaj1999.6351055x

van Oosterom, E. J., Borrell, A. K., Chapman, S. C., Broad, I. J., & Hammer, G. L. (2010). Functional dynamics of the nitrogen balance of sorghum: I. N demand of vegetative plant parts. *Field Crops Research*, *115*(1), 19–28. https://doi.org/10.1016/j.fcr.2009.09.018

Veenstra, R. L., & Ciampitti, I. A. (2021). Corn tillers: Rethinking the "sucker" theory. *ASA, CSSA, SSSA International Annual Meeting, Salt Lake City, UT.* https://scisoc.confex.com/scisoc/2021am/meetingapp.cgi/Paper/134925

Veenstra, R. L., Messina, C. D., Berning, D., Haag, L. A., Carter, P., Hefley, T. J., Prasad, P. V. V., & Ciampitti, I. A. (2021). Effect of tillers on corn yield: Exploring trait plasticity potential in unpredictable environments. *Crop Science*, *61*(5), 3660–3674. https://doi.org/10.1002/csc2.20576

von Wettberg, E., Davis, T. M., & Smýkal, P. (2020). Editorial: Wild plants as source of new crops. *Frontiers in Plant Science*, *11*. https://doi.org/10.3389/fpls.2020.591554

Wang, X., Vignjevic, M., Jiang, D., Jacobsen, S., & Wollenweber, B. (2014). Improved tolerance to drought stress after anthesis due to priming before anthesis in wheat (Triticum aestivum L.) var. Vinjett. *Journal of Experimental Botany*, *65*(22), 6441–6456. https://doi.org/10.1093/jxb/eru362

Wang, Y., & Li, J. (2011). Branching in rice. *Current Opinion in Plant Biology*, *14*(1), 94–99. https://doi.org/10.1016/j.pbi.2010.11.002

Williams, C. B. (1912). Economic value of corn suckers. *Agronomy Journal*, *4*(1), 152–157. https://doi.org/10.2134/agronj1912.00021962000400010027x

Williams, P. J., & Hooten, M. B. (2016). Combining statistical inference and decisions in ecology. *Ecological Applications*, *26*(6), 1930–1942. https://doi.org/10.1890/15-1593.1

Wood, S. N. (2017). *Generalized Additive Models*. Chapman and Hall/CRC. https://doi.org/10.1201/9781315370279

Xue, Y., Duan, H., Liu, L., Wang, Z., Yang, J., & Zhang, J. (2013). An improved crop management increases grain yield and nitrogen and water use efficiency in rice. *Crop Science*, *53*(1), 271–284. https://doi.org/10.2135/cropsci2012.06.0360

Yamaguchi, J. (1974). Varietal traits limiting the grain yield of tropical maize IV. Plant traits and productivity of tropical varieties. *Soil Science and Plant Nutrition*, *20*(3), 287–304. https://doi.org/10.1080/00380768.1974.10433251

Yan, Y., Zhao, N., Tang, H., Gong, B., & Shi, Q. (2020). Shoot branching regulation and signaling. *Plant Growth Regulation*, *92*(2), 131–140. https://doi.org/10.1007/s10725-020-00640-1

Zhi, X., Tao, Y., Jordan, D., Borrell, A., Hunt, C., Cruickshank, A., Potgieter, A., Wu, A., Hammer, G., George-Jaeggli, B., & Mace, E. (2022). Genetic control of leaf angle in sorghum and its effect on light interception. *Journal of Experimental Botany*, *73*(3), 801–816. https://doi.org/10.1093/jxb/erab467

Zhu, J., Werf, W., Anten, N. P. R., Vos, J., & Evers, J. B. (2015). The contribution of phenotypic plasticity to complementary light capture in plant mixtures. *New Phytologist*, *207*(4), 1213–1222. https://doi.org/10.1111/nph.13416

Appendix A - Chapter 2 Supplementary Material

Table A.1 Site-year monthly climatic summaries of mean solar radiation, mean maximum temperature, mean minimum temperature, and water supply considering precipitation and irrigation sources.

Site-Year	**Mean Daily Solar Radiation** (MJ m^{-2} day^{-1})					**Water Supply** (Precipitation + Irrigation) (mm)				
	Apr	*May*	*Jun*	*Jul*	*Aug*	*Apr*	*May*	*Jun*	*Jul*	*Aug*
Manhattan 2019	19.7	20.9	26.1	25.0	20.9	42.5	353.1	162.3	102.1	252.9
Garden City 2019	21.5	23.1	26.5	27.5	23.5	13.4	260.6	167.4	110.8	105.4
Goodland 2019	21.1	21.7	26.6	26.5	23.7	20.4	255.0	127.2	90.0	365.4
Keats 2020	19.4	19.9	27.1	23.6	22.7	52.0	146.6	96.6	175.1	46.0
Buhler 2020	20.0	21.5	26.9	24.5	23.9	27.2	144.1	91.5	177.6	42.1
Greensburg 2020	20.9	24.7	27.1	26.1	23.4	29.0	79.1	144.9	194.6	30.1
Garden City 2020	21.7	25.6	27.4	26.8	24.1	5.1	93.6	106.9	174.0	59.4
Goodland 2020	20.8	24.7	26.8	26.0	24.4	2.9	66.8	128.1	97.1	61.5
Colby (A & B) 2020	21.1	23.5	27.1	25.9	24.3	2.7	55.3	46.0	126.4	41.1
Site-Year	**Mean Maximum Temperature** (°C)					**Mean Minimum Temperature** (°C)				
	Apr	*May*	*Jun*	*Jul*	*Aug*	*Apr*	*May*	*Jun*	*Jul*	*Aug*
Manhattan 2019	20.8	22.0	29.5	31.9	29.6	7.8	11.7	17.0	20.0	19.2
Garden City 2019	21.4	21.8	29.7	33.2	33.3	4.1	8.8	14.3	17.9	17.9
Goodland 2019	19.4	18.7	28.1	33.2	30.4	2.3	6.0	12.2	16.2	15.8
Keats 2020	17.9	21.0	30.9	30.6	29.9	4.3	11.3	19.3	20.4	17.9
Buhler 2020	20.2	23.0	33.1	32.2	31.6	4.3	11.1	19.7	20.8	17.9
Greensburg 2020	19.9	23.5	32.9	32.3	32.1	2.3	9.8	17.1	18.7	17.0
Garden City 2020	19.7	25.1	34.2	32.3	31.4	1.8	9.6	17.1	18.6	16.5
Goodland 2020	18.0	23.1	32.7	32.0	31.8	-0.7	7.4	15.0	16.6	15.1
Colby (A & B) 2020	17.9	22.8	32.5	31.5	31.2	-0.6	7.4	15.4	17.0	15.2

Table A.2 Site-year water supply (WS) summary and apparent crop water budget (AWB) estimation [calculated as the observed water supply (irrigation + precipitation) less the apparent crop water demand (crop evapotranspiration, ETc)] by crop development stage period – Pre-V4 (one month prior to planting through fourth-leaf stage), V4-V7 (fourth leaf to seventh leaf), V7-V14 (seventh leaf to fourteenth leaf), and V14-R6 (pre-tasselling to physiological maturity).

Site-Year	**Pre-V4 WS** (mm)	**Pre-V4 AWB** (mm)	**V4-V7 WS** (mm)	**V4-V7 AWB** (mm)	**V7-V14 WS** (mm)	**V7-V14 AWB** (mm)	**V14-R6 WS** (mm)	**V14-R6 AWB** (mm)
Manhattan 2019	394.5	362.7	140.4 +362.7	471.4	105.8 +471.4	513.4	276.3 +513.4	506.5
Garden City 2019	158.6	117.4	51.7 + 117.4	139.7	66.8 + 139.7	109.4	85.4 +109.4	-186.3
Goodland 2019	163.2	123.2	33.2 + 123.2	120.4	24.5 + 120.4	29.3	289.6 + 29.3	-94.5
Keats 2020	198.6	167.7	28.6 + 167.7	162.7	68.0 + 162.7	148.0	221.1 +148.0	50.4
Buhler 2020	172.9	138.1	10.5 + 138.1	112.3	86.4 + 112.3	83.8	218.7 + 83.8	-73.2
Greensburg 2020	108.1	66.8	9.8 + 66.8	34.0	135.1 + 34.0	58.6	224.7 + 58.6	-116.3
Garden City 2020	81.3	73.8	44.8 + 73.8	73.2	79.1 + 73.2	38.6	257.4 + 38.6	-136.7
Goodland 2020	69.7	25.2	49.3 + 25.2	34.1	111.8 + 34.1	17.0	166.7 + 17.0	-330.8
Colby A 2020	59.0	10.8	23.2 + 10.8	-12.6	34.5 – 12.6	-81.4	172.3 - 81.4	-380.0
Colby B 2020	70.9	25.2	27.2 + 25.3	3.0	36.8 + 3.0	-54.8	172.3 - 54.8	-345.2

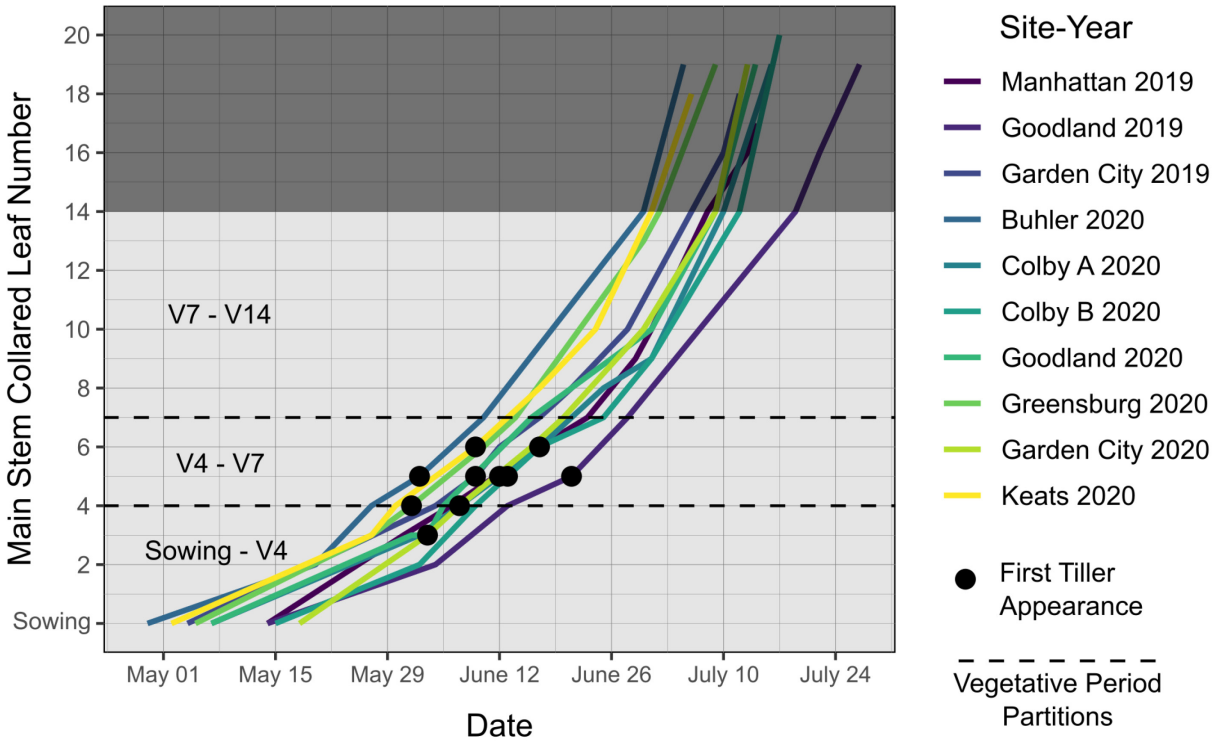

Figure A.1 Observed phenological stage progression (based on main stem collared leaf number) for all site-years. Lines are colored by site-year and connect observations without regression. Black points indicate the date of first tiller appearance for a given site-year. Black dashed lines indicate separation of vegetative period intervals Sowing-V4, V4-V7, and V7-V14. Shaded portion of plot above the fourteenth leaf indicates stages not considered in vegetative period partitioning, and data is shown only to provide full phenological progression dates and final leaf number.

Equation A.1

$$y_{ijklmnp} = \mu + \alpha_i + \beta_j + \theta_k + \delta_l + \alpha_i\beta_j + \alpha_i\theta_k + \alpha_i\delta_l + \beta_j\theta_k + \beta_j\delta_l + \theta_k\delta_l + \alpha_i\beta_j\theta_k + \alpha_i\beta_j\delta_l + \beta_j\theta_k\delta_l + \alpha_i\beta_j\theta_k\delta_l + b_m + d_{n(m)} + h_{p(n(m))} + \varepsilon_{ijklmnp},$$

$$b_m \sim N(0, \sigma_b^2),$$

$$d_{n(m)} \sim N(0, \sigma_d^2),$$

$$h_{p(n(m))} \sim N(0, \sigma_h^2), and$$

$$\varepsilon_{ijklmnp} \sim N(0, \sigma_\varepsilon^2).$$

In this case, $y_{ijklmnp}$ is the observed yield of a plot with tiller presence level k of genotype j of target plant density i of site-year l, observed in sub-plot p of whole plot n of block m; μ is the overall mean (intercept); α_i is the fixed effect of the i^{th} level of target density; β_j is the fixed effect of the j^{th} level of genotype; θ^k is the fixed effect of the k^{th} level of tiller presence; δ_l is the fixed effect of the l^{th} site-year; all combinations of the factors α_i, β_j, θ_k, and δ_l indicate double, triple, and quadruple interactions between them at double, triple, and quadruple levels; b_m is the random intercept effect of block m; $d_{n(m)}$ is the random intercept effect of the whole plot within block m; $h_{p(n(m))}$ is the random intercept effect of the sub-plot within whole plot n within block m; and $\varepsilon_{ijklmnp}$ is the residual term.

Equation A.2

$$y_{ijkln} = \mu_i + \alpha_i m_{j(i)} + \beta_i t_{j(i)} + \gamma_i m_{j(i)} t_{j(i)} + b_k + d_{l(k)} + h_{n(l(k))} + \varepsilon_{ijkln},$$

$$b_k \sim N(0, \sigma_b^2),$$

$$d_{l(k)} \sim N(0, \sigma_d^2),$$

$$h_{n(l(k))} \sim N(0, \sigma_h^2), and$$

$$\varepsilon_{ijkln} \sim N(0, \sigma_\varepsilon^2).$$

In this case, y_{ijklm} is the yield of j^{th} observation of the i^{th} site-year, which was collected in sub-plot n of whole plot l in block k; $m_{j(i)}$ is the true main plant density of the j^{th} observation in site-year i; $t_{j(i)}$ is the true tiller density of the j^{th} observation in site-year i; μ_i is the overall mean (intercept) for site-year i; α_i is the fixed effect associated with observed main plant density in site-year i; β_i is the fixed effect associated with observed tiller population in site-year i; γ_i is the fixed effect of the interaction between observed main plant density and tiller density in site-year i; b_k is the random intercept effect of block k; $d_{l(k)}$ is the random intercept effect of whole plot l within block k; $h_{n(l(k))}$ is the random intercept effect of sub-plot n within whole plot l within block k; and ε_{ijkln} is the residual term.

Appendix B - Chapter 3 Supplementary Material

Table B.1 ANOVA results for ear density given treatment factors target plant density (D), genotype (G), tiller presence (P), and interactions; and observed variables main plant density (M), observed tiller density (T), yield environment (E), and interactions. Tested source of variation (Source), degrees of freedom (df), degrees of freedom of residuals (Residual df), F value, and the associated *p* value significance are presented. All sources with *p* values ≤ 0.05 are shown in boldface font. Coefficient of determination (R^2) and root mean square error (RMSE) values for model fit are presented below each section.

Response Variable	Source	df	Residual df	F value	p value
Main stalk ears ha^{-1} (treatment factors, 10 site-years)	**Plant Density (D)**	**3**	**49.59**	**263.29**	***
	Genotype (G)	1	264.00	0.02	Ns
	Tiller Presence (P)	**1**	**198.00**	**55.68**	***
	D × G	2	264.00	0.92	Ns
	D × P	**2**	**198.00**	**16.22**	***
	G × P	1	198.00	0.12	Ns
	D × G × P	2	198.00	0.26	Ns
Marginal R^2 = 0.23, Conditional R^2 = 0.55, RMSE = 5360 ears ha^{-1}					
Comprehensive ears ha^{-1} (treatment factors, 10 site-years)	**Plant Density (D)**	**3**	**47.38**	**321.70**	***
	Genotype (G)	1	251.34	0.00	Ns
	Tiller Presence (P)	**1**	**198.00**	**39.63**	***
	D × G	2	251.34	1.64	Ns
	D × P	**2**	**198.00**	**10.83**	***
	G × P	1	198.00	0.96	Ns
	D × G × P	2	198.00	0.32	Ns
Marginal R^2 = 0.52, Conditional R^2 = 0.77, RMSE = 6933 ears ha^{-1}					
Main stalk ears ha^{-1} (observed variables, 17 site-years)	**Observed Plant Density (M)**	**1**	**183.32**	**35.11**	***
	Observed Tiller Density (T)	**1**	**307.84**	**28.51**	***
	Yield Environment (E)	**3**	**82.72**	**146.17**	***
	M × T	**1**	**334.69**	**9.94**	**
	M × E	2	195.43	2.58	Ns
	T × E	2	341.09	0.09	Ns
	M × T × E	2	375.77	0.53	Ns
Marginal R^2 = 0.62, Conditional R^2 = 0.79, RMSE = 4892 ears ha^{-1}					

Comprehensive ears ha^{-1} (observed variables, 17 site-years)	**Observed Plant Density (M)**	**1**	**186.46**	**25.42**	***
	Observed Tiller Density (T)	**1**	**326.98**	**10.24**	**
	Yield Environment (E)	**3**	**92.78**	**127.19**	***
	M × T	**1**	**360.31**	**9.42**	**
	M × E	2	200.27	2.18	Ns
	T × E	2	354.39	1.21	Ns
	M × T × E	2	390.76	0.27	Ns
Marginal R^2 = 0.32, Conditional R^2 = 0.55, RMSE = 6386 ears ha^{-1}					

*** significant at $p \leq 0.001$; ** significant at $p \leq 0.01$; Ns, not significant

Table B.2 Analysis of variance results for kernel density given treatment factors target plant density (D), genotype (G), tiller presence (P), and interactions; and observed variables main plant density (M), observed tiller density (T), yield environment (E), and interactions. Tested source of variation (Source), degrees of freedom (df), degrees of freedom of residuals (Residual df), F value, and the associated *p* value significance are presented. All sources with *p* values ≤ 0.05 are shown in boldface font. Coefficient of determination (R^2) and root mean square error (RMSE) values for model fit are presented below each section.

Response Variable	Source	df	Residual df	F value	p value
Main stalk kernels m^{-2} (treatment factors, 10 site-years)	**Plant Density (D)**	**3**	**40.78**	**97.78**	***
	Genotype (G)	1	227.15	2.91	Ns
	Tiller Presence (P)	**1**	**198.00**	**24.43**	***
	D × G	2	227.15	1.21	Ns
	D × P	**2**	**198.00**	**4.60**	*
	G × P	1	198.00	0.08	Ns
	D × G × P	2	198.00	0.03	Ns
Marginal R^2 = 0.31, Conditional R^2 = 0.84, RMSE = 243 kernels m^{-2}					
Comprehensive kernels m^{-2} (treatment factors, 10 site-years)	**Plant Density (D)**	**3**	**42.25**	**79.28**	***
	Genotype (G)	1	253.36	2.51	Ns
	Tiller Presence (P)	1	198.00	2.75	Ns
	D × G	2	253.36	1.08	Ns
	D × P	2	198.00	1.85	Ns
	G × P	1	198.00	1.70	Ns
	D × G × P	2	198.00	0.64	Ns
Marginal R^2 = 0.15, Conditional R2 = 0.77, RMSE = 307 kernels m^{-2}					
Main stalk kernels m^{-2} (observed variables, 17 site-years)	Observed Plant Density (M)	1	186.50	1.75	Ns
	Observed Tiller Density (T)	**1**	**287.00**	**11.17**	***
	Yield Environment (E)	**3**	**108.57**	**74.14**	***
	M × T	1	306.28	3.77	Ns
	M × E	**2**	**191.68**	**20.68**	***
	T × E	2	323.51	0.00	Ns
	M × T × E	2	354.50	0.01	Ns
Marginal R^2 = 0.66, Conditional R^2 = 0.84, RMSE = 235 kernels m^{-2}					
	Observed Plant Density (M)	1	183.72	2.95	Ns

Comprehensive ears ha^{-1} (observed variables, 17 site-years)	Observed Tiller Density (T)	1	315.22	0.09	Ns
	Yield Environment (E)	**3**	**70.96**	**61.60**	***
	M × T	1	343.49	0.13	Ns
	M × E	**2**	**196.35**	**20.57**	***
	T × E	**2**	**345.99**	**4.33**	*
	M × T × E	2	380.61	2.53	Ns
Marginal R^2 = 0.57, Conditional R^2 = 0.76, RMSE = 293 kernels m^{-2}					

*** significant at $p \leq 0.001$; * significant at $p \leq 0.05$; Ns, not significant

Table B.3 Analysis of variance results for kernel weight given treatment factors target plant density (D), genotype (G), tiller presence (P), and interactions; and observed variables main plant density (M), observed tiller density (T), yield environment (E), and interactions. Tested source of variation (Source), degrees of freedom (df), degrees of freedom of residuals (Residual df), F value, and the associated *p* value significance are presented. All sources with *p* values ≤ 0.05 are shown in boldface font. Coefficient of determination (R^2) and root mean square error (RMSE) values for model fit are presented below each section.

Response Variable	Source	df	Residual df	F value	p value
Main stalk kernel weight (treatment factors, 10 site-years)	**Plant Density (D)**	**3**	**45.50**	**189.75**	***
	Genotype (G)	**1**	**249.84**	**5.06**	*
	Tiller Presence (P)	1	198.00	3.36	Ns
	D × G	2	249.84	1.42	Ns
	D × P	**2**	**198.00**	**3.16**	*
	G × P	1	198.00	0.01	Ns
	D × G × P	2	198.00	0.06	Ns
Marginal R^2 = 0.08, Conditional R^2 = 0.60, RMSE = 42.5 mg kernel^{-1}					
Comprehensive kernel weight (treatment factors, 10 site-years)	**Plant Density (D)**	**3**	**45.31**	**187.62**	***
	Genotype (G)	**1**	**248.72**	**5.34**	*
	Tiller Presence (P)	1	198.00	2.05	Ns
	D × G	2	248.72	1.50	Ns
	D × P	2	198.00	2.89	Ns
	G × P	1	198.00	0.66	Ns
	D × G × P	2	198.00	0.36	Ns
Marginal R^2 = 0.32, Conditional R2 = 0.54, RMSE = 41.9 mg kernel^{-1}					
Main stalk kernel weight (observed variables, 17 site-years)	**Observed Plant Density (M)**	**1**	**187.83**	**6.05**	*
	Observed Tiller Density (T)	1	332.13	1.49	Ns
	Yield Environment (E)	**3**	**89.95**	**388.45**	***
	M × T	1	367.25	2.87	Ns
	M × E	2	201.68	0.81	Ns
	T × E	2	357.11	0.24	Ns
	M × T × E	2	393.53	0.72	Ns
Marginal R^2 = 0.32, Conditional R^2 = 0.54, RMSE = 46.1 mg kernel^{-1}					
	Observed Plant Density (M)	**1**	**188.11**	**6.35**	*

Comprehensive kernel weight (observed variables, 17 site-years)	Observed Tiller Density (T)	1	332.89	0.42	Ns
	Yield Environment (E)	**3**	**88.59**	**420.86**	***
	M × T	1	368.32	1.69	Ns
	M × E	2	201.95	0.91	Ns
	T × E	2	357.34	0.09	Ns
	M × T × E	2	393.71	0.91	Ns
Marginal R^2 = 0.32, Conditional R^2 = 0.54, RMSE = 44.6 mg kernel $^{-1}$					

*** significant at $p \leq 0.001$; * significant at $p \leq 0.05$; Ns, not significant

Table B.4 Analysis of variance results for yield response given observed variables primary ears ha^{-1}, secondary ears ha^{-1}, tiller axillary ears ha^{-1}, and tiller apical ears ha^{-1} by yield environment (E). Tested source of variation (Source), degrees of freedom (df), degrees of freedom of residuals (Residual df), F value, and the associated *p* value significance are presented. All sources with *p* values ≤ 0.05 are shown in boldface font. Coefficient of determination (R^2) and root mean square error (RMSE) values for model fit are presented below each section.

Source	df	Residual df	F value	*p* value
Primary Ears × Yield Environment (E)	**3**	**119.67**	**568.12**	***
Secondary Ears × E	**3**	**527.00**	**38.69**	***
Tiller Axillary Ears × E	**3**	**524.34**	**81.03**	***
Tiller Apical Ears × E	3	522.37	2.30	Ns
Marginal R^2 = 0.84, Conditional R^2 = 0.84, RMSE = 1.16 Mg ha $^{-1}$				

*** significant at $p \leq 0.001$; * significant at $p \leq 0.05$; Ns, not significant

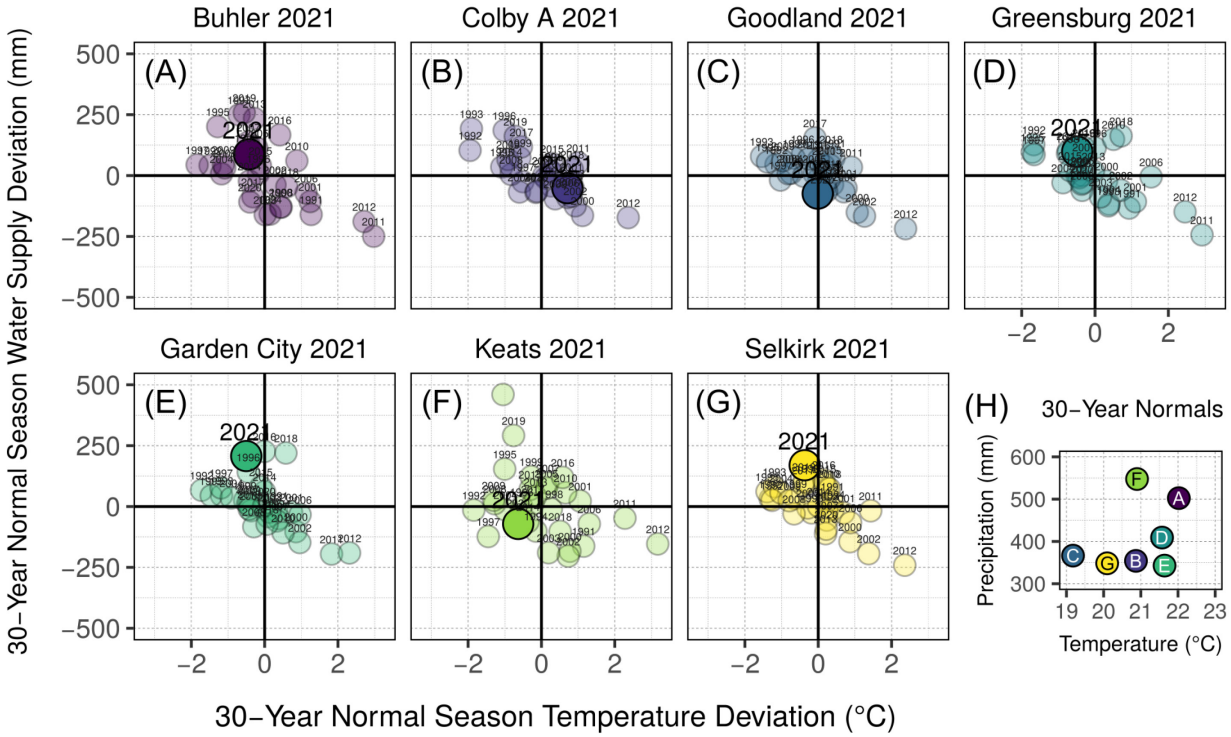

Figure B.1 Environmental characterization of site-years added to those described previously in Figure 2.1. Annual season normal precipitation and temperature deviation for 1991-2020 are presented for site-years (a) Buhler 2021, (b) Colby A 2021, (c) Goodland 2021, (d) Greensburg 2021, (e) Garden City 2021, (f) Keats 2021, and (g) Selkirk 2021. Season normal precipitation and temperature characterization by site-year are shown in panel h, referring to the panel letter of described site-years. Bold vertical lines in panels a - g indicate normal average temperature for site-year season date ranges, while bold horizontal lines indicate normal precipitation accumulation for site-year season date ranges. Year of study for each site-year (panels a - g) is indicated with a large, opaque point and enlarged text, and considers both precipitation and irrigation in the water supply value (y-axis). All other years in panels a - g are shown with transparent points and smaller text, and water supply (y-axis) includes only precipitation. Base period for all climate normal calculations was 1991-2020.

Equation B.1

$$y_{ijklmnq} = \mu + \alpha_i + \beta_j + \theta_k + \delta_l + \alpha_i\beta_j + \alpha_i\theta_k + \alpha_i\delta_l + \beta_j\theta_k + \beta_j\delta_l + \theta_k\delta_l + \alpha_i\beta_j\theta_k + \alpha_i\beta_j\delta_l + \beta_j\theta_k\delta_l + \alpha_i\beta_j\theta_k\delta_l + b_m + d_{n(m)} + h_{q(n(m))} + \varepsilon_{ijklmnq},$$

$$b_m \sim N(0, \sigma_b^2),$$
$$d_{n(m)} \sim N(0, \sigma_d^2),$$
$$h_{q(n(m))} \sim N(0, \sigma_h^2), and$$
$$\varepsilon_{ijklmnq} \sim N(0, \sigma_\varepsilon^2).$$

In this case, $y_{ijklmnp}$ is one of the observed yield component responses for site-years with a complete three-way factorial treatment structure, namely

- main stalk ear density (ears ha^{-1}),
- total ear density (ears ha^{-1}),
- main stalk kernel density (kern m^{-2}),
- total kernel density (kern m^{-2}),
- main stalk kernel weight (mg $kern^{-1}$), or
- total kernel weight (mg $kern^{-1}$),

of a plot with tiller presence level k of genotype j of target plant density i of site-year l, observed in sub-plot q of whole plot n of block m; μ is the overall mean (intercept); α_i is the fixed effect of the i^{th} level of target density; β_j is the fixed effect of the j^{th} level of genotype; θ_k is the fixed effect of the k^{th} level of tiller presence; δ_l is the fixed effect of the l^{th} site-year; all combinations of the factors α_i, β_j, θ_k, and δ_l indicate double, triple, and quadruple interactions between them at double, triple, and quadruple levels; b_m is the random intercept effect of block m; $d_{n(m)}$ is the random intercept effect of the whole plot within block m; $h_{p(n(m))}$ is the random intercept effect of the sub-plot within whole plot n within block m; and $\varepsilon_{ijklmnp}$ is the residual term.

Equation B.2

$$y_{ijklmn} = \mu + \alpha_j + \beta m_i + \gamma t_i + \theta m_i t_i + \delta_j m_i + \tau_j t_i + \zeta_j m_i t_i + s_k + b_{l(k)} + d_{m(l(k))} + h_{n(m(l(k)))} + \varepsilon_{ijklmn},$$

$$s_k \sim N(0, \sigma_s^2),$$

$$b_{l(k)} \sim N(0, \sigma_b^2),$$

$$d_{m(l(k))} \sim N(0, \sigma_d^2),$$

$$h_{n(m(l(k)))} \sim N(0, \sigma_h^2), and$$

$$\varepsilon_{ijklmn} \sim N(0, \sigma_\varepsilon^2).$$

In this case, y_{ijklmn} is one of the observed yield component responses, namely

- main stalk ear density (ears ha^{-1}),
- total ear density (ears ha^{-1}),
- main stalk kernel density (kern m^{-2}),
- total kernel density (kern m^{-2}),
- main stalk kernel weight (mg kern^{-1}), or
- total kernel weight (mg kern^{-1}),

of the i^{th} plot, found in sub-plot n of whole plot m of block l in site-year k of environmental cluster j; m_i is the observed main plant density of plot i; t_i is the observed tiller density of plot i; μ is the overall mean (intercept); α_j is the fixed effect of the j^{th} level of environmental cluster; β is the fixed effect associated with observed main plant density; γ is the fixed effect associated with observed tiller density; θ is the fixed effect associated with the interaction of observed main plant density and observed tiller density; δ_j is the fixed effect associated with observed main plant density in environment cluster j; τ_j is the fixed effect associated with observed tiller density in environment cluster j; ζ_j is the fixed effect associated with interaction of observed main plant density and observed tiller density within environment cluster j; s_k is the random intercept effect of site-year k; $b_{l(k)}$ is the random intercept effect of block l within site-year k; $d_{m(l(k))}$ is the random intercept effect of the whole plot within block l within site-year k; $h_{n(m(l(k)))}$ is the random intercept effect of the sub-plot within whole plot m within block l within site-year k; and ε_{ijklmn} is the residual term.

Appendix C - Chapter 4 Supplementary Material

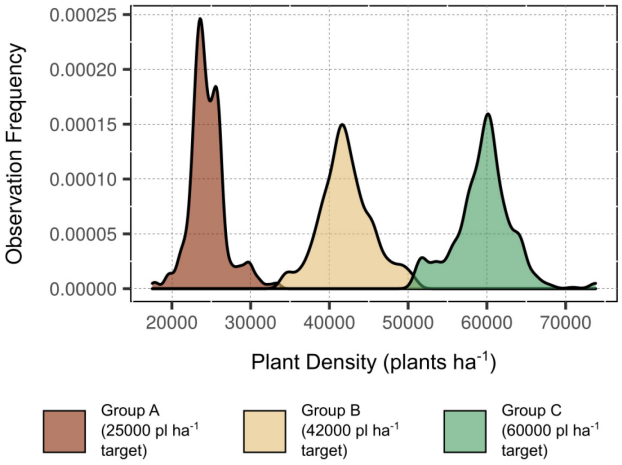

Figure C.1 Observation density of true plant density for each of the three defined plant density groups. Groups were based on target plant density levels of 25000 pl ha^{-1} (rust), 42000 pl ha^{-1} (gold), and 60000 pl ha^{-1} (green).

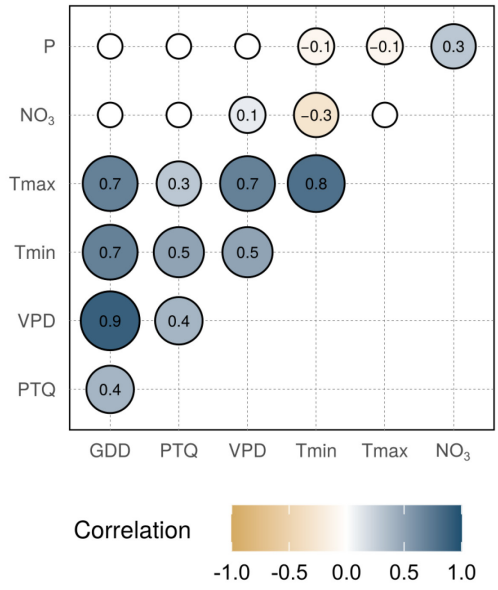

Figure C.2 Correlations among environmental variables shown independently in Figure 4.2. Point size indicates the magnitude of correlation, while color indicates the sign (-, gold; +, blue). GDD, cumulative growing degree days; PTQ, growing period photothermal quotient; T_{min}, mean daily minimum growing period temperature; T_{max}, mean daily maximum growing period temperature; VPD, cumulative vapor pressure deficit; NO_3, soil test nitrate; P, soil test phosphorus.

Equation C.1 Selected model for prediction of tiller densities in corn fields of various target plant densities and nutrient management strategies, considering non-limiting moisture availability and sufficiency of other potential limiting factors not listed.

- Data model: $z_i = y_i$ or $z_i \propto y_i$.
- Process model: $[y_i|\alpha_i] \equiv \text{Binomial}(\alpha_i)$, where
  $\alpha_i = \text{inverse logit } [\beta_0 + f_{1d}(g_{id}) + f_{2d}(q_{id}) + f_{3d}(l_{id}) + f_{4d}(x_{id}) + f_{5d}(v_{id}) + f_{6d}(n_{id}) + f_{7d}(p_{id})]$.
- Parameter model: $\beta_0 \propto 1$.

That is,

- z_i is the observed tiller density ha^{-1}, assumed to be the same as y_i, the true density;
- α_i is the bulk of the process model as described above;
- β_0 is the y-intercept of fitted model;
- d is a plant density cluster with factor levels A (25000 plants ha^{-1}), B (42000 plants ha^{-1}), or C (60000 plants ha^{-1});
- f_{1d} is the smooth effect of cumulative growing degree days (GDD) for plant density cluster d;
- g_{id} is the cumulative GDD of observation i in plant density cluster d;
- f_{2d} is the smooth effect of photothermal quotient (PTQ) for plant density cluster d;
- q_{id} is the PTQ of observation i in plant density cluster d;
- f_{3d} is the smooth effect of mean minimum temperature for plant density cluster d;
- l_{id} is the mean seasonal minimum temperature of observation i in plant density cluster d;
- f_{4d} is the smooth effect of mean maximum temperature for plant density cluster d;
- x_{id} is the mean seasonal maximum temperature of observation i in plant density cluster d;
- f_{5d} is the smooth effect of the cumulative vapor pressure deficit (VPD) for plant density cluster d;
- v_{id} is the cumulative VPD of observation i in plant density cluster d;
- f_{6d} is the smooth effect of soil test nitrate (NO_3) for plant density cluster d;
- n_{id} is the soil test NO_3 (ppm) of observation i in plant density cluster d;
- f_{7d} is the smooth effect of soil test phosphorus (P) for plant density cluster d; and
- p_{id} is the soil test P (ppm) of observation i in plant density cluster d.

Appendix D - Chapter 5 Supplementary Material

Table D.1 Biomass ANOVA p-values. AB, aboveground dry biomass; R, reproductive dry biomass; S, stem dry biomass; L, leaf dry biomass; (ha), kilograms per hectare; (pl), kilograms per plant; D, plant density; G, genotype; P, tiller presence; T, sampling.

Source	AB (ha)	AB (pl)	R (ha)	R (pl)	S (ha)	S (pl)	L (ha)	L (pl)
Plant Density (D)	***	***	***	***	***	***	***	***
Genotype (G)								
Tiller Presence (P)	***	***			***	***	***	***
Sampling (T)	***	***	***	***	***	***	***	***
D × G								
D × P	*	***			***	***	***	***
D × T	***	***		***	***		***	*
G × P								**
G × T						*		
P × T	***	***			***	***	***	***
D × G × P								
D × G × T								
D × P × T	*	***			***	***	**	***
G × P × T								
D × G × P × T								

*, $p \leq 0.05$; **, $p \leq 0.01$; ***, $p \leq 0.001$

Table D.2 Water-soluble carbohydrate ANOVA p-value results. WSC, water-soluble stem carbohydrates; (m^2), grams per square meter; (pl), grams per plant; D, plant density; G, genotype; P, tiller presence; T, sampling.

Source	WSC (m^2)	WSC (pl)
Plant Density (D)	***	***
Genotype (G)		
Tiller Presence (P)	***	***
Sampling (T)	***	***
D × G		
D × P	***	***
D × T	***	
G × P		
G × T		
P × T	***	***
D × G × P		
D × G × T		
D × P × T	***	***
G × P × T		*
D × G × P × T		

*, $p \leq 0.05$; **, $p \leq 0.01$; ***, $p \leq 0.001$

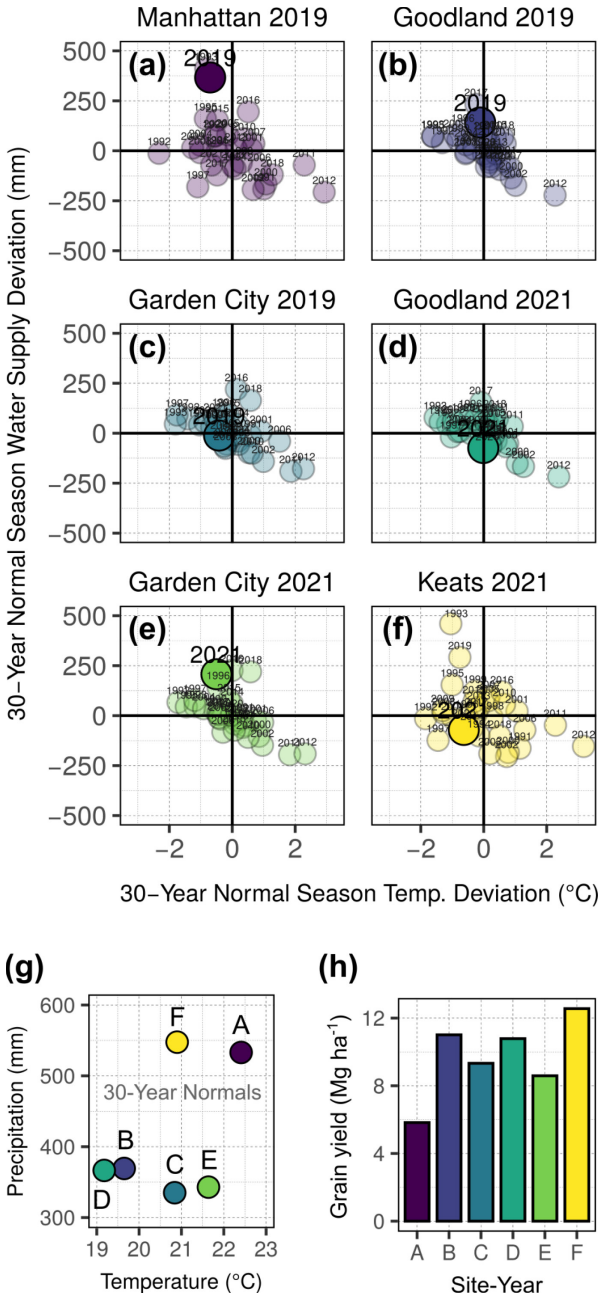

Figure D.1 Environmental characterization of evaluated site-years. Annual season normal precipitation and temperature deviation for 1991-2020 are presented for site-years (a) Manhattan 2019, (b) Goodland 2019, (c) Garden City 2019, (d) Goodland 2021, (e) Garden City 2021, and (f) Keats 2021. Season normal precipitation and temperature characterization by site-year are shown in panel g, and average grain yields by site-year are shown in panel h – both refer to the panel letter of described site-years. Bold vertical lines in panels a - f indicate normal average temperature for site-year season date ranges, while bold horizontal lines indicate normal precipitation accumulation for site-year season date ranges. Year of study for each site-year (panels a - f) is indicated with a large, opaque point and enlarged text, and considers both precipitation and irrigation in the water supply value (y-axis). All other years in panels a - f are shown with transparent points and smaller text, and water supply (y-axis) includes only precipitation. Base period for all climate normal calculations was 1991-2020.